A GIS EXPERT SYSTEM FOR THE DELINEATION OF WATERSHEDS IN LOW-RELIEF REGIONS WITH RURAL INFRASTRUCTURE

Guy D. Duke
B.Sc., University of Lethbridge, 2001

A Thesis
Submitted to the School of Graduate Studies
of the University of Lethbridge
in Partial Fulfillment of the
Requirements for the Degree

MASTERS OF SCIENCE

Department of Geography
University of Lethbridge
LETHBRIDGE, ALBERTA, CANADA

Abstract

Grid-based digital elevation models (DEMs) are used to simulate overland flow paths in hydrological models. The accuracy of these drainage patterns are dependent upon how well the DEM represents the terrain features that control runoff patterns. Often regional DEMs are not produced at scales small enough to represent rural infrastructure. The scale of runoff patterns that can be accurately modeled is, therefore, restricted, particularly when the terrain is relatively flat.

The RIDEM (Rural Infrastructure Digital Elevation Model) model is presented that utilizes commonly available ancillary data to downscale grid-based runoff patterns. The resulting drainage patterns reflect drainage modifications imposed by rural infrastructure including: roads, ditches, culverts, and irrigation canals. Downscaling runoff patterns enables the completion of runoff studies at smaller scales. The model was implemented within the Oldman River watershed, Alberta, Canada to determine the spatial patterns of potential runoff contributing areas in three agricultural watersheds regularly contaminated by pathogens.

Acknowledgements

Table of Contents

List of Tables

List of Figures

viii

Chapter 1

1 Overview

1.1 Introduction

A watershed (also called a drainage basin, or catchment) is defined as the area that on the basis of topography contributes all the water to a particular stream cross-section (Dingman, 2002). The characteristics within the watershed (viz. climate, geology, soils, topography, land use, and land cover) control the flow pathways, rates of movement, magnitude, and quality of stream flow. Because the processes that determine the fate of water in the land phase of the hydrological cycle operate at the watershed scale, effective water management strategies must also take this perspective (Dingman, 2002).

The study area used to complete this thesis research was contained within the Oldman River watershed in southern Alberta, Canada (Figure 1). The Oldman River drains approximately 22,641 km^2 to the confluence of the Oldman and Bow Rivers that form the South Saskatchewan River (ORBWQI, 2000). The headwaters of the Oldman River watershed are located in the Rocky Mountains. The area downstream of the Rocky Mountains, lying within the Northern Great Plains, is primarily agricultural. The Lethbridge Northern Irrigation District (LNID) and the Saint Mary Irrigation District (SMRID) operate within the watershed with a basin population of approximately 200,000 (ORBWQI, 2000).

A five-year review of infection by Waters et al. (1994) found that southern Alberta had the highest rate of gastrointestinal illness in the province. More recently, outbreaks of

1

waterborne illness in Walkerton, Ontario in 2000 and North Battleford, Saskatchewan in 2001, boil water orders, temporary shutdowns of water treatment facilities, and a series of water treatment plant upgrades have raised public concern regarding the quality of water in the Oldman River watershed (Gannon et al., 2002). In 1997 a cooperative program between the University of Lethbridge, Health Canada, the LNID, Alberta Environment, Alberta Agriculture, and the Oldman River Basin Water Quality Initiative (ORBWQI) began. Since that time, water samples from 30 locations within the watershed have revealed routine contamination of water supplies from bacterial pathogens (*E. coli* 0157:H7 and *Salmonella* spp) as well as bacterial indicator species (viz. total and fecal coliforms) (Gannon et al., 2002; Hyland et al., 2003; Johnson et al., 2003).

Investigating the relationships between pathogen occurrence and the spatial characteristics of the Oldman River watershed is a major objective of the cooperative study that involves the University of Lethbridge (Gannon et al., 2002). Accurately determining the watersheds, for each of the 30 water quality-sampling locations, would facilitate the analysis of the spatial and temporal influence of watershed properties on waterborne pathogen occurrence. During the completion of this thesis a stand-alone computer model called RIDEM (Rural Infrastructure Digital Elevation Model) was written in Microsoft Visual Basic that corrects runoff transport pathways in low-relief areas that have been altered by rural infrastructure. The watersheds derived with RIDEM can be used to guide new management strategies in the Oldman River watershed.

2

1.2 Objectives

The objective of this research is to delineate the watershed, or runoff contributing area, of several water-quality monitoring sites that are part of the Oldman River Basin Water Quality Initiative. Although watersheds can be derived manually using hard-copy topographic maps, automated processes that utilize a digital representation of terrain and implement a flow direction algorithm are preferred because they follow a predetermined logic and are repeatable. Therefore, to delineate watersheds accurately using a digital representation of terrain requires the following:

- an assessment of the terrain characteristics in the study area,

- an evaluation of the digital terrain representation, and

- an evaluation of currently available flow direction algorithms.

3

Figure 1 Oldman River watershed study area

Image reprinted with the permission of Wendy Devent, Project Coordinator, Oldman River Basin Water
Quality Initiative. Image creator: Brian Coffey, Alberta Agriculture, Food and Rural Development

<center>**Chapter 2**</center>

2 Literature Review

2.1 Runoff Hydrology

Although gross watersheds are the plane area that on the basis of topography contributes

all the water to a specified stream cross-section, only a fraction of the gross watershed

actually produces runoff that enters local surface waters most of the time (Dingman,

2002). The portion of the watershed that actually contributes runoff to the outlet is called

the effective watershed (PFRA, 1983). Gross watershed boundaries also contain areas

that do not contribute runoff even under extremely wet conditions. Godwin and Martin

(1975) referred to these areas as dead drainages. While gross watersheds and dead

drainages are defined based on topography alone, the extent of effective watersheds is

conditional upon additional hydrological factors such as soils, precipitation, and

vegetation (PFRA, 1983).

All of the water that passes through the outlet of a watershed originates as precipitation.

A portion of all precipitation is evaporated and returns to the atmosphere. Another

portion percolates through the soil under the force of gravity, eventually becoming part of

the groundwater. Following underground flow paths, groundwater either exfiltrates, to

become surface water, or it may discharge directly into a surface water body (i.e.,

stream). A third portion of the precipitation flows above ground. This portion of the

precipitation that reaches the stream channel is referred to as runoff (Strahler and

Strahler, 1996). The timing, magnitude, and quality of stream flow at the watershed

<center>5</center>

outlet is, therefore, dependent upon the flow pathway taken through the landscape (Dingman, 2002).

Runoff contributing areas within a watershed are primarily the result of two processes. The first process called infiltration-excess (or Hortonian flow), occurs when the precipitation intensity exceeds the rate of water infiltration (Juracek, 2000; Dingman, 2002). The area contributing runoff to a stream via infiltration-excess flow is called the critical source area (CSA) (Quinn, 2002). The second process of runoff contribution to a stream is called saturation-excess overland flow. Saturation-excess runoff occurs when precipitation falls on areas where the water table is located at the land-atmosphere interface (Juracek, 2000; Dingman, 2002). The area contributing runoff to a stream via saturation-excess overland flow is referred to as the variable source area (VSA) (Quinn, 2002). Usually non-point source pollutants are transported from the land to a water body through via runoff (Cooke et al., 2002). Consequently, the determination of overland flow paths enables the study of land-use impacts on water quality.

This thesis is concerned solely with the determination of overland flow paths governed by topography, and does not consider evaporation or infiltration. The temporal dynamics of varying VSA's and CSA's are, therefore, outside the scope of this research.

2.2 Watershed Delineation

Conventionally, watersheds were delineated using paper topographic maps or stereoscopically viewed air photographs. Watersheds were delineated starting at the watershed outlet and tracing elevation contour lines at right angles. Constant visual inspection was often necessary to ensure that an imaginary rain droplet would flow downslope to the outlet location, assuming the ground surface was impermeable (Dingman, 2002). Manual delineation of watersheds is, however, tedious, prone to error, and subject to individual judgment (Band, 1986).

The advent of Geographic Information Systems (GIS), the increased processing power of computers, and the availability of digital elevation models (DEM) have made automated watershed delineation possible. In addition to the speed advantage automated watershed delineation has over manual procedures, deriving watersheds within a GIS also has the advantage of reproducibility and ease of distribution (Tribe, 1992). Automated watershed delineation within a GIS is based upon digital representations of the landscape referred to as DEMs. DEMs enable the determination of flow pathways in the landscape because overland and near surface flow pathways are controlled by topography (Moore et al., 1991). The algorithms used to derive flow pathways in the GIS environment are commonly referred to as routing or flow direction algorithms.

7

2.2.1 Digital Elevation Models (DEM)

Originally, DEMs were created simply to orthorectify air photos (Burrough and

McDonell, 1998), however, because topography impacts hydrological, geomorphological,

and biological landscape processes the application potential of DEMs has greatly

expanded. Currently, DEMs are not only used to extract primary topographic attributes

(e.g., elevation, slope, aspect, drainage lines, catchment areas, and others), but also to

characterize the spatial variability of complex processes occurring in the landscape

(Moore et al., 1991). These secondary (or compound) topographic attributes are used for

many types of applications, including the prediction of the following:

- precipitation,

- soil moisture,

- soil salinization,

- erosion potential,

- sedimentation rates,

- catchment runoff response,

- non-point-source pollution,

- assessing and managing biological productivity, and others.

Moore et al. (1991) summarized the application potential of DEMs used in hydrological,

hydraulic, water resources, and environmental applications.

The application potential of a DEM is, however, dependent upon its data storage

structure. DEMs are generally stored in one of the following three data structures:

8

- 2-dimensional arrays (or grids),

- triangulated irregular networks (TIN),

- or as contours (Figure 2).

Grid structures consist of a matrix of square grid cells (known as raster cells) with an

average elevation value that is representative for the area that comprises each cell. The

spatial location of each grid cell within the matrix is defined by the row and column

coordinate. Thus, the memory requirement to store grid data structures is minimal

because only the location of a single cell needs to be stored. The grid data structure is

known as the raster data model. TINs represent the elevation surface as interconnected

triangles with locational and elevation values stored for each triangle vertex. TINs

require three values (x, y, and z) for each vertex and are, therefore, not stored as

efficiently as the grid data structure (Kumler, 1994). The irregular structure of a TIN also

hinders some types of spatial analysis, which is the major drawback of TINs (Burrough

and McDonnell, 1998). Contour-based DEMs consist of digitized contour lines with

associated elevation values for each contour. Similar to TINs, the drawbacks of contour-

based DEMs include storage inefficiency, and processing complexity. Contour-based

DEMs are referred to as digital line graphs (DLG).

The grid data structure is not, however, without its disadvantages. These disadvantages

include:

- data redundancy in areas of homogeneous terrain because of the inability to

    represent differing areas of relief complexity with variable grid cell sizes,

- failure to accurately represent discontinuities in elevation,

9

- exaggerated emphasis along the axis of the grid for some types of analysis, and

- grid size dependency of many computed topographic parameters (Fairchild and

  Leymarie, 1991; Moore et al., 1991; Burrough and McDonnell, 1998; Garbrecht

  and Martz, 2000).

Despite the limitations of the grid data structure it remains the most widely used form of

DEM because of its simplicity, processing ease, and computational efficiency (Moore et

al., 1991; Burrough and McDonell, 1998; Garbrecht et al., 2001). Additionally, the grid

data structure is inherently compatible with pixel-based remotely sensed imagery that can

be used to characterize the landscape. This research is concerned solely with grid-based

DEMs. From this point forward, the term DEM will refer to an elevation model with a

grid data structure.

2.2.2 Grid-Based Flow Direction Algorithms

DEM-based watershed derivation requires the prediction of overland flow paths that

define the connectivity of the landscape with respect to water, sediment, and pollutant

transport. The simplest and most commonly used flow direction algorithm, proposed by

O'Callaghan and Mark (1984), is commonly referred to as the deterministic eight

neighbour or D8. The D8 flow direction algorithm first calculates the slope between the

central grid cell and each orthogonal and diagonal neighbour in a moving 3-by-3-grid cell

window (Figure 3). The slope is calculated by subtracting the elevations of two

neighbouring grid cells, and dividing by the horizontal distance between the grid cell

centers. For orthogonal neighbours (viz. N, E, S, W) the horizontal distance is equal to

the grid cell size. To compensate for the increased path length between the center cell

and each diagonal neighbour the horizontal distance is determined by multiplying with a

factor of $1/\sqrt{2}$ for each diagonal slope calculation. Based on the slope values calculated a

single flow direction is assigned to the cell in which the path of steepest downward

descent exists (Figure 3). Because the flow from each cell is allocated to only one

neighbour, the D8 algorithm is a discretized (or single) flow direction algorithm. Thus,

the flow directions possible within the D8 framework is limited to the eight major

compass directions (viz. N, NE, E, SE, S, SW, W, NW) in accordance to the alignment of

the grid cell matrix.

The original D8 algorithm proposed by O'Callaghan and Mark (1984) was, however,

problematic when grid cells lacking a downslope neighbour occurred in the DEM. This

11

situation, referred to as a "sink", resulted in flow paths that terminated at the grid cell with the lowest elevation, producing a discontinuous drainage pattern. Because discontinuous drainage patterns are uncommon in the real world (O'Callaghan and Mark, 1984), Jensen and Domingue (1988) developed a new procedure to eliminate all "sinks" prior to the assignment of flow directions. The methodology of Jensen and Domingue (1988), commonly referred to as "pit filling", either raises local DEM "sinks" to the minimum elevation required to fill the depression, or reduces the elevation of grid cells responsible for the formation of "sinks". The result of applying this algorithm is a continuous drainage pattern in which all flow paths progress off the edge of the DEM matrix. The requirement of a continuous flow direction matrix has become a fundamental requirement for conventional grid-based hydrological models.

In addition to watershed and sub-catchment boundaries, producing a flow direction matrix also enables the automated extraction of drainage networks (or streams). Drainage accumulation functions determine the number of grid cells that drain to each grid cell element. If each grid cell is given a weighting of 1, drainage accumulation functions determine the runoff contributing, or specific catchment area (SCA) for each grid cell in the flow direction matrix (O'Callaghan and Mark, 1984). Channel networks (or streams) are then defined as those cells with an accumulated drainage area greater than a user-defined threshold. As the specified threshold value decreases, the density of extracted drainage networks increase (Figure 4).

Extracting channel networks with a specified flow accumulation threshold has been criticized because the selected SCA if often chosen arbitrarily, resulting in inaccurate representations of cannel networks (Tarboton, 1991). Consequently, several more complex procedures that account for slope or terrain curvature have also been proposed (Tarboton et al., 1991; Montgomery and Foufoula-Georgiou, 1993). These methodologies are, however, outside the scope of this thesis.

Watersheds are derived analogously to flow accumulation functions that determine the SCA for each grid cell. Given a specified grid cell representing the watershed outlet all cells whose flow path ultimately leads through the outlet grid cell are included in the watershed. Using the conventional approach incorporated into many GIS packages (e.g., ArcView, ArcInfo) automated DEM-based watershed delineation processing is a three-step approach:

- fill spurious DEM sinks,

- derive local flow directions (e.g., D8),

- determine the contributing area to a specified outlet grid cell.

Figure 5 shows the progression of DEM-derived hydrological data layers including a hillshade rendition of a DEM, a flow direction matrix, a stream network, and a watershed boundary grid.

2.3 Grid-Based Watershed Modelling Error

The fundamental step of all grid-based hydrological models is the assignment of flow

directions (Freeman, 1991; Desmet and Govers, 1996). The accuracy of modeled flow

paths is, therefore, dependent upon the accuracy of the DEM and the conceptual accuracy

of the flow direction algorithm (Quinn and Beven, 1991; Garbrecht and Martz, 2000,

Wise, 2000; Endreny and Wood, 2001). Since O'Callaghan and Mark proposed the D8

flow direction algorithm in 1984, several authors have developed alternative flow

direction algorithms that attempt to mitigate the limitations of the D8 methodology.

These limitations are:

- bias in the flow path orientation due to the alignment of the grid cell matrix,

- the creation of parallel flow paths across DEM sinks,

- failure to represent flow accurately on convex slopes, and

- sensitivity to small DEM elevation errors.

Similarly, many researchers have analyzed the impact DEMs have on derived drainage

patterns. DEM-based accuracy analysis has included studies regarding the effects of:

- DEM elevation accuracy,

- data source properties used to interpolate DEMs,

- DEM horizontal resolution (viz. grid cell size), and

- DEM vertical resolution (viz. elevation increment).

The following two sections review research that has contributed to the progression of

grid-based hydrological modeling in regards to flow direction and DEM error.

14

2.3.1 Flow Direction Algorithm Error

Three types of grid-based flow direction algorithms exist, including: single flow direction algorithms that allocate all of the flow from a source cell to a single downslope cell, multiple flow direction algorithms that restrict flow to a maximum of two downslope cells, and multiple flow direction algorithms that partition flow to all neighbouring downslope cells (Desmet and Govers, 1996). While single flow direction algorithms allow parallel and convergent flow only, multiple flow direction algorithms can also model divergent flow. Consequently, the extent of DEM-derived watersheds is sensitive to the choice of flow direction algorithm implemented.

The earliest grid-based flow direction algorithm developed was the deterministic eight neighbour (D8) introduced by O'Callaghan and Mark (1984). The D8 algorithm assigns a single flow direction from each cell to the neighbouring cell to which the steepest downslope path exists. Because the flow direction is discretized into one of eight directions, the modeled flow direction can deviate from the true flow direction by as much as 22.5° (Figure 6). Due to the inability of the D8 algorithm to represent flow directions continuously (i.e., from 0-360°), the D8 algorithm produces preferential flow directions that correspond to the alignment of the grid cell matrix and its diagonals. As a result, the D8 algorithm produces unrealistic parallel flow patterns on hillslopes where the aspect is not aligned with the grid cell matrix (Freeman, 1991; Costa-Cabral and Burges, 1994; Gallant and Wilson, 1996; Tarboton, 1997; Rieger, 1998; Orlandini et. al., 2003). Fairchild and Leymaire (1991) suggested breaking up the parallel flow paths by

15

incorporating a random factor with the Rho8 (random eight node) algorithm. However, introducing a random component to the process makes reproducing results nearly impossible and is, therefore, counterproductive (Costa-Cabral and Burges, 1994; Gallant and Wilson, 1996; Tarboton, 1997; Rieger, 1998). Because single flow direction algorithms cannot model dispersion, flow patterns derived with the D8 algorithm are also unrealistic on divergent (i.e., convex) surfaces (Freeman, 1991; Costa-Cabral and Burges, 1994; Tarboton, 1997). The effect is to create sharp boundaries between grid cells with large SCAs and grid cells with small SCAs (Figure 7a). This conceptual inaccuracy can potentially lead to the prediction of concentrated flow patterns (or stream channels) on hillslopes dominated by sheet flow. Single flow direction algorithms are also sensitive to erroneous concavities in DEMs that can lead to the inaccurate prediction of drainage patterns (Desmet and Govers, 1996).

In order to eliminate the preferential flow directions of the D8 algorithm, several authors have suggested the use of multiple flow direction algorithms (Freeman, 1991; Quinn et al., 1991). The multiple flow direction algorithms proposed by Freeman (1991) and Quinn et al. (1991) (referred to jointly as the MF algorithm) partition the flow from each grid cell to all downslope neighbours in proportion to their slope. The MF algorithm produces smooth transitions from zones with small SCAs to areas with large SCAs (Figure 7b). Although flow patterns derived with the MF algorithm are more realistic than D8-derived drainage patterns on hillslopes (Freeman, 1991; Quinn et. al., 1991; Desmet and Govers, 1996; Gallant and Wilson, 1994; Rieger, 1998), the weakness of the MF algorithm becomes apparent in areas where concentrated flow patterns dominate (i.e.,

16

river valleys). After reviewing the MF algorithm, Costa-Cabral and Burges (1994), Desmet and Govers (1996), and Tarboton (1997) all concluded that partitioning the flow from a single grid cell to as many as eight neighbours is inconsistent with the concept of drainage area because it produces overly divergent flow patterns. This inaccuracy occurs primarily in low-relief areas. The modeled drainage patterns are, therefore, more representative of diffuse sheet flow than channelized (or concentrated) flow patterns along watercourses. Freeman (1991) suggested the implementation of the D8 single flow direction approach in concentrated flow areas (viz. areas upwardly curved) and the MF algorithm on adjacent hillslopes. This however, prompts the question of when, or where, to switch from the MF algorithm to a single flow direction algorithm. To address this concern, Desmet and Govers (1996) developed the flux decomposition algorithm that partitions flow into two orthogonal (i.e., N or S, E or W) cells. When the orthogonal cells are at a higher elevation than the diagonal cell (i.e., within sharp concavities) the algorithm switches to the D8 approach. Although the resulting drainage patterns are more realistic along main drainage lines than those produced with the MF algorithm, the flux decomposition algorithm is not effective when the concavities are greater than one cell size in width (Desmet and Govers, 1996). Gallant and Wilson (1996) proposed transitioning from multiple to a single flow direction algorithm at a user-defined SCA threshold. However, choosing the proper SCA to represent the transition from hillslope to concentrated flow patterns is problematic because the SCA chosen is arbitrary (Tarboton et al., 1991).

17

Tarboton (1997) developed the D-Infinity algorithm that minimizes dispersion by restricting flow from a single cell to as many as two downslope cells. Based on mathematical terrain surfaces, the D-Infinity algorithm has been shown to produce more accurate flow patterns than the MF and D8 algorithm (Tarboton, 1997). Because the D-Infinity maintains dispersion it is, however, also inconsistent with the concept of drainage area (Moore and Grayson, 1991; Orlandini et al., 2003). Because the D-Infinity algorithm also disperses flow to more than one downslope neighbour, the extent of watersheds derived with the D-Infinity algorithm are erroneously large (Figure 8).

The development of multiple flow direction algorithms fostered a new concept in grid-based flow direction routing called dispersal area mapping (e.g., Endreny and Wood, 2001). Dispersal area mapping quantifies the proportion of each grid cell that contributes runoff to a specified location. This concept can be extended to introduce uncertainty into overland flow routing if one assumes the proportion that each grid cell contributes is analogous to the likelihood of that grid cell contributing to the outlet. In this regard, Tarboton (pers. comm.) developed the dependence function to eliminate watershed commission errors that hinder routing algorithms that support divergence. The dependence function proportionately assigns a continuous value to each grid cell from 0 to 1. Values of 1 are assigned to cells that contribute entirely to the outlet. Cells that do not contribute to the outlet are given a value of 0. The dependence watershed in Figure 9b shows that the majority of the grid cells that comprise the watershed do not contribute significantly to the outlet, yet they are included in the D-Infinity watershed (Figure 9a). Tarboton (pers. comm.) recommends selecting a membership function of greater than or

18

equal to 0.5 to exclude the grid cells unlikely to contribute runoff to the outlet (Figure

9c). While the result of this process is a watershed that resembles the watershed derived

with the single flow direction algorithm D8 (Figure 9d), the dependence function is

hindered by the same subjectivity as attempts to switch from MF algorithms to single

flow direction algorithms at a user-specified SCA.

In an attempt to remove the restrictions of grid-based data structures entirely, Lea (1992)

and Costa-Cabral and Burges (1994) developed DEMON (Digital Elevation Model

Networks), an aspect driven flow tube method to simulate overland flow paths. The

algorithm fits a plane based on the elevations of four grid cells and calculates a single

flow direction between 0 and 360°. Although DEMON has been shown to outperform

the D8 algorithm (Costa-Cabral and Burges, 1994; Gallant and Wilson, 1996; Tarboton,

1997) as well as the MF algorithm (Tarboton, 1997), DEMON is not robust and cannot

manage all landscape patterns (Tarboton, 1997).

In contrast to multiple flow direction algorithms, single flow direction algorithms are

appealing because they are:

- computationally efficient,

- consistent with the physical definition of drainage area, and

- relatively easy to incorporate into existing distributed hydrological models.

Consequently, several authors have attempted to improve the D8 methodology proposed

by O'Callaghan and Mark (1984). Jensen and Domingue (1988) made the algorithm

more robust by incorporating a new methodology to define flow directions in DEM sinks

19

of all types and sizes. The refined D8 methodology proposed by Jensen and Domingue

(1988) has since been incorporated into ESRI GIS software (ArcView, ArcGIS, ArcInfo).

From this point forward, this methodology is referred to as the conventional D8 flow

direction algorithm.

The conventional D8 algorithm has been shown to produce unrealistic parallel flow

patterns over flat areas (areas with a slope of zero) created during the filling process of

the DEM (Garbrecht and Martz, 1997; Martz and Garbrecht, 1999; Rieger, 1998;

Turcotte et al., 2001). Martz and Garbrecht (1999) suggested this as perhaps the single

largest inconsistency of the D8 approach and subsequently developed a new flat area

algorithm, referred to as D8-TOPAZ. The conventional D8 flat area algorithm identifies

grid cells at the edge of flat areas (or sinks) with the lowest elevation. Grid cells within

the flat area are subsequently routed to the nearest outlet as previously identified. In

contrast, the D8-TOPAZ algorithm routes flow in flat areas both away from higher terrain

and towards lower terrain by introducing minor elevation changes to the flat areas of the

DEM (Garbrecht and Martz, 1997). The resulting flow patterns converge in flat areas,

eliminating the parallel flow patterns that plagued the approach introduced by Jensen and

Domingue (1988) (Figure 10). Given that the D8-TOPAZ algorithm produces more

realistic results than the conventional D8 algorithm, the importance of implementing the

D8-TOPAZ algorithm increases in areas of low relief areas because the proportion of flat

areas increases following the DEM filling process (Garbrecht and Martz, 1997).

20

Orlandini et al. (2003) developed the D8-least transversal deviation (D8-LTD) method, which attempts to solve the problems associated with grid bias (viz. preferential flow directions) without the disadvantage of introducing dispersion. The D8-LTD algorithm keeps in memory the deviation of the discretized D8 flow direction (i.e., 0, 45, 90, 135, 180, 225, 270, 315, and 360°) from the theoretical slope direction (i.e., 0-360°) as calculated within the D-Infinity method proposed by Tarboton (1997). The next downstream grid cell is assigned a flow direction minimizing the sum of the transversal deviations between the current and previous grid cell (Orlandini et al., 2003). The effect is to periodically correct flow directions on hillslopes that are misaligned with the grid matrix. Drainage patterns derived with the D8-LTD algorithm have been shown to outperform the conventional D8 algorithm on both mathematical surfaces and DEMs of real landscapes (Orlandini, et. al., 2003).

Although multiple flow direction algorithms have been used successfully to model soil moisture (e.g., Quinn et al., 1995) and predict ephemeral gullies (e.g., Desmet et al., 1999), single flow direction algorithms remain the algorithm of choice for identifying streamlines and delineating watersheds (Freeman, 1991; Orlandini et al., 2003). By taking into consideration deviations between the direction of steepest downslope descent and the orientation of the grid cell matrix, the D8-LTD algorithm (Orlandini et al., 2003) may reduce the problem of grid bias that plagues the D8 algorithm without adding the complexity introduced through dispersion. However, due to the inability to successfully implement the D8-LTD executable programs obtained from Dr. Stefano Orlandini, the D8-TOPAZ algorithm was implemented for this research.

2.3.2 Digital Elevation Model Error

The first step required to create a DEM is the collection of point elevation data or a

topographic contour map. Methods for collecting point elevation data include:

- *in-situ* measurement of elevations using surveying instruments,

- photogrammmetric techniques based on stereoscopic aerial photography,

- interferometric synthetic aperture radar (IFSAR), and

- active light detection and ranging (LIDAR) (Raber et al., 2002).

Once point elevation data (or a contour map) have been collected, an interpolation

algorithm is required to replace the original observations by a regular distribution of

points, thereby creating the grid data structure (e.g., Hutchinson, 1989). However,

information is inevitably lost during the DEM creation process because DEMs are

discrete representations of a continuous surface (Huang, 2000; Wise, 2000; Schneider,

2001; Quinn, 2002). Stated more simply, information is lost because each cell within the

grid data structure has one elevation value, while the real world area each grid cell

represents has an infinite number of elevations. As a result, grid DEMs are not

continuous, and all topographic parameters derived from a DEM will contain some aspect

of error even if the DEM is error-free (Wise, 2000; Schneider, 2001).

Quinn et al. (1991) recognized the creation of the DEM as the most difficult part of

digital terrain analysis and flow path determination. Filling the gaps between the

sampled elevation points creates a generalized terrain representation, as well as erroneous

"sink" and "dam" features. Sinks within a DEM are a collection of grid cells (or a single

22

cell) that lack a downslope neighbour and are caused by elevation under-estimates

(Garbrecht and Martz, 1999). Because sinks larger than 30-m in size occur only in

special landscapes (e.g., karst landscapes), sinks within DEMs are considered erroneous

(O'Callaghan and Mark, 1984). Dams are created when narrow strips of cells produce an

impoundment, and therefore sinks by creating blockages across flow paths. Dams are

caused by interpolation overestimates, and the orientation of the grid matrix (Reiger,

1998; Garbrecht and Martz, 1999). A third consequence of DEM interpolation is the

generalization of small incised channels (e.g., canals, ditches) and small raised terrain

features (e.g., roads), and as a result, only the general pattern of terrain is preserved.

The normal method of assessing DEM error is to compare a sample of heights from

within the DEM against the known heights from a more accurate data source. The

accuracy of the DEM is normally reported as the root mean square error (RMSE):

$$\text{RMSE} = \sqrt{\frac{\sum\limits_{i=1}^{N}(\hat{Y}_i - Y_i)^2}{n}} \qquad \text{(Equation 1)}$$

where: $\hat{Y}_i$ = estimated elevation value in the DEM
Y_i = true elevation value
n = the number of test points

Garbrecht and Martz (2000) subdivided DEM accuracy into DEM resolution and DEM

quality. DEM quality refers to the closeness of the elevation values compared to the true

values and is quantified by the RMSE. DEM resolution refers to the precision of the

elevation values including both horizontal grid cell size and the elevation value

increment. DEM quality is a function of three factors, including the following:

- the accuracy, density, and distribution of the source data,

23

• the roughness of the terrain surface, and

• the interpolation method used to derive the DEM (Gong et al., 2000; Huang, 2000).

Gong et al. (2000) measured the magnitude of effect from each of the above factors and

concluded that the point-elevation sampling interval is the single greatest factor affecting

DEM quality. As the sampling interval used to generate DEMs increases, DEM error

increases linearly, although the magnitude of change in error decreases as terrain

becomes less rugged (Gong et al., 2000; Huang, 2000).

While minimizing the RMSE of a DEM is always beneficial, minimizing the grid cell

size is not always advantageous. It is generally recognized that the appropriate DEM

resolution is a function of the scale of the processes modeled, and the size of the land

surface features that govern these processes (Garbrecht and Martz, 2000). Walker and

Willgoose (1999) stated that the grid cell size required to accurately represent the

landscape should be based upon the roughest terrain in the study area. Such a statement

is not, however, very useful because the surface phenomenon "terrain" is only

meaningful within a certain range of scales (Schneider, 2001). Viewed from space,

terrain features on earth are irrelevant. Similarly, if one observes terrain from close

enough, the principal components become discrete entities such as rocks and soil

aggregates (Schneider, 2001). Consequently, several authors have made more specific

suggestions regarding the appropriate resolution of DEMs. Zhang and Montgomery

(1994) and Quinn et al. (1995) found that a grid cell size of 10-m adequately represents

topography for hydrological applications.

Optimizing DEM horizontal resolution is not, however, a question of identifying the size

of features that are required to be represented in the DEM, but rather determining what

resolution the point-elevation sampling interval supports (Garbrecht and Martz, 1996;

Walker and Willgoose, 1999). Kienzle (2004) examined the information gained by

decreasing the grid cell size of a DEM, and concluded that in relatively flat terrain (viz.

southern Alberta, Canada) with a point sampling distribution of 100-m (plus mass points

and break lines) the optimal DEM resolution is 10 m. Thus, it is the properties of the

point data set used to interpolate the DEM that limits DEM horizontal resolution (or grid

cell size). Decreasing the resolution of the DEM beyond the resolution of the original

data set does not increase the accuracy of the DEM, nor the topographic parameters

derived from it (Figure 11) (Zhang and Montgomery, 1994; Garbrecht and Martz, 1996;

Brasington and Richards, 1998; Walker and Willgoose, 1999; Garbrecht et al., 2001;

Kienzle, 2004).

The second component of DEM resolution is the elevation increment or vertical

resolution. At the regional scale, commercially available DEMs (e.g., 30-m United States

Geological Survey [USGS] DEMs) typically have a 1-m vertical resolution, and are

therefore in integer format. The implications of DEM vertical resolution depend on the

nature of the terrain. In relatively flat terrain a 1-m vertical resolution creates erroneous

1-m high terraces increasing the proportion of flat areas (Veregin, 1997). In areas with

large slope values these DEM artifacts are less pronounced. Gyasi-Agyei et al. (1995)

studied the effect DEM vertical resolution had on hydrological parameters and concluded

that the vertical resolution is satisfactory if the ratio between the average elevation drop

per grid cell and the vertical resolution is greater than one.

2.4 Landscape Feature Impacts on Drainage Feature Derivation

Moore et al. (1991), Grayson et al. (1993), and Band and Moore (1995) stated that flow

paths predicted with grid-based models are often grossly simplified and unrealistic due to

their inability to account for the effects of terrain on flow processes. The inability to

account for terrain can be attributed to the poor representation of the terrain features that

influence drainage patterns. Band and Moore (1995) reiterated this statement by

describing the development of fully distributed parameter hydrological models as little

more than "academic exercises" due to the difficulty of collecting input terrain data

(among others), of significant detail to capture the heterogeneity within a watershed.

Thus, regional scale DEMs often do not represent the critical sources of landscape

drainage variation. The scale of grid-based model outputs are, therefore, rarely in tune

with the scale required by decision makers (Finke and Bierkens, 2002). Beven (1995)

described this as the "scale problem", where information gained at one scale is used to

make predictions at either larger or smaller scales. In this regard, several authors have

studied the effect that land surface heterogeneity (or micro-topography) imposes on

hydrological modeling at different spatial scales. These studies suggest new

methodologies are needed to incorporate small-scale terrain features into grid-based

hydrological models. The following section reviews:

- the spatial disturbance pattern of land use change in the Canadian grasslands,

- the effect anthropogenic features such as roads, ditches, tillage furrows, and culverts
  have on hydrological processes, and

27

- the steps taken to incorporate these terrain features into grid-based hydrological models.

2.4.1 Anthropogenic Terrain Features

In the late 19th century the federal government of Canada promoted mass immigration by

advertising free 160-acre (0.65 km^2 or 1 quarter-section) homesteads (Chicalo, 2002).

Following this influx of settlement the landscape of the Canadian prairies was subdivided

into a rectangular network of townships and quarter sections (Figure 12). This network

became the template for the construction of a system of roads that has been built across

the Canadian grasslands (Figure 13). A provincial road inventory in 1999 determined

that approximately 15, 462 km of primary highways, 15, 083 km of secondary highways,

and 137, 298 km of local roads (i.e., gravel) have been constructed in the province of

Alberta alone (Henning, pers. comm.). Settlement in areas frequently confronted with

water deficits have also lead to the development of 13 irrigation districts in Alberta

totaling 5,132 km^2 of irrigable land (Alberta Agriculture, Food and Rural Development,

1997). In 2002, approximately 72,034 km^2 of land was seeded to principal crops, and

thus subject to tillage and other agricultural practices in Alberta (Alberta Agriculture,

Food and Rural Development, 2003). It is estimated that only 28%, or 42,087 km^2, of

native grassland remains on the Canadian prairies (United States Geological Survey,

2003). The spatial extent of these disturbance patterns has prompted research to assess

the impact these land use changes impose on environmental processes.

The results from several research studies indicate that anthropogenic terrain features

common in southern Alberta significantly affect the hydrological and geomorphological

processes within a watershed. For example, tillage furrows as small as 2-cm in depth can

29

significantly modify flow networks and erosion patterns (Ludwig et al., 1996; Souchere et al., 1998; Cerdan et al., 2001; Takken et al., 2001 [a, b, c]; Souchere et al., 2003). A study by Dijck (2000) demonstrated that the density, continuity, and total length of the "between-field runoff network" (i.e., ditches) are more influential on runoff hydrographs in agricultural areas of France than field properties (viz. levelling and surface roughness). Ludwig et al. (1996) and Dijck (2000) suggested that agricultural fields are frequently hydrologically isolated. Runoff that is generated from one field is seldom transferred to an adjacent field due to the presence of ditches at field edges.

When few drainage features (i.e., culverts) are present, roads can also cause substantial inter-basin water transfers (Luce and Wemple, 2001). Studies conducted in the United States by Montgomery (1994) and in Ethiopia by Nyssen et al. (2002) concluded that roads concentrate runoff, significantly increasing the formation of gullies, as well as changing the size and shape of watersheds. In the study conducted by Nyssen et al. (2002), changes in runoff patterns resulting from road construction significantly increased the drainage area of gullies from 5.8 to 8.5 hectares (P < 0.001). In a study in the western cascades of Oregon, Wemple et al. (1996) reported a 21 to 50% increase in watershed drainage density as a result of roadside ditches and culverts. Similarly, Montgomery (1994) reported a 60% increase in drainage density following road construction. The consequence of extending the channel network is a more rapid delivery of runoff to streams, resulting in shorter times to peak flow and increased total discharges (Dijck, 2000; Jones et al., 2000; La Marche and Lettenmaier, 2001). Additionally, Tague and Band (2001) showed that road induced runoff modification significantly affected soil

30

moisture conditions. Roads have also been reported as a significant mechanism of soil, water, and air quality pollution (Van Bohemen and Van De Laak, 2003). Because of their tendency to run across topographic gradients, the construction of linear features such as roads (and irrigation canals) influence watershed scale processes to a much greater extent than their aerial coverage suggests (Luce and Wemple, 2001).

The results of these studies indicate that anthropogenic terrain features significantly affect hydrological processes, including:

- flow pathways,

- rates of movement,

- magnitude, and

- quality of stream flow.

Consequently, new routines are required to capture the effects of anthropogenic disturbances (e.g., tillage, roads, irrigation) in order to accurately model runoff transport processes. In turn, this will improve grid-based hydrological models and enable the accurate delineation of watershed boundaries, as well as the successful implementation of new water management strategies.

2.4.2 Scaling Grid-Based Drainage Patterns with Ancillary Data

Because the accuracy of DEM-derived drainage patterns is contingent upon the accuracy of the DEM, it is crucial that the elevation values within DEMs capture the terrain features that influence drainage patterns (Jensen and Domingue, 1988). This requirement is particularly important in low-relief landscapes where small-scale terrain features (i.e., roads, ditches, irrigation canals) significantly affect runoff flow paths. Hydrological models, however, do not frequently account for the limitations of DEMs to accurately represent the landscape (Walker and Willgoose, 1999; Schneider, 2001). Consequently, anthropogenic terrain features are not accounted for in traditional grid-based models that utilize conventional flow direction algorithms. True watershed boundaries can, therefore, differ significantly from watersheds derived using conventional flow direction algorithms that rely upon a generalized representation of topography (Ludwig et al., 1995; Souchere et al., 1998; Cerdan et al., 2001).

Linear landscape features as small as tillage furrows have the ability to modify overland flow directions (Souchere et al., 1998; Cerdan et al., 2001; Takken et al., 2001 [a, b, c]; Souchere et al., 2003) suggesting the need to interpolate DEMs from datasets with point-elevation sampling intervals at the scale of centimeters. Recognizing the limitations of current technology, hydrological modelers have begun to incorporate ancillary data when deriving flow directions from DEMs. Saunders (2000) utilized ancillary stream data to impose or "burn" stream vector data to improve the accuracy of flow direction matrices near streams. "Burning" streams refers to the process of decreasing the elevation of grid

cells representing watercourses to enforce the known drainage patterns on the flow

direction matrix. Saunders (2000) concluded that vector hydrography networks are

accurately replicated through the stream burning process. Takken et al. (2001c)

developed the tillage-controlled runoff pattern (TCRP) algorithm that incorporates

knowledge regarding tillage orientation into the Limburg Soil Erosion Model (LISEM).

In-field flow direction mapping revealed that the runoff direction on 75% of all hillslopes

was controlled by the orientation of tillage and not the naturally occurring topographic

aspect (Takken et al., 2001b). In the Belgium Loess Belt, Takken et al. (2001c) reduced

predicted field scale erosion rates by 35% after taking into consideration the impact

tillage orientation imposed on drainage patterns with the TCRP algorithm. Similarly,

Cerdan et al. (2001) and Souchere et al. (2003) used the expert-based Sealing and

Transfer by Runoff and Erosion related to Agricultural Management (STREAM) model

to simulate erosion in agricultural watersheds. By manipulating the flow direction in

tilled fields according to furrow depth and slope, and enforcing flow directions along

dead furrows, the STREAM model accurately replicated the observed runoff network

(Cerdan et al., 2001).

By incorporating ancillary data into grid-based hydrological models (e.g., Saunders,

2000; Cerdan et al., 2001; Takken et al., 2001c; Souchere et al., 2003) runoff flow

patterns can be modeled more precisely. Thus, the scale of processes modeled can be

reduced below the scale of processes governed by the DEM alone. Analysts that use

ancillary data when modelling must, however, be aware of the inaccuracies associated

with the additional data. The variables included for integration into the model should be

33

of conceptual and practical significance (Jensen, 1996). Therefore, ancillary data incorporated into grid-based hydrological models should enable the scale of output results to match the scale required for analysis (Finke and Bierkens, 2002). This process requires hydrological modelers to identify the features in the landscape that influence runoff patterns and develop new routines that simulate their effects for surface drainage derivation.
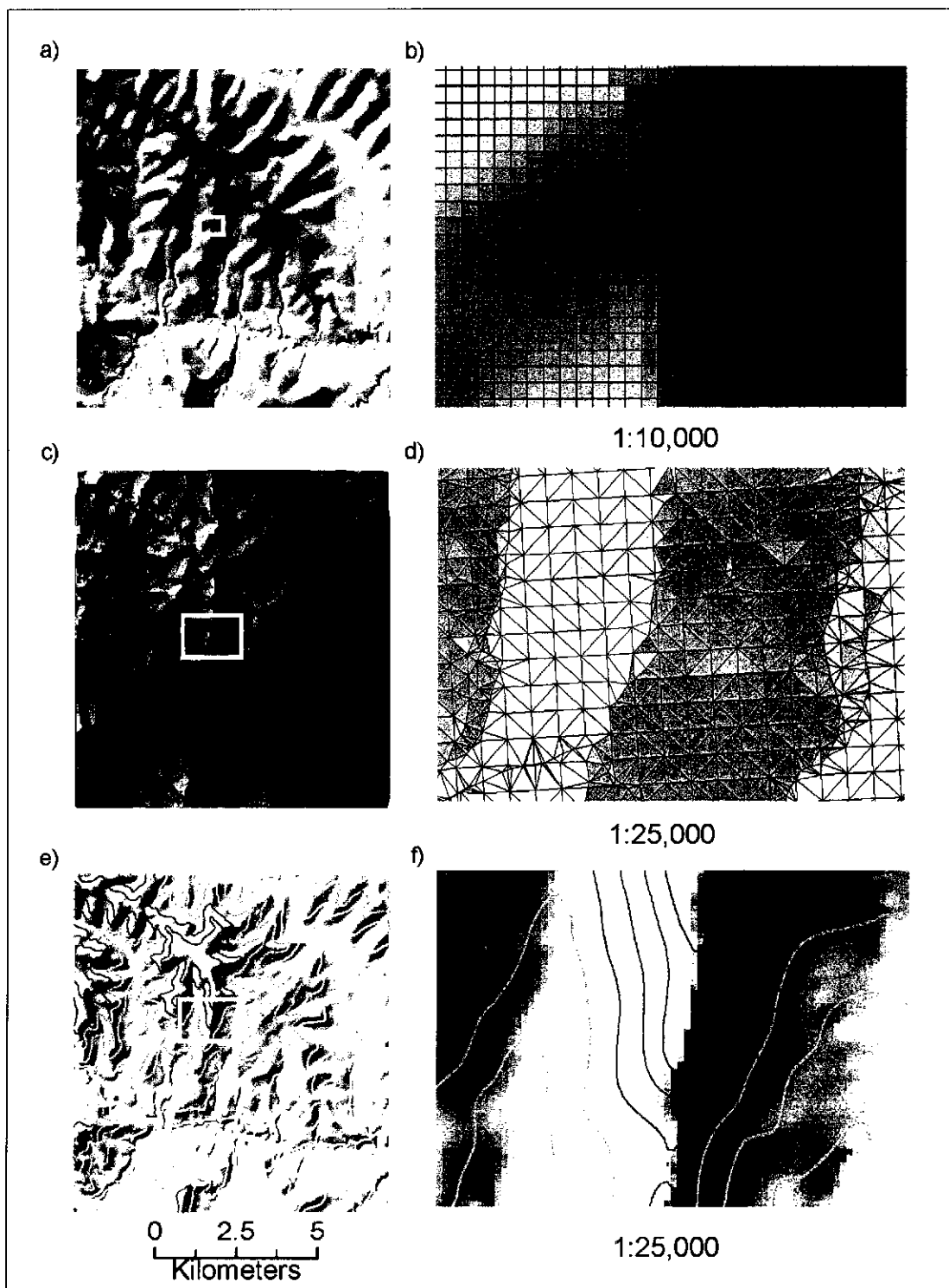
Figure 2 Digital Elevation Model (DEM) data structures

a) grid, b) grid inset showing 25-m square grid elements, c) triangular irregular network (TIN), d) TIN inset showing the triangle alignment, e) contour-based (50-m contour interval), f) contour-based inset (25-m contour interval).

35
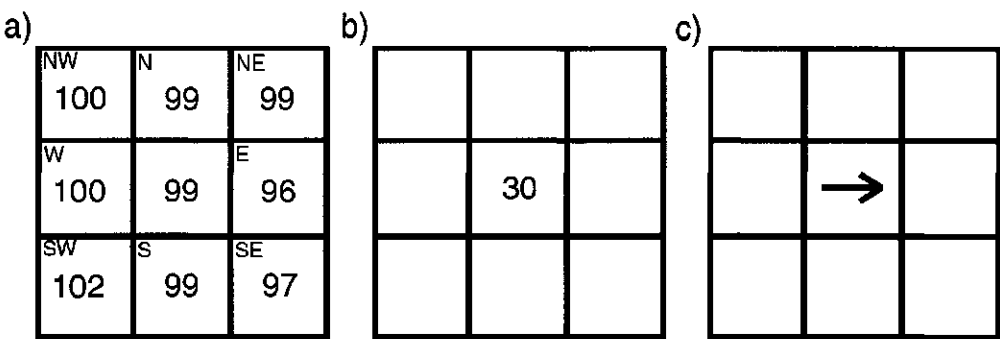
Figure 3 D8 flow direction sequence of analysis

a) 3-by-3-grid cell window representing elevations (m) with a 10-m grid cell size, b) the steepest downwards descent (percent slope) to a grid cell "E" ((3/10)*100%), and c) the corresponding D8 flow direction.
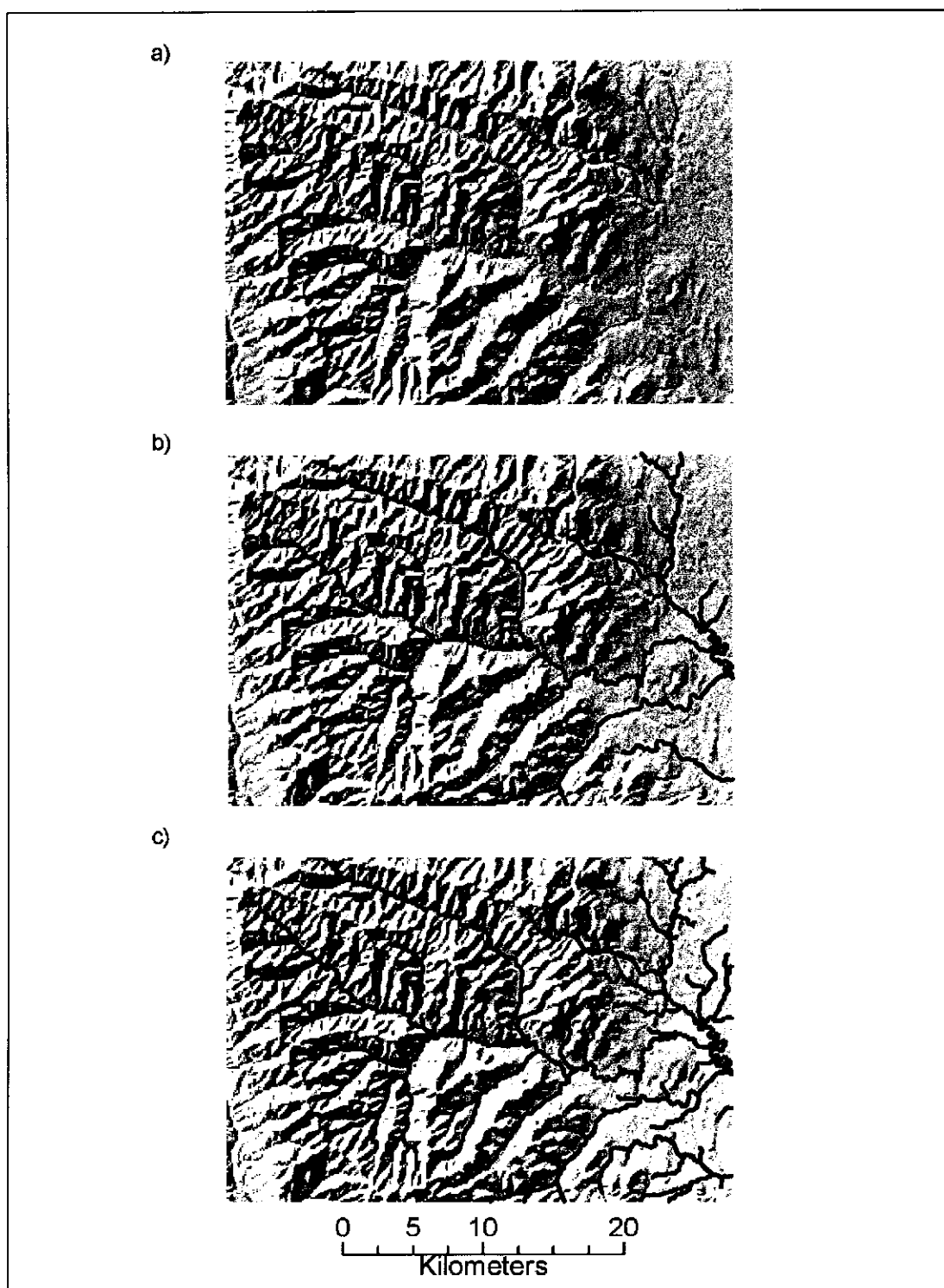
Figure 4 DEM-derived drainage network sensitivity to SCA threshold

a) Hillshaded DEM grid, b) a DEM-derived stream network SCA 12.5 km^2, c) a DEM-derived stream network SCA 2.5 km^2.

37
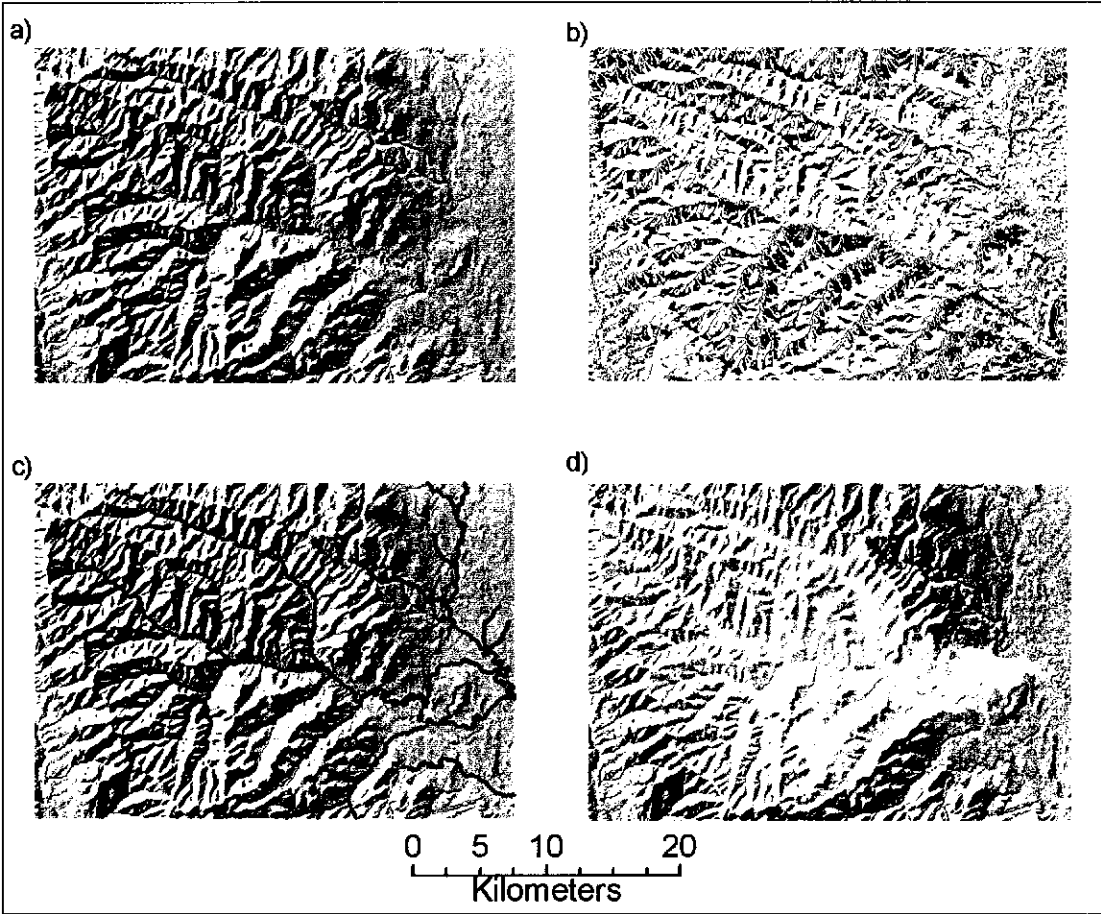
Figure 5 Progression of hydrological information extracted from DEMs

a) DEM hillshade grid, b) a D8 flow direction grid, c) a DEM-derived stream network grid, d) a watershed boundary grid.
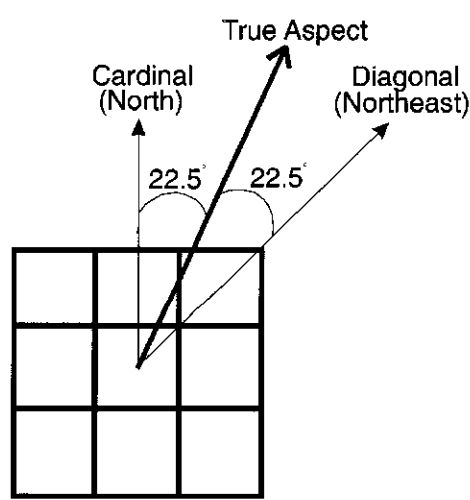
Figure 6 Potential D8 routing algorithm flow path error
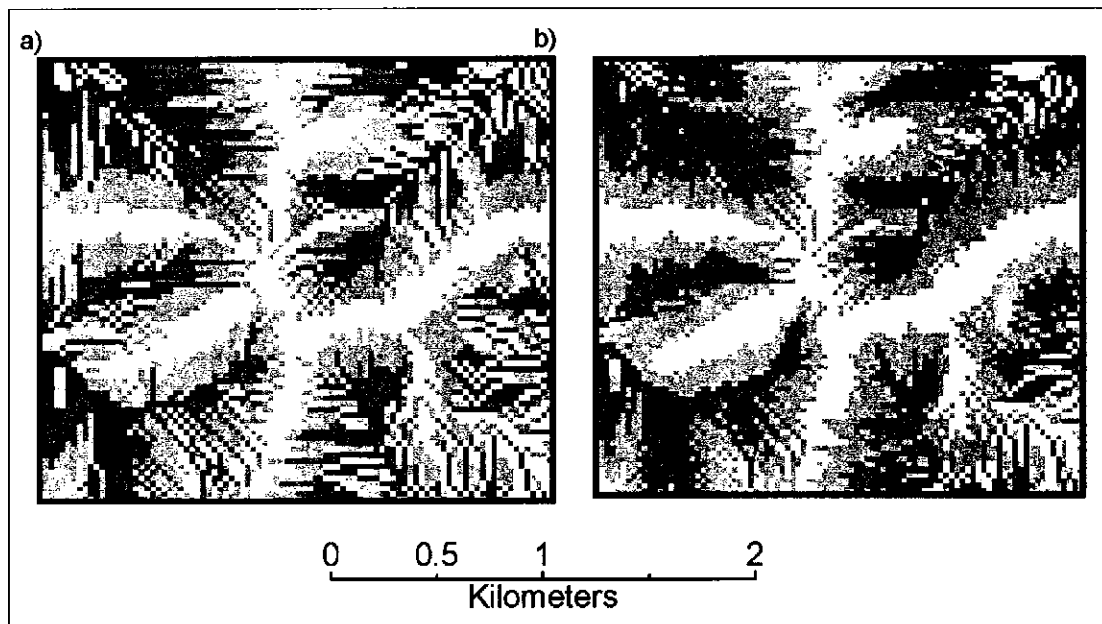
Figure 7 Discretized vs. divergent flow direction algorithm dispersal areas

Light coloured areas represent ridges, while dark coloured areas represent valleys. a) D8 flow direction algorithm, b) MF flow direction algorithm that supports divergent flow paths.
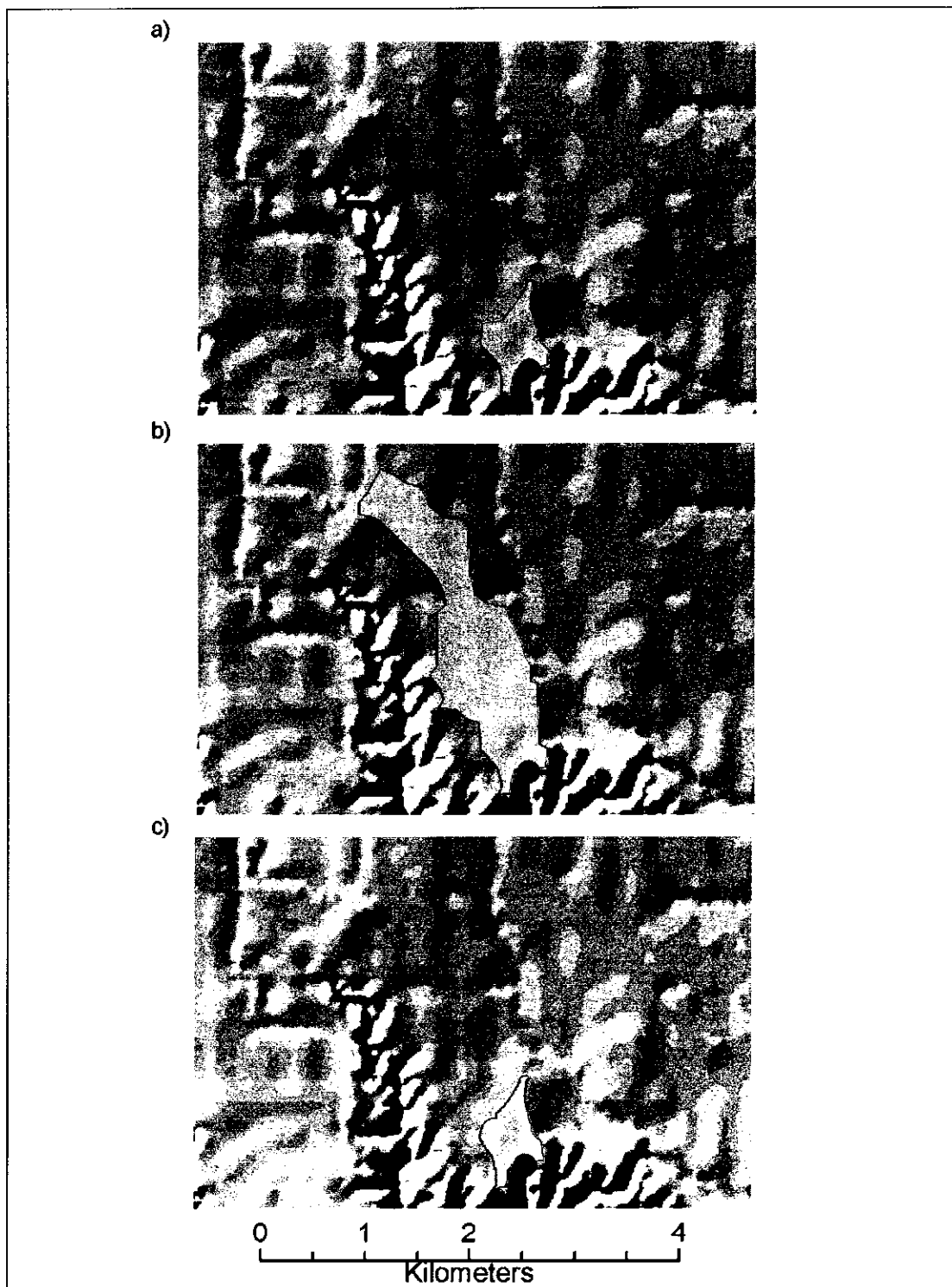
Figure 8 Discretized vs. divergent flow direction algorithm watershed boundary comparison

a) the discretized D8 algorithm, and b) the multiple flow direction D-Infinity algorithm, c) a watershed delineated by manually tracing DEM-derived contours.

40
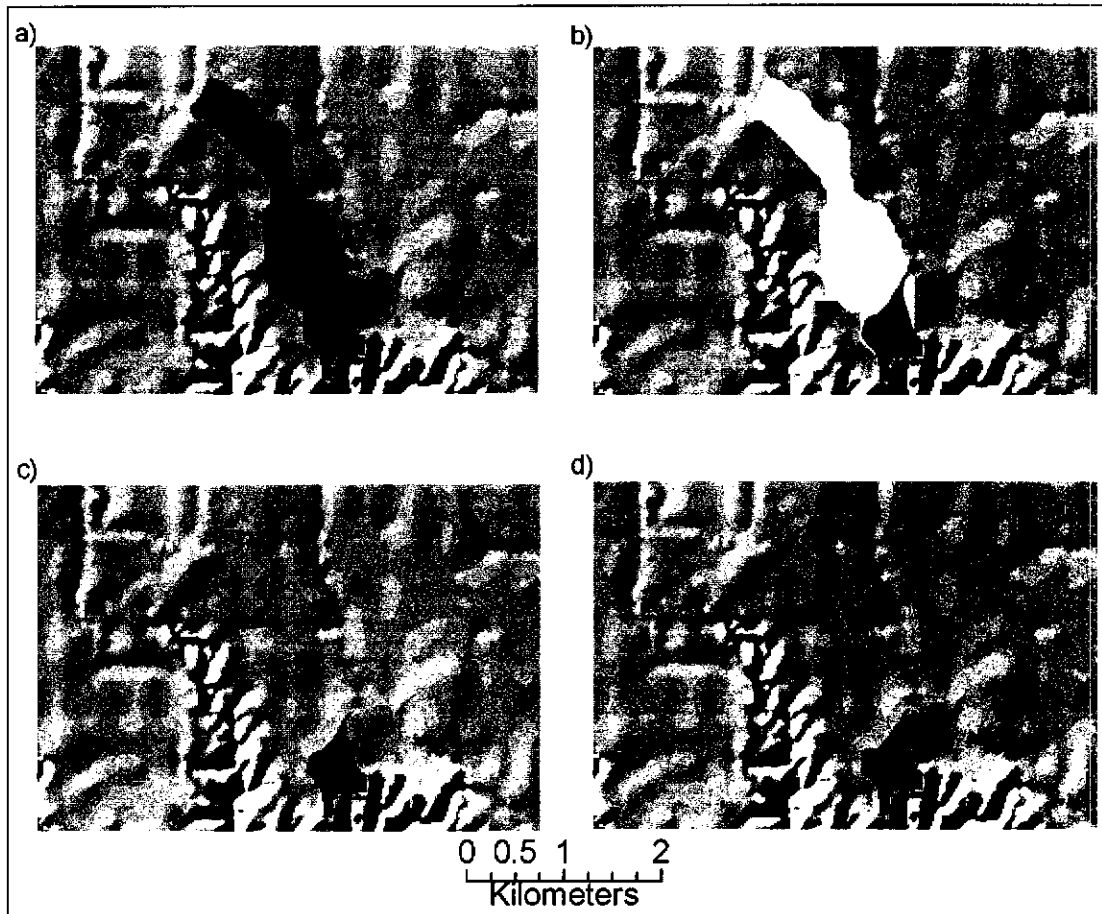
Figure 9 Discretized vs. divergent vs. dependence flow direction algorithm watershed boundary comparison

a) the multiple flow direction D-Infinity algorithm, b) the fuzzy logic dependence algorithm where yellow represents very low proportions of the grid cells contributing, orange represents grid cells contributing approximately half of their outflow, and red grid cells contributing a very large proportion of their outflow to the watershed outlet, c) a dependence membership value greater than or equal 0.5, d) the D8 flow direction algorithm.

41
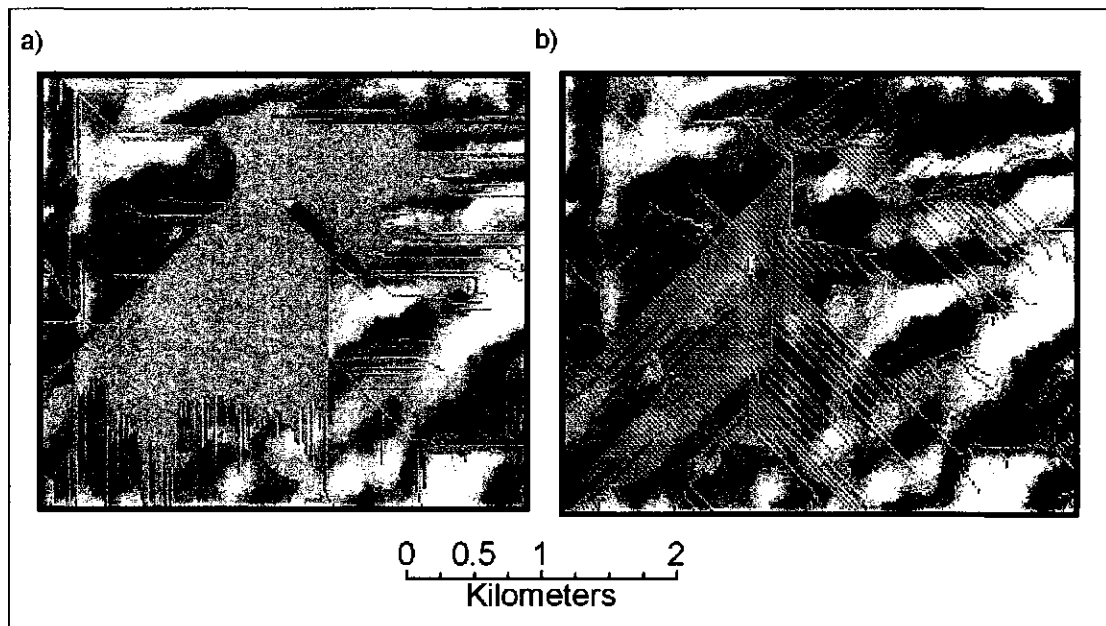
Figure 10 Drainage networks in flat areas

a) D8 flow direction algorithm, b) D8-TOPAZ flow direction algorithm.
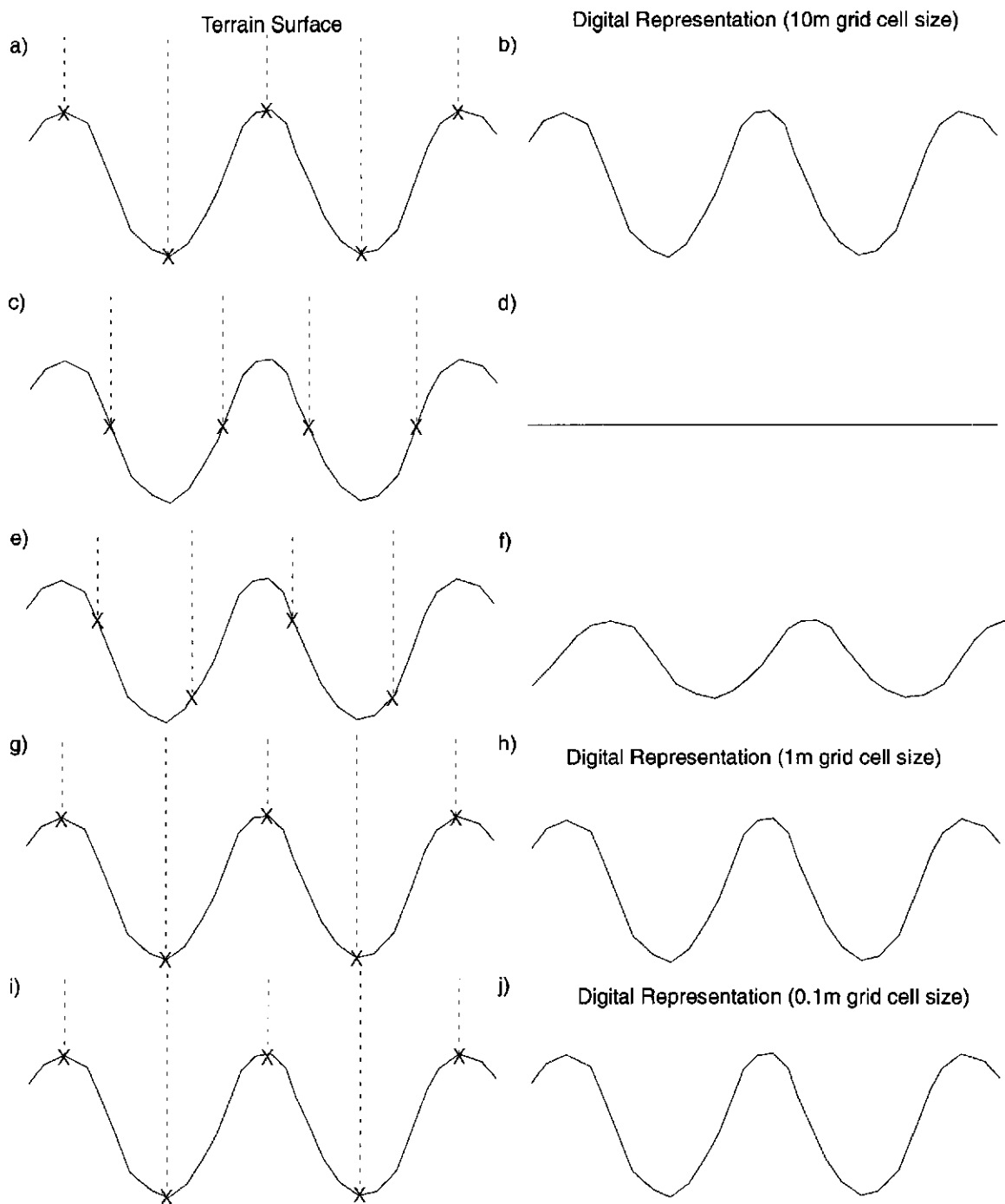
Figure 11 Influence of point-elevation properties and grid cell size on DEM accuracy

X indicates an point-elevation sample.
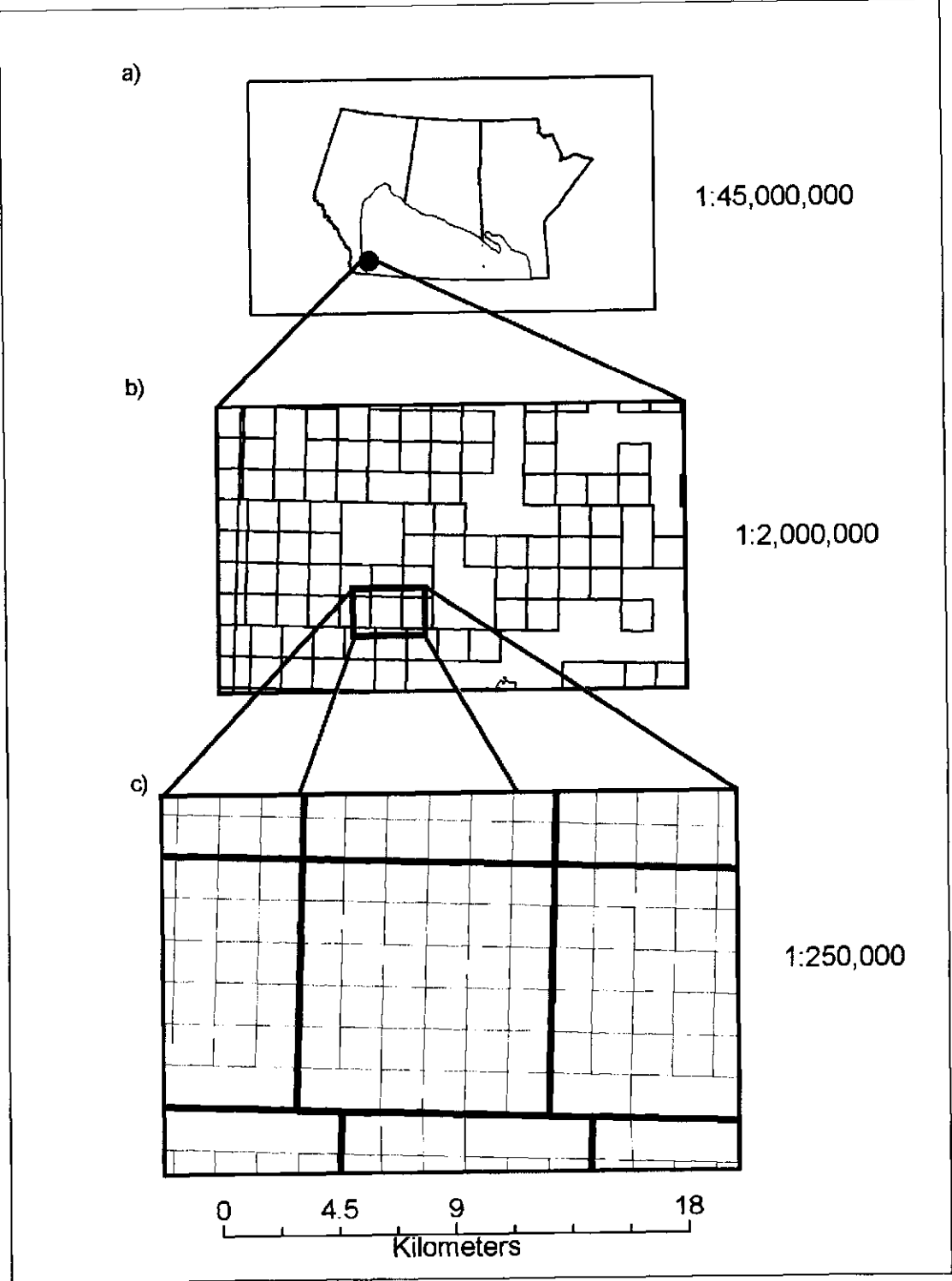
Figure 12 Spatial survey patterns in the Canadian grasslands

a) The extend of Canadian grasslands relative to the provinces Alberta, Saskatchewan, and Manitoba, as well as the study area near Lethbridge, Alberta. b) shows 6-mile by 6-mile (9.65-km by 9.65-km) township squares, and c) shows the grid of 36 sections that make up one township.

44
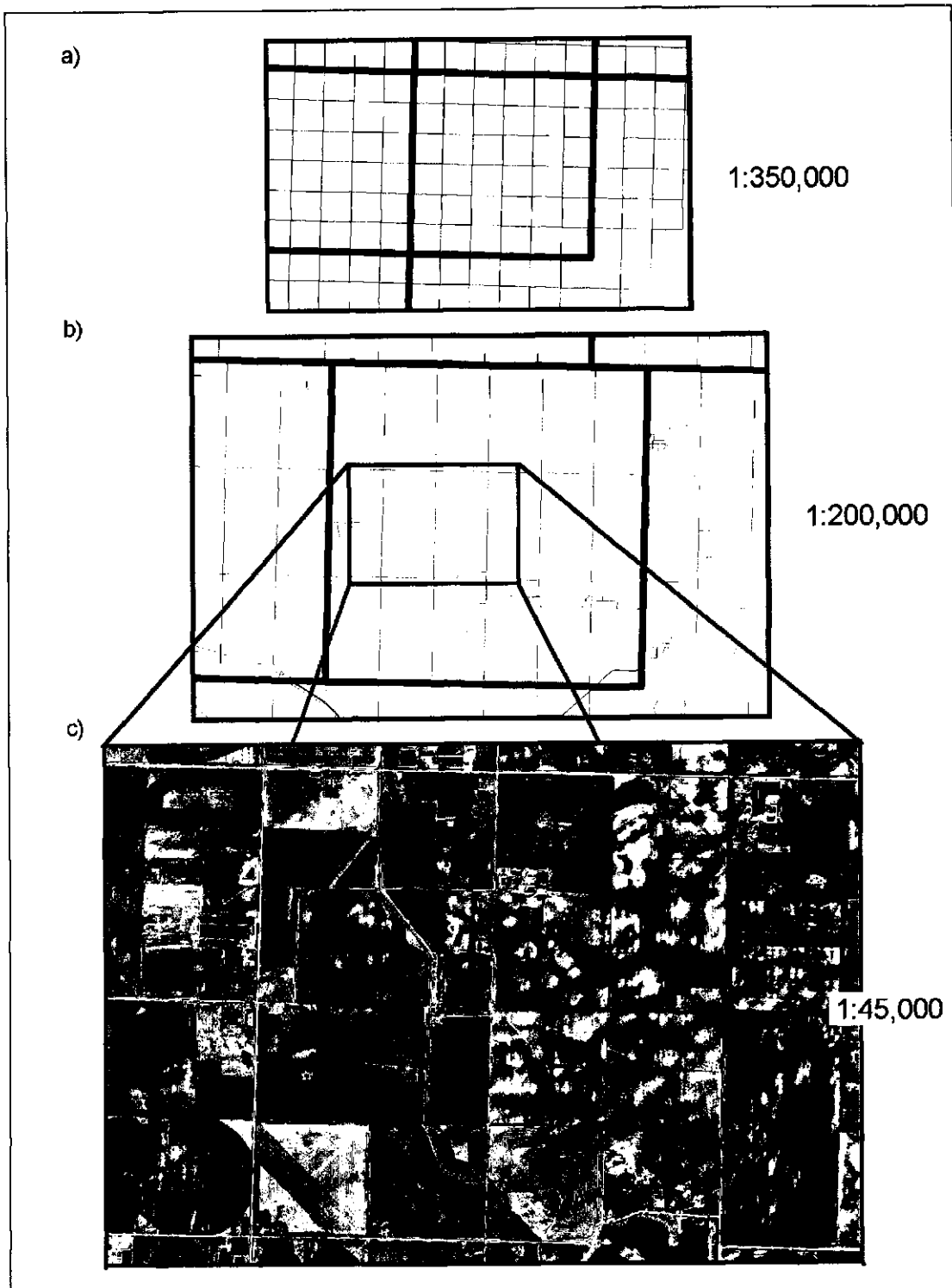
Figure 13 Rural road network in the Canadian grasslands

a) A township containing 36 sections in green, b) shows the rectangular road network that dissects the grasslands. Road segments are located every mile (1.6-km) in the west-east direction, and every 2 miles (3.2-km) in the north-south direction, c) shows how the system of roads has influenced the size and shape of individual farming plots.

45

Chapter 3

3 Flow Path Modelling Pre-assessment for Southern Alberta

3.1 Watershed Delineation Scale Assessment

Due to the inability of grid-based DEMs to represent the continuous nature of topography
and inadequate point-elevation data sets, information is inevitably lost during the DEM
creation process (Gao, 1998; Huang, 2000; Wise, 2000; Schneider, 2001; Quinn, 2002).
Therefore, even though small-scale terrain features are hydrologically significant they are
often not represented in DEMs. It was this characteristic of DEMs that Moore et al.
(1991), Grayson et al. (1993), and Band and Moore (1995) concluded causes
oversimplified drainage patterns when implementing grid-based models. As a result,
Schneider (2001) stated that it is crucial to clearly identify the properties that a DEM
must possess before a DEM-based model can be successfully implemented. The
consequence of DEM generalization is, therefore, a restriction on the scale of processes
that can be successfully modeled. Finke and Bierkens (2002) stated that model outputs
rarely match the scale required by decision makers. Because the outputs derived using
the model presented in this thesis are intended for analysis at the watershed scale, the
flow processes modeled must include the processes that affect watershed boundaries.
The question then becomes how to obtain results at the scale appropriate for analysis
(Finke and Bierkens, 2002). When confronted with the problem of identifying probable
source areas of water pollution in the Oldman River watershed, a qualitative assessment
was completed. The initial assessment was intended to answer the following questions:

- Which features in the landscape effect overland flow pathways?

46

- Which data are available to model flow pathways in the study area?

- Can a DEM created from the available elevation data set represent the

  hydrologically significant terrain features identified?

- What new procedures are required to account for hydrologically significant terrain

  features in a grid-based watershed model?

3.1.1 Which features in the landscape impact overland flow pathways?

Between the years of 1908 and 1998 Lethbridge, Alberta received an annual average of

264.6-mm of rainfall (Environment Canada, 1998). In June, 2002 over 140-mm of rain

fell in three consecutive days, effectively saturating the entire region with rainfall

(Gallant, 2002). In-field observations of runoff patterns during this period of excess

precipitation made it clear that roads, ditches, culverts, and irrigation canals significantly

influence overland flow pathways in southern Alberta. Because these features are

frequently misaligned with the naturally occurring topographic aspect, they enforce

anthropogenic drainage patterns (Figure 14). The flat nature of the topography in the

study area exacerbated the impact of the anthropogenic runoff misrouting, leading to

significant deviations from the drainage patterns that would have naturally predominated.

The spring flood also made it clear that irrigation canals increase the drainage density of

nearby streams by capturing runoff (Figure 15). Although natural depressions in the

landscape are relatively uncommon (O'Callaghan and Mark, 1984), potholes in recently

glaciated terrain, and depressions caused by the construction of roads are commonplace

(Band, 1986). During the spring flood these depression features accumulated runoff that

eventually infiltrated into the soil or evaporated into the atmosphere (Figure 16).

However, when culverts were located at road-induced depressions (or sinks), runoff

progressed towards irrigation canals and natural drainage networks (Figure 17).

Although the majority of research previously conducted on the hydrological effects of

roads was conducted in forested regions (e.g., Montgomery, 1994; Wemple, 1996; Jones

et al., 2000; Tague and Band, 2001; La Marche and Lettenmaier, 2001), these

observations indicate that the combination of roads, culverts, and irrigation canals

enforce similar hydrological impacts in the grasslands of southern Alberta, even though

no studies have addressed this issue in Alberta.

3.1.2 Which data are available to model flow pathways in the study area?

The point-elevation data set available to interpolate the DEM consisted of the province-

wide elevation data managed by AltaLIS (Calgary, Alberta), the agent for Spatial Data

Warehouse, which is a not-for-profit organization maintaining and promoting Alberta's

digital mapping. The elevation data were comprised of photogrammetricaly derived

elevation points regularly spaced at 100-m with additional spot points (e.g., road

intersections), and elevation points along landscape break-lines (e.g., coulee ravine

thalwegs and ridges). The AltaLIS provincial hydrography vector data was also available

that included major drainage courses. Vector (or line) coverages of the LNID canal

system, as well as digital orthophotos covering the entire irrigation district were available

from Kevin Haggert at the LNID. Dennis Sheppard of the Lethbridge Community

College provided DMTI Spatial's (Markham, Ontario) CanMap Streetfile Version 5.1.

48

The vector road coverage from DMTI Spatial included paved highways as well as gravel township and range roads.

3.1.3 Can a DEM created from the available elevation data set represent the hydrologically significant features identified?

An initial assessment of the density of the point-elevation data set was conducted by overlaying the data set with the orthophotos supplied by the LNID. A quick visual assessment confirmed that point samples were lacking along roads, ditches, and many irrigation canals (Figure 18). A DEM interpolated from the AltaLIS point-elevation data set would, therefore, be unable to represent these features. Field elevation surveys of 52 road cross-sections were completed and used to determine the typical road cross-sectional profiles within the study area (Appendix 9.1). Figure 19a is an example of a typical road cross-sectional profile obtained through surveying. In contrast, Figure 19b shows the digital representation of the same location derived from a 20-m DEM interpolated from the AltaLIS point-elevation data set. The graphs clearly indicate that the point-elevation-sampling interval is too coarse to represent the terrain complexity associated with roads and other hydrologically significant features that are sufficiently large to cause the re-routing of surface runoff. The deficiency of the AltaLIS point-elevation data set to represent roads, ditches, and canals would, therefore, lead to the generalized flow patterns that Moore et al. (1991), Grayson et al. (1993), and Band and Moore (1995) stated plague many hydrological models. Even though it was clear the information loss within the DEM was significant, an error assessment was conducted to determine the legitimacy of flow patterns derived using the conventional D8 flow direction algorithm. This

49

assessment confirmed that frequently the DEM-derived (D8) drainage patterns

inaccurately crossed linear terrain features such as roads and irrigation canals that were

deemed hydrologically significant (Figure 20). In Figure 20 the modeled flow paths

progress across the canal because the canal channel is not adequately represented in the

DEM.

3.1.4 What new procedures are required to account for hydrologically significant terrain features in a grid-based watershed model?

Based on the assessment of the requirements to accurately model the overland flow

processes in the Oldman River watershed it was determined that:

- Irrigation canals must be explicitly enforced in the flow direction matrix to ensure

  the simulated flow paths do not inaccurately proceed across them.

- Roads and ditches must be explicitly enforced into the flow direction matrix

  contingent upon the cross-sectional profile of the road.

- The split flow patterns that result from branching irrigation canals must be

  simulated and incorporated into the watershed delineation procedure.

- Culverts must be explicitly enforced in the model because they facilitate the

  progression of runoff across roads.

Similar to the approaches of Saunders (2000), Cerdan et al. (2001), Takken et al. (2001

[a, b, c]), and Souchere et al. (2003), a methodology was required to utilize the available

ancillary data to enhance the precision (or scale) of runoff flow paths below the scale

derived from conventional grid-based flow routing with the elevation data set from

AltaLIS. Following the June, 2002, flood it was hypothesized that accurately accounting

for the rural infrastructure in the landscape (viz. roads, ditches, culverts, and canals) would capture the processes that dominate flow pathways in the study area. Thus, the proposed methodology would enable the accurate delineation of the watersheds for each of the 30 water quality sampling locations as part of the Oldman River Basin Water Quality Initiative.

3.2 Research & Model Introduction

The methodologies for this thesis were automated into a stand-alone computer model written in Microsoft Visual Basic. The computer model, called RIDEM (Rural Infrastructure Digital Elevation Model) requires input files in ArcView / ArcInfo gridascii format (Appendix 9.2). Appendix 9.3 contains several snippets of code that were written and included in RIDEM. RIDEM is a tool that manipulates grid flow direction matrices to account for small-scale anthropogenic terrain features (viz. roads, ditches, culverts, siphons/flumes, and irrigation canals) that are not typically represented in regional DEMs. By implementing the algorithms included in RIDEM the scale of runoff flow paths modeled is reduced below the scale produced using conventional grid-based processes. Therefore, RIDEM has the potential to improve the predictive capability of previous models used to study the impact of land use on water quality (e.g., Cooke et al., 2002; Gannon et al., 2002; Hyland et al., 2003; Johnson et al., 2003).

RIDEM is comprised of two algorithms. The first algorithm called the road enforcement algorithm (REA) manipulates flow direction matrices by incorporating known road cross-sectional profiles and culvert locations. The methodology of the REA model, along with

51

the results from a test watershed are presented as submitted to the Journal of Spatial

Hydrology (JOSH) in chapter four of this thesis entitled "Improving Overland Flow

Routing by Incorporating Ancillary Road Data into Digital Elevation Models". The

second component of the RIDEM model is the canal enforcement algorithm (CEA). The

CEA manipulates flow direction matrices derived from the REA model, or any flow

direction matrix in ESRI D8 format, by enforcing known flow directions within irrigation

distribution systems. The CEA also simulates cross-flow drainage patterns at locations

containing siphon / flume structures. The result of applying the CEA algorithm is an

enforced flow direction matrix and gross watershed boundary. The CEA is presented as

submitted to the journal Agricultural Water Management, in chapter five of this thesis

entitled "Overland Flow Path Modelling with Digital Elevation Models in Irrigated

Landscapes".

The sixth chapter of this thesis entitled "RIDEM: a Grid-Based Model to Downscale

Flow Paths in Landscapes with Rural Infrastructure" presents the results from combining

the REA and CEA for three water-quality monitoring stations, including: Piyami Drain,

Sientza Drain and, Battersea Drain. This portion of the thesis was submitted to the

journal Water Resources Research for publication, and is also currently under review.

a)
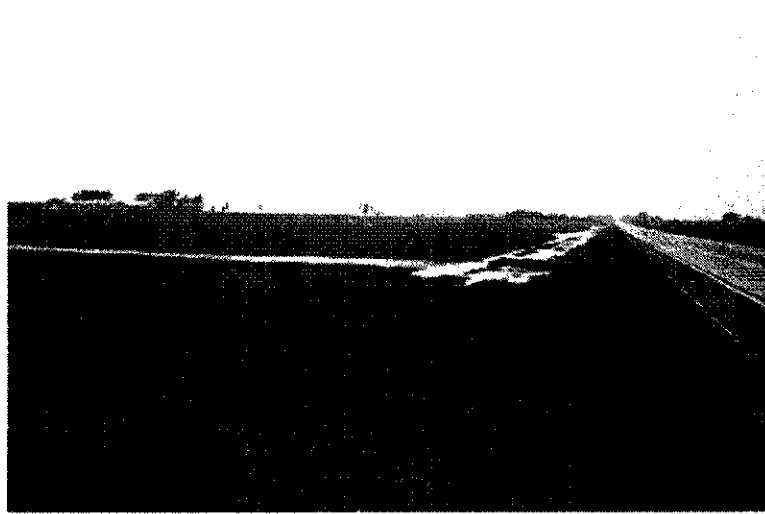
b)

Figure 14 Road induced runoff flow path modification

a) Runoff flowing along the topographic slope from the left side of the picture towards the road on the right is deflected 90 degrees by a raised road and continues to flow towards the top of the picture.

b) A secondary highway (right side of image) conveys runoff originating in the adjacent field towards the top of the image. A road-crossing culvert located under the local road in the foreground of the image facilitates the progression of runoff.

a)

b)
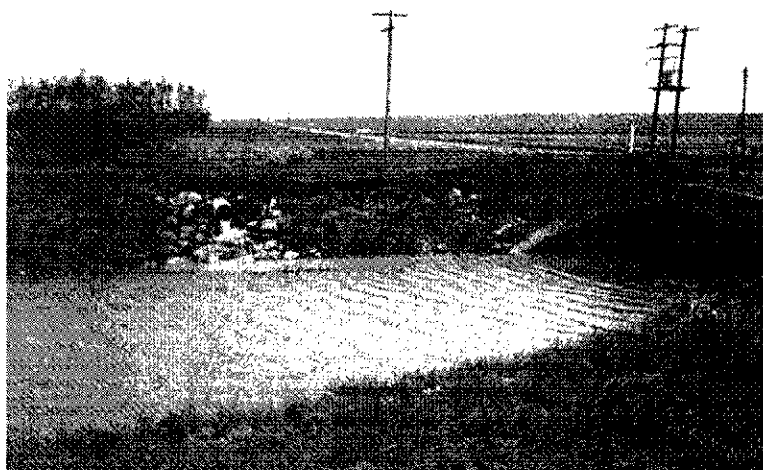
Figure 15 Drainage network extension via irrigation canals

a) Runoff concentrated in a ditch along a highway enters an irrigation canal through a culvert.

b) Runoff originating in a fallow field (image background) enters an irrigation canal through a drainage culvert.

a)

b)

Figure 16 Road induced runoff accumulation

a) Runoff flows towards a very large pool next to a road with a raised profile. Because a drainage culvert is not installed at this location runoff accumulates, and either infiltrates into the soil or evaporates into the atmosphere.

b) A body of water accumulates in a road-induced depression lacking a drainage culvert.

a)
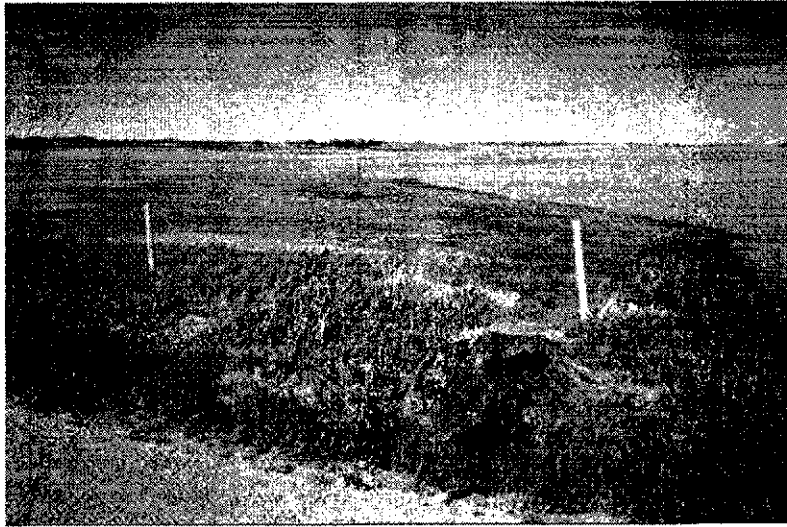
b)

Figure 17 Hydrological linkages via culverts

a) A culvert installed under this road enables runoff to progress across the road and into the adjacent field (Image background).

b) Concentrated runoff flows underneath a local road intersection via a road-crossing culvert (foreground) and towards the outlet of Szietna several km downslope of this location.
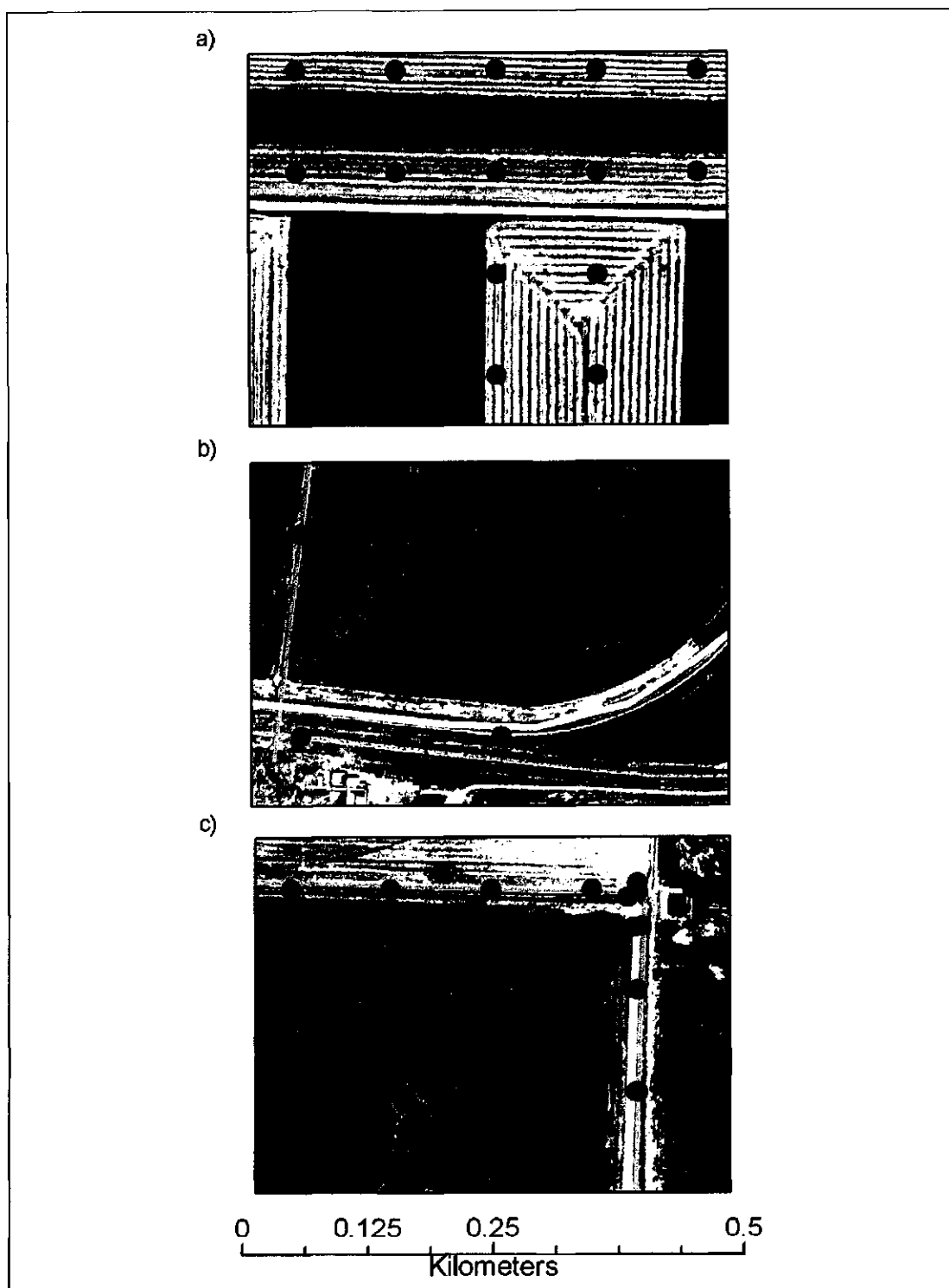
Figure 18 Point distribution of AltaLIS point-elevation data.

Sampled elevation locations are shown in red, irrigation canals in blue, and roads in yellow. a) a local raised road, b) an open channel irrigation canal as well as a secondary highway, and c) an open channel irrigation canal.

57

a)

Surveyed Road Cross Section

b)

DEM Road Representation
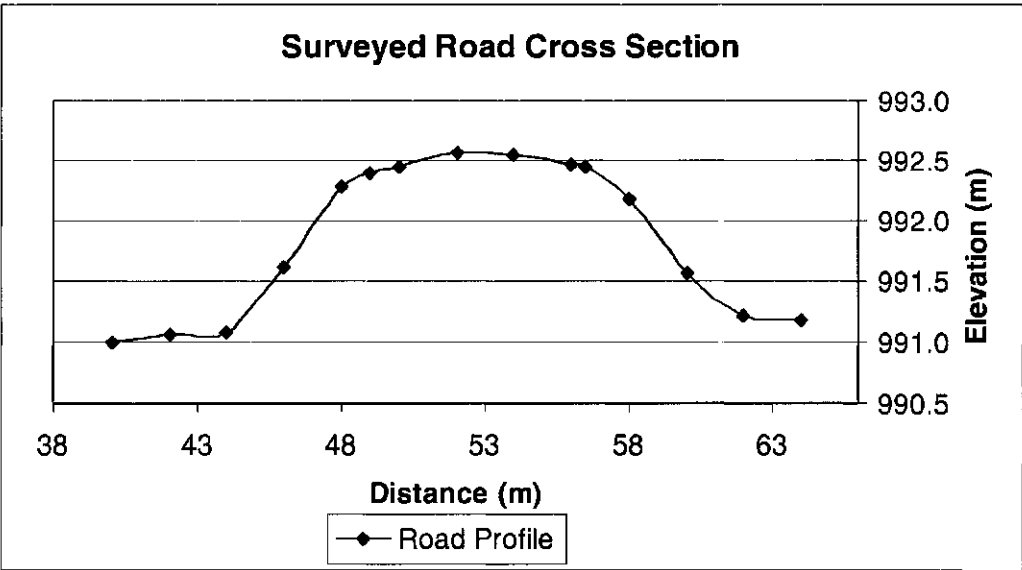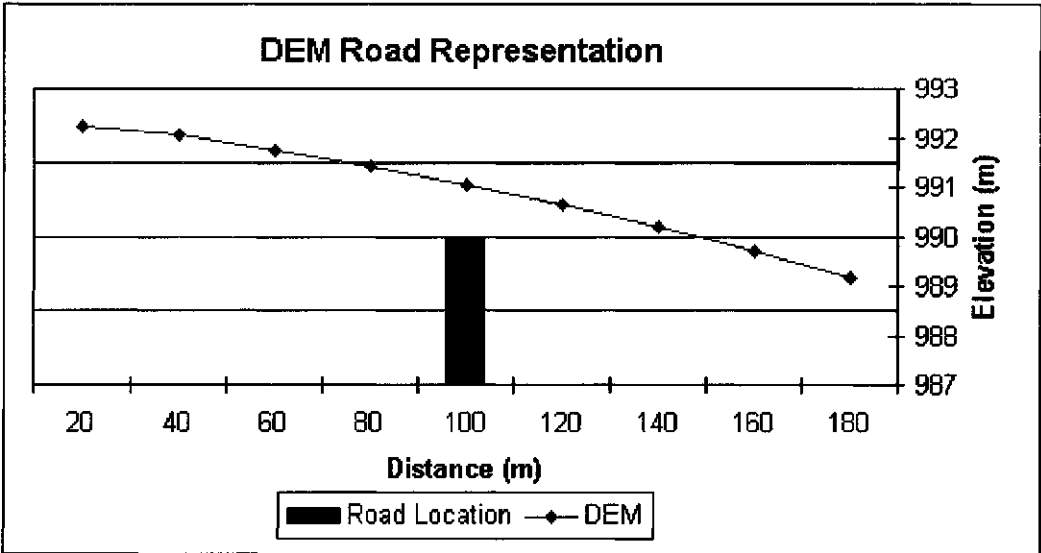
Figure 19 Road cross-sectional profiles

a) surveyed road cross-sectional profile determined using a theodolite, b) road cross-sectional profile
extracted from a 20-m DEM interpolated from AltaLIS point-elevation data.

58
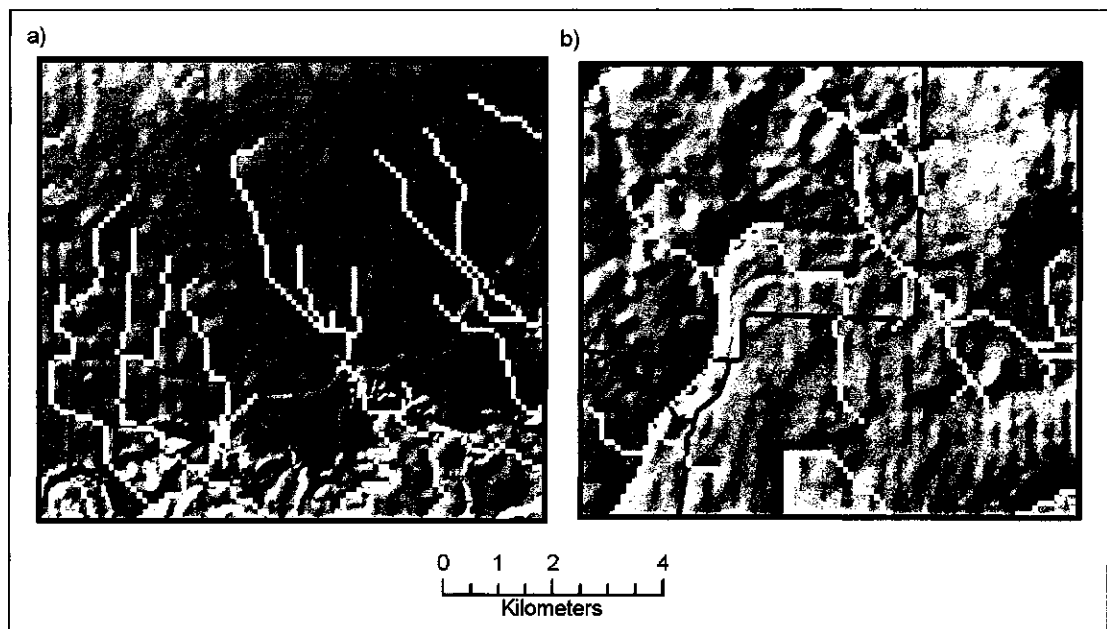
Figure 20 Overland flow networks derived using the conventional D8 flow direction algorithm

The DEM-derived flow networks shown in a) and b) erroneously progress across several irrigation canals segments.

Chapter 4

4 Improving Overland Flow Routing by Incorporating Ancillary Road Data into Digital Elevation Models

4.1 Introduction

Digital elevation models (DEM) are routinely used for hydrological applications because

overland flow routing is controlled by topography (Moore et al., 1991). DEMs are used

to delineate watersheds (Jensen and Domingue, 1988), analyze channel networks (Quinn

and Beven, 1991; Tarboton, 1991), predict soil water content (Quinn and Beven, 1993;

Quinn et al., 1995), predict erosion potential (Ludwig et al., 1996; De Roo and Jetten,

1999; Taken et al., 2001b, c), model non-point-source pollution (Cluis, et al., 1996), and

carry out flood and hydrograph analysis (Oliveria and Maidment, 1999). However,

Moore et al. (1991) also stated that the deficiency of many hydrological and water quality

models is their inability to account for the effects of terrain on flow processes. The

results from hydrological models are, therefore, often grossly simplified and unrealistic.

Linear landscape features can significantly affect the hydrological and geomorphological

processes within a watershed (See section 2.4.1 Anthropogenic Terrain Features).

However, hydrological models often do not account for the limitations of DEMs to

accurately represent the landscape (See section 2.4.2 Scaling Grid-Based Drainage

Patterns with Ancillary Data). This paper proposes a methodology to utilize ancillary

road, ditch, and culvert data to account for linear landscape features in hydrological

models. The need to develop an algorithm to incorporate ancillary road, ditch, and culvert data into existing grid-based flow direction algorithms stemmed from:

- the observation that the location of roads frequently cannot be ascertained by examining DEM-derived channel networks,

- the effects linear landscape features impose on several biophysical processes within watersheds,

- the potential severity of consequences of inaccurate watershed delineations, for example, the movement of "contaminated" water across watershed boundaries (PFRA, 1983).

If cross-sectional attributes of roads were known, it may seem as though manipulating pre-existing DEMs accordingly would be an effective method to enforce the effects of artificial linear features on flow direction matrices. For instance, grid cells representing roads could be raised, and grid cells representing ditches could be lowered. However, conventional grid-based routing procedures (e.g., D8) require the removal of closed depressions with a flooding algorithm (Martz and Garbrecht, 1998; Rieger, 1998), therefore, alterations made to the DEM prior to "filling" would be nullified. In fact, altering the DEM in this way would exacerbate the extent of flat areas (i.e., grid cells lacking a neighbour at a lesser elevation). Because flow directions within flat areas must be defined arbitrarily, the accurate modelling of runoff in these areas is impossible (Turcotte et al., 2001). Martz and Garbrecht (1998) suggested this as the single greatest weakness of conventional grid-based routing algorithms, and developed a flat area algorithm that produces more realistic results than the conventional D8 algorithm,

although it remains dependent on arbitrary decision rules (Turcotte et al., 2001). The procedure described in the present study was developed to utilize DEM elevation values prior to the filling process. Although several authors have stated that depressions are spurious features created during the interpolation process of DEMs (e.g., Martz and Garbrecht, 1998; Rieger, 1998), depressions are actually common features in glaciated terrain (Mark, 1988). Additionally, the construction of roads has also created many artificial landscape depressions. The assignment of flow directions prior to filling is, therefore, an effective way to identify the lowest points, or thalwegs in the landscape. The procedure described herein simulates raising road elevations and lowering ditch elevations within the DEM to produce a manipulated flow direction matrix. With approximately 2.5 million km^2 of flat prairie grassland in North America (Figure 30 and 31) the REA is applicable in a significant portion of North America and many other parts of the world.

4.2 Methodology

4.2.1 The Road Enforcement Algorithm

The algorithm, a stand-alone program written in Microsoft Visual Basic, is referred to as the road enforcement algorithm (REA). The REA defines a flow direction matrix for the grid cells adjacent to roads and imposes this matrix on the topographically derived (DEM) flow direction matrix. Thus, a single flow direction matrix is produced that accounts for roads, ditches, and culverts that can be used in any grid-based hydrological model.

4.2.2 Conceptual Model of Roads, Ditches, and Culverts

The extent to which hillslopes are linked to stream channels depends on the runoff

pathway to the stream (Wemple et al., 1996). Ludwig et al. (1996) subdivided this

relationship into runoff contributing areas (viz. fields) and the "runoff collector network".

For this study, the runoff collector network is composed of linear depression features

(viz. ditches) and areas adjacent and upslope to raised roads. The runoff collector

network can influence overland flow directions in three ways:

- elevated roads can form overland flow barriers and flow path sinks, thereby re-

  routing flow along their orientation on the upslope side of the road (Figure 21).

- roadside ditches can create flow path corridors and flow path sinks (Figure 22).

- roads with flat cross-sectional profiles do not influence overland flow directions and

  are, therefore, excluded from the runoff collector network (Figure 23).

4.2.3 Data Requirements of the Road Enforcement Algorithm

The REA requires input files in ESRI ArcView / ArcInfo grid ascii format (Appendix

9.2). The model requires a minimum of four input data layers including:

- a DEM (floating point),

- a topographically defined flow direction matrix,

- a topographically defined flow accumulation matrix,

- a road layer, and

- culvert locations (optional).

The REA model was created keeping in mind the restriction of data availability,

therefore, the model contains three levels that enable the user to implement progressively

more detailed road and ditch information.

4.2.3.1 REA Level I

The first level of the REA model is a single template model. Within the single template

model a common cross-sectional template is assigned to all roads. This model requires

the least amount of knowledge regarding the location and attributes of roads and ditches

within an area. Road construction cross-sectional templates, as defined by government

agencies (i.e., Alberta Department of Transportation), could be used to guide these

assumptions. Within the conceptual view of roads described earlier, one of two cross-

sectional road templates must be assigned to each road to enforce flow directions along

its orientation, categorized as follows:

- a raised road template without adjacent ditches (i.e., an influence on the flow

  direction on the upslope side of the road only), or

- roads with adjacent ditches (i.e., an influence on the flow direction on both sides of

  the road).

If the road with adjacent ditches template is selected, the user must provide two values.

The first value, referred to as the ditch-to-road height, defines the height of the road

relative to the deepest part of the ditch (Figure 24). The second value, referred to as the

ditch-to-field height, defines the depth of the ditch relative to the adjacent field (Figure

24). If the raised road template is selected, the ditch-to-road height is required, and the

ditch-to-field height is effectively set to zero.

4.2.3.2 REA Level II

The second level of the REA model is known as the variable template model. Within this model, segments of roads are classified into each cross-sectional category separately. The variable template model requires separate road input files for both the raised roads and roads with adjacent ditches categories. The model assumes a common cross-sectional template within each classification category. Thus, a single ditch-to-road height is required for each category. If the category road with ditches is included, the ditch-to-field height is also required.

4.2.3.3 REA Level III

The third level of the REA model is called the custom template model. This model was designed to remove the inherent road profile shape restrictions of the first and second level models. In contrast to the first and second level models that accept a single ditch-to-road and ditch-to-field height for each road category, the custom template model accepts separate data layers for the ditch-to-road and ditch-to-field heights for each grid point along the runoff collector network. The custom template model can, therefore, be used to assign spatially variable road cross-sectional templates within each classification category. Thus, the custom template model permits detailed road cross-sectional profile data to be incorporated into the model from GPS or ground survey data. The third level provides two major benefits, including:

• the ability to represent road heights and ditch depths as continuous surfaces, and

• the modeled cross-sectional profiles on the left and right side of the road are

independent.

4.2.4 Calculation of the Runoff Collector Network Flow Directions

Although slight variations of the REA exist, depending on the model level selected, the

logic of each procedure is identical.

Step 1: Derive topographic watershed parameters

The first step of the algorithm requires the creation of the topographical flow direction

and flow accumulation matrices. Deriving the flow direction and flow accumulation

matrices can be accomplished in most GIS software packages that support raster analysis.

Step 2: Identification of grid cells to enforce (the runoff collector network)

The algorithm first extracts all grid cells adjacent to the specified road locations. Based

on the cross-sectional attributes defined by the input parameters, the algorithm then

defines the runoff collector network as the grid cells whose flow direction would be

influenced by a linear landscape feature. This includes all ditch locations, and grid cells

that flow across elevated roads within the topographic flow direction matrix. Depending

upon whether culvert data are included, the algorithm then adds the grid cells

representing culvert locations to the runoff collector network.

Step 3: Defining convergence grid cells

Elevation values from the input DEM are assigned to the runoff collector mask defined in

the previous step. Flow directions are then calculated using the conventional D8

approach (O'Callaghan and Mark, 1984). Grid cells with converging flow patterns occur

in the thalwegs (i.e., the lowest points in the landscape) of the runoff collector network,

and are flagged as potential breach locations. These locations correspond to the grid cells

where runoff may exit the runoff collector network, either over a road or into a field.

Convergence grid cells with a single inflow and outflow are considered spurious

depressions, and are assigned a flow direction into their outflow grid cell (Figure 25).

Step 4: Assign flow directions to convergence grid cells

Convergence grid cells, analogous to the TCRP model incorporated in the soil erosion

model LISEM (Takken et al., 2001b), are then assigned the flow direction from the

topographically defined flow direction matrix. A continuous runoff collector network is

then created by assigning the topographically defined flow directions to the grid cells

adjacent to the road locations that are not influenced by a linear landscape feature. Next,

the flow direction matrix of the runoff collector network is superimposed on the DEM

derived flow direction matrix. To ensure loops are not introduced to the flow direction

matrix, the grid cells within the runoff collector network that are routed to each

convergence site are identified. If the combined flow direction matrix loops back to the

current convergence segment (the portion of the runoff collector network draining to the

current breach grid cell), the algorithm assigns a flow direction to the grid cell on the

opposite side of the runoff collector network. If this flow direction also creates a loop,

67

the grid cell is flagged and the breach point is moved to the location within the convergence segment with the highest topographically defined flow accumulation value. At this stage the requirement to move convergence locations occurs exclusively in areas that were closed depressions in the DEM, and were therefore filled during the creation of the DEM derived flow direction matrix. Following the completion of this step, a continuous flow direction matrix is produced with the runoff collector network enforced and the identification of all convergence locations within the collector network.

Step 5: Reroute flow within the runoff collector network

In step four each convergence grid cell was assigned a flow direction to breach (or exit) the runoff collector network. Runoff can exit the runoff collector network either across a road, or into an adjacent field. The depth of the runoff collector network relative to the adjacent road (or field) determines whether runoff would pool until a sufficient depth of water was attained to breach the runoff collector network, or simply overtop a ridge at a point within the runoff collector network (Figures 26a, b). For example, consider the two following scenarios of a road breach location that was assigned a ditch-to-road height of 1-m. If the elevation of the potential breach site was 100-m and it had two ridges within the runoff collector network at an elevation of 105-m and 110-m respectively, runoff would accumulate at the breach location until the runoff pool was 1-m deep. At that point runoff would breach the road (Figure 26a). However, if the elevation of the potential breach site was 100-m and it had two ridges within the runoff collector network at 100.5-m and 110-m respectively, runoff would accumulate in the runoff collector

68

network until the runoff pool was 0.5-m deep. Thus, runoff would continue to flow within the runoff collector network without breaching the road (Figure 26b).

Flow within the runoff collector network cascades down-slope because the rerouting algorithm proceeds from the breach grid cell with the highest elevation to the breach grid cell with the lowest elevation. For each potential breach grid cell the convergence segment (the portion of the runoff collector network draining to each breach site) is once again identified. The algorithm retrieves the elevation and row and column coordinates of each ridge grid cell. Additionally, the grid cells adjacent to each ridge grid cell (i.e., within one row and column) are recorded. If the grid cell is within the runoff collector network and has a higher elevation than the current ridge, the algorithm flags the elevation and row and column coordinates of this grid cell. The neighbouring grid cell with the lowest elevation, but higher than the adjacent ridge within the convergence segment, becomes the appropriate ridge through which to reroute flow. However, if runoff has already been rerouted into the current convergence segment through the potential ridge, the grid cell is excluded as a potential ridge. Thus, flow is not rerouted over a potential ridge more than once. The elevations of each ridge in the convergence segment are subtracted from the elevation of the breach grid cell. If the difference is less than the height of water required to pool, and subsequently breach the runoff collector network, its location and elevation are flagged. After the lowest ridge within the runoff collector network has been identified, the entire convergence segment is rerouted through the ridge grid cell. Therefore, runoff continues to cascade downslope until a significantly

69

deep convergence grid cell is located to facilitate breaching the runoff collector network (Figure 27).

4.3 Results and Discussion

The REA was tested in the south fork of the Piyami Drain watershed in southern Alberta, Canada. The south fork of Piyami Creek drains approximately 110 km^2 to the Oldman River. The topography is comprised of gently rolling hills near Piyami Creek, as well as extensive flat areas around the outer edges of the watershed. The total relief of the watershed is 204 meters, with an average basin slope of 2.5%. The watershed contains approximately 202-km of gravel and paved roads. The results of implementing the REA are first presented at the field scale, followed by the results for the entire watershed. Field verification of the model was based on the following observations:

- culvert locations,

- road side cattails (*Typha latifolia*),

- runoff ponding,

- dead vegetation following a rare prolonged spring precipitation event,

- prominent topographic depressions, or

- an irrigation canal.

The DEM for the Piyami Drain watershed was interpolated from point-elevation data using the TOPOGRID command within ArcInfo (Hutchinson, 1989). The elevation data were provided by AltaLIS (Calgary, Alberta), the agent for Spatial Data Warehouse (See

section 3.1.3 Which data are available to model flow pathways in the study area?).

Following the work of Quinn et al. (1991) and Kienzle (2004) the DEM was interpolated

to a 10-m grid cell size. The 10-m grid cell size also corresponded to the average road

width in the study area. Matching the grid cell size with the average road width

maximizes the locational accuracy of the runoff patterns on either side of the roads. The

resulting grid cell values were kept as floating point numbers to avoid the flow direction

problems associated with integer grids (Freeman, 1991; Garbrecht and Martz, 1997;

Rieger, 1998; Turcotte et al., 2001).

4.3.1 Field Scale Results

The variable template model (Level II) was implemented for the field scale application.

The extent of the field scale study consisted of an area enclosed by two adjacent township

roads and three adjacent range roads (Figure 28a). Thus, the study area dimensions were

approximately 3.2-km by 3.2-km (2 by 2-miles), with a total road length of

approximately 16-km (10-miles). Approximately 4.8-km of road (3-miles) were assigned

to each of the three classification categories (viz. flat cross-sectional profile, raised road,

road with adjacent ditches) (Figure 28a). A ditch-to-road height of 1-m was assigned to

the raised road template. The roads with adjacent ditches were assigned a ditch-to-field

height of 0.5-m and a ditch-to-road height of 1.5-m.

The drainage pattern derived using the conventional DEM-derived approach (D8) does

not show any indication of the presence of a runoff collector network adjacent to the road

locations (Figure 28b). In contrast, Figure 28c shows the modified drainage pattern

71

created with the variable template model. The runoff collector network is easily

distinguishable on both sides of the road when the road is classified as road with ditches

(Figure 28c). The presence of a runoff collector network is also clearly visible on the

upslope side of the road classified into the raised road template. Because the grid cells

adjacent to the road with a flat cross-sectional profile were not identified as being

influenced by the adjacent road, the modified drainage pattern is identical to the DEM

derived pattern. When the modified drainage pattern is examined in its entirety, the field

scale test application effectively shows that roads and ditches significantly modify

drainage patterns at the field scale. Therefore, one can infer that biophysical processes

modeled within the watershed, such as erosion patterns, would also differ due to the

effect of roads on overland flow directions (e.g., Desmet and Govers, 1996; Ludwig et

al., 1995; Desmet et al., 1999; De Roo and Jetten, 1999; Cerdan et al., 2001; Takken et

al., 2001 [b]; Souchere et al., 2003).

To demonstrate the implications of DEMs failing to represent roads and ditches, the REA

was also implemented using the single template model (Level I). A raised road cross-

sectional profile was assigned to the previously described road network with a ditch-to-

road height of 1-m. Figure 29a shows the location of all grid cells that the DEM derived

flow direction matrix predicted runoff would cross, or breach a road. In contrast, Figure

29b shows the locations of all predicted road breach locations following rerouting with

the REA. The total length of road breaches predicted by the topographical (DEM)

derived flow direction matrix corresponded to 79% of the total road length (1,620 breach

grid cells out of 2,043 road grid cells). Following re-routing with the REA the number of

road breach locations reduced to 18 (<1% of the total road length). Because significant overland flow could theoretically cross the road at each predicted road breach location, these locations are likely to correspond to either culvert locations or show some indication of historic runoff ponding (viz. cattail growth, dead vegetation). A field investigation revealed 14 of the 18 predicted breach locations contained culverts (78%). One of the 14 confirmed culvert locations was located approximately 75-m from the predicted breach location within a relatively flat area. Of the 4 locations without culverts, one contained standing water, and a second corresponded to an area of dead vegetation along the edge of a cultivated field that was flooded during a rare spring precipitation event. The ditch-to-road height at one of the remaining three locations was significantly higher than 1-m. Therefore, a larger ditch-to-road height would have been more appropriate and may have eliminated this breach location. The field investigation also revealed that two additional road crossing culverts were located in the study area, but were not predicted by the REA. Although a single road cross-sectional template for the approximately 16.1-km (10-miles) of roads is a gross generalization, the modified flow direction matrix seems to be more realistic than the flow direction matrix derived from the DEM alone.

4.3.2 Watershed Scale Results

The drainage patterns were modified for the entire south fork of Piyami Drain using the variable template model (Level II). Through a field survey each road segment in the watershed was classified into one of the three categories, including: flat cross-sectional

73

profiles, raised roads, roads with adjacent ditches (Figure 30). To gain a better

understanding of the typical road cross-sectional profiles within Piyami Drain, 10 road

cross-sections were initially surveyed with a theodolite (Table 1). The surveyed cross-

section locations were selected to include the range of road cross-sectional profiles in the

watershed. The ditch-to-road and ditch-to-field heights were set from a subjective

analysis of the roads within the watershed and taking into consideration the surveyed

cross-sections. A ditch-to-road height of 1-m was implemented for the raised road

template. For the roads with adjacent ditches template a ditch-to-road height of 1.5-m

and a ditch-to-field height of 0.5-m was used.

Table 1 Surveyed ditch-to-field and ditch-to-road heights within Piyami Drain

Ditch to Field Height (meters)	Ditch to Road Height (meters)
1.600	1.615
0.440	1.810
--*	1.240
0.670	2.050
0.460	0.870
0.175	0.635
--*	0.910
0.020	0.590
--*	1.070
0.675	1.730
--*	0.440
--*	0.680
0.160	0.800
0.120	1.120
0.650	1.290
0.460	1.090
--*	1.490
--*	1.340
0.165	0.555
--*	0.190
--*	1.615
Average = 0.47	Average = 1.08
Standard Deviation = 0.40	Standard Deviation = 0.50

* The ditch-to-field height is not reported because there was not a ditch as these locations, the field may
have been either at the same or a greater elevation than the location next to the road.

Figure 31a shows the watershed delineated using the conventional D8 flow direction

algorithm (108 km^2) and the watershed delineated after accounting for roads, ditches, and

culverts with the REA (114 km^2). The watershed boundary was modified in 14 separate

locations, however, 93% of the area discrepancy was located in two regions. The

difference between the two watershed delineations was quantified using a statistic we

refer to as the percent agreement according to Equation 2.

$$XPA = \frac{WB}{WD8 + WREA + WB} \times 100\% \qquad \text{(Equation 2)}$$

Where:
XPA   = watershed % agreement
WB   = area delineated by both the D8 and the REA algorithms
WD8   = area delineated by the D8 algorithm only
WREA   = area delineated by both the REA algorithm only

The percent agreement statistic is meaningful because regular area comparisons do not

take into consideration the spatial agreement of two regions, whereas the percent

agreement statistic does. The percent agreement between the Piyami Drain watershed

derived with the D8 flow direction matrix and the watershed derived from the flow

direction matrix following the implementation of the road enforcement algorithm was

94%.

Whereas the DEM derived flow direction matrix predicted 152.19-km of road breaches,

the road enforcement algorithm predicted 4.81-km (number of grid cells crossing road

multiplied by the grid cell size of 10 m). Because a 3.2-km road segment was classified

as flat, the breach points along this road were not included in the analysis results.

Subsequently, the DEM derived flow direction matrix predicted 149.64-km of road

breaches, corresponding to 14, 964 locations (74% of the entire classified road length).

75

In contrast, the REA predicted 2.16-km of road breaches, corresponding to 216 separate locations (1% of the entire classified road length). Because predicted breach locations indicate where overland flow would cross roads, these locations are likely to correspond to road crossing culvert locations. However, the installation of a culvert is conditional upon the local landscape actually producing runoff (Alberta Department of Transportation, 1996). Of the 216 predicted road breach locations, a field survey confirmed 90 (42%) of the predicted culvert locations. Of the remaining 128 predicted breach locations 65 were either flooded during a very significant spring rainfall, currently contained standing water, or were prominent topographic depressions. Therefore, 155 (72%) of the predicted road breach locations either contained a culvert or showed direct evidence that confirmed the accuracy of the model. Although 50 (23%) locations did not contain a culvert nor show direct evidence of overland flow convergence during the field investigation, their appropriateness as road breach locations is neither confirmed nor denied because the local landscape hydrological properties may not have necessitated the installation of a culvert. However, 11 (5%) of the predicted breach locations were considered erroneous, which is likely due to inaccuracies of the DEM.

Culverts located within the runoff collector network facilitate the progression of runoff towards the watershed outlet. In contrast, breach locations without culverts correspond to depressions in the runoff collector network and/or road barriers along landscape thalwegs where runoff accumulates and either evaporates or infiltrates. Thus, the absence of a culvert effectively isolates the areas upstream of road breach locations from the watershed outlet. We argue that studies concerned solely with runoff parameters

76

measured at the outlet (i.e., water quality, stream flow, sediment concentrations) could

benefit from eliminating the hydrologically disconnected areas from the watershed.

Further investigations could focus on the areas that are linked to the outlet by overland

flow. After the hydrologically disconnected areas were excluded from the Piyami Drain

watershed the predefined area contributing water, sediment, and contaminants decreased

from 114 km^2 to 61 km^2 (Figure 31b). Figure 31b also shows that runoff collector

networks create artificial dead drainages, creating a fragmented hydrolocially connected

watershed. These results support the conclusions of Wemple (1996), Dijck (2000),

Tague and Band (2001), and Jones et al. (2001), that runoff collector networks not only

influence overland flow directions, but can also increase the runoff efficiency in some

areas, while reducing or effectively eliminating it in others.

4.4.0 Conclusions

Roads, ditches, and culverts are hydrologically significant landscape features that are not

frequently represented in DEMs, necessitating the use of ancillary information to account

for their effects when conducting distributed hydrological modelling. The road

enforcement algorithm (REA) presented in this paper manipulates flow direction matrices

alongside roads. The algorithm converges flow within the "runoff collector network",

thereby predicting locations where runoff exits runoff collector networks into fields and

across roads. Because culverts are installed to facilitate the adequate drainage of roads

and field runoff, many of the predicted road crossing locations corresponded to culvert

locations (42%). However, ditches and elevated roads can also create overland flow

barriers. Failing to install culverts effectively disconnects the upslope area from

77

contributing runoff to the watershed outlet. Because the REA can predict culvert locations, a subsequent field investigation revealed that almost half the Piyami Drain watershed delineated with the conventional grid based approach (D8) was hydrologically disconnected from the outlet.

Furthermore, from a subjective analysis of all the roads in the Piyami Drain watershed, we suggest that roads that do not impose overland flow directions according to their orientation are rare in this type of landscape. Thus, we propose that by explicitly accounting for the location of roads, ditches, and culverts the REA makes more realistic assumptions than defining flow direction matrices using DEMs alone.

a)

b)

c)
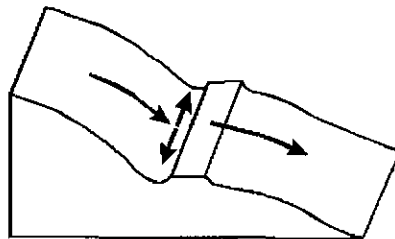
Figure 21 REA Raised roads

a) A large pool of runoff accumulates on the upslope side of an elevated road after a rare prolonged precipitation event in June, 2002. The downslope side of the road (not shown) showed no signs of runoff accumulation.

b) A linear drainage pattern is enforced due to an elevated road. Overland flow is seen here draining from the trees in the background to a culvert located in the foreground.

c) Conceptual model of elevated road enforcement. Runoff is re-routed on the upslope side of the raised road, but is not affected on the downslope side of the road.

79

a)

b)

c)
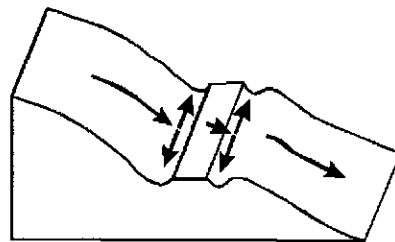
Figure 22 REA Roadside ditches

a) Runoff accumulates in a ditch on the downslope side of a road. The majority of the runoff originated in a very significant rainfall event two months before this picture was taken.

b) An abrupt change in the runoff direction due to the presence of a road. The runoff in the picture is flowing from the field towards the road, at which point, the road imposes a ninety degree change in direction. Thus, the roadside ditch enforces the progression of the runoff along the road perpendicular to the natural drainage pattern.

c) Conceptual model of ditch runoff enforcement. Runoff is re-routed on both the upslope and downslope sides of the road.

a)
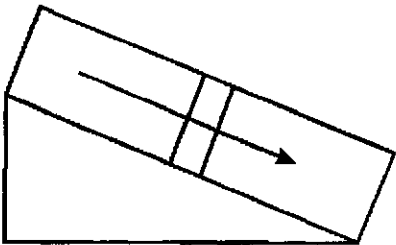
Figure 23 REA Flat cross-sectional road profiles

a) Conceptual model of runoff across a flat road. Runoff is not significantly affected by the road and continues to follow the topographic slope.

Figure 24 Road cross-section Ditch-to-Field and Ditch-to-Road heights
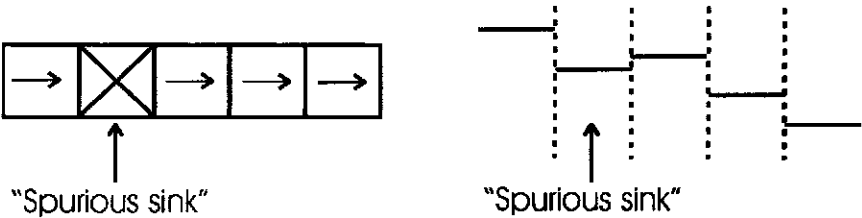
Figure 25 Spurious depression features

81

a)
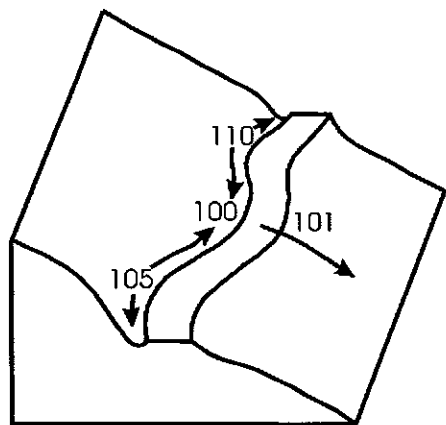
b)
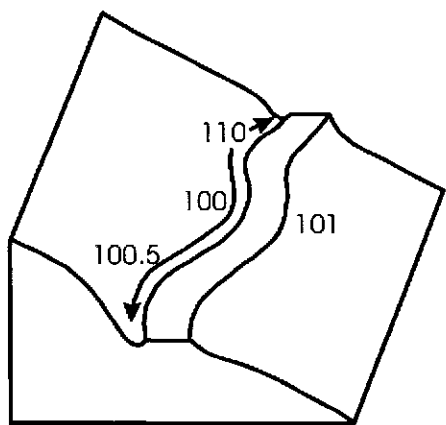
Figure 26 Runoff patterns within the runoff collector network

a) Road breach scenario. Figure 26a shows the elevations of four key locations and the resulting drainage pattern. The runoff progresses from the two ridges in the runoff collector network towards the breach grid cell in the center. Runoff flows from the depression on the upslope side of the road across the road and progresses downslope.

b) Road height too high to enable breaching. Figure 26b shows the same scenario as Figure 26a, but with a different ridge top elevation. Due to the reduced height of the ridge located at the bottom of the figure, runoff no longer breaches the road. Instead the runoff continues to flow alongside the road perpendicular to the natural drainage pattern (hillslope direction).
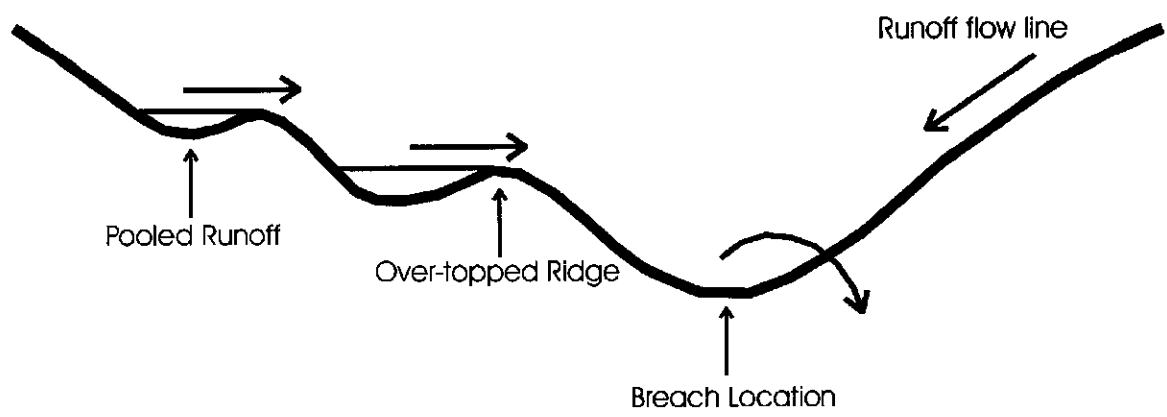
Figure 27 Runoff collector network rerouting model
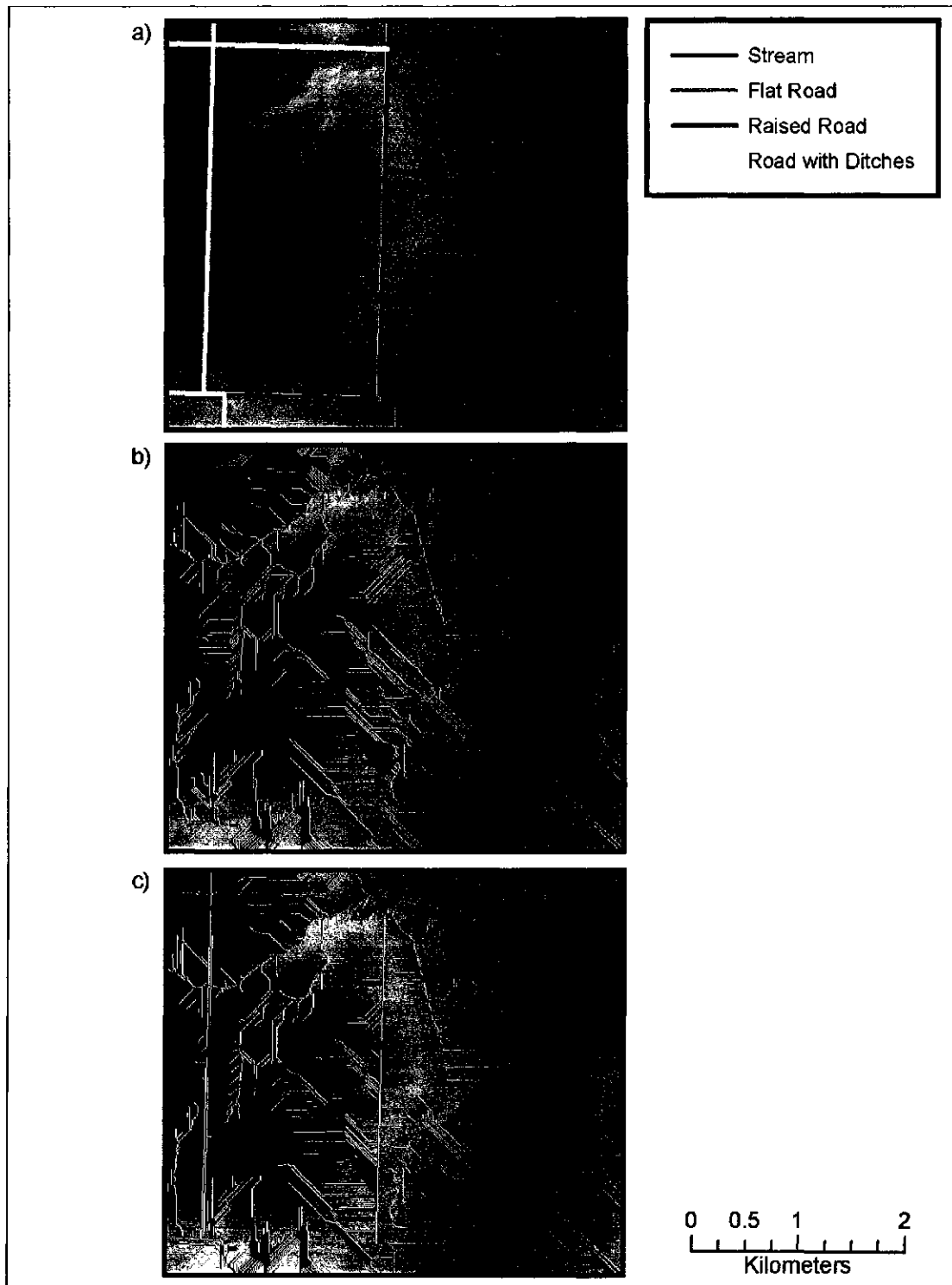
Figure 28 Field scale drainage patterns

a) Road classification base map used for the variable template model.
b) Flow accumulation map showing the DEM derived drainage pattern.
c) Flow accumulation map showing the REA derived drainage pattern.

84
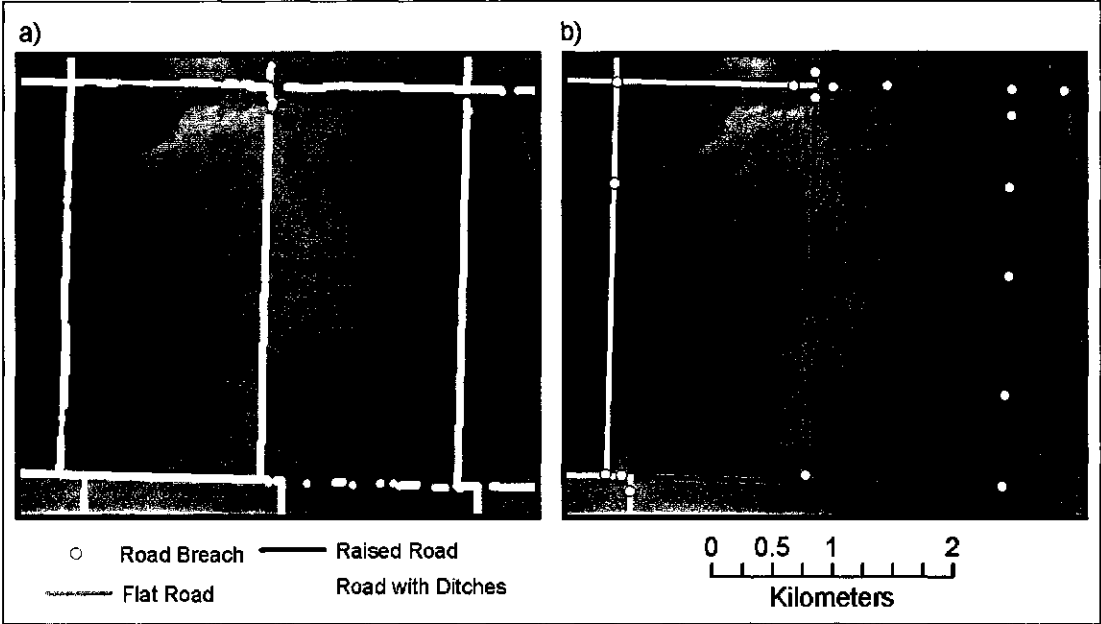
Figure 29 Field scale road breach locations

a) DEM derived drainage pattern (2, 043 road breach locations).

b) REA derived drainage pattern (18 road breach locations).
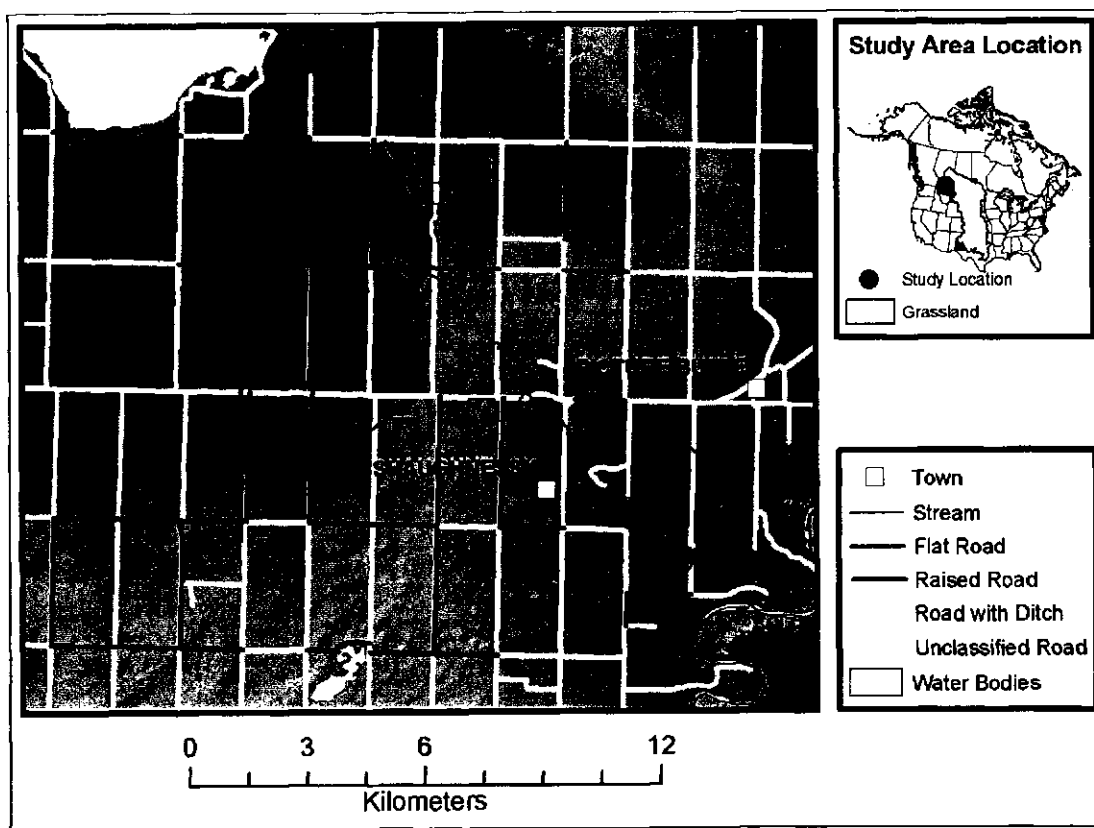
Figure 30 Watershed scale road classification base map used for the variable template model
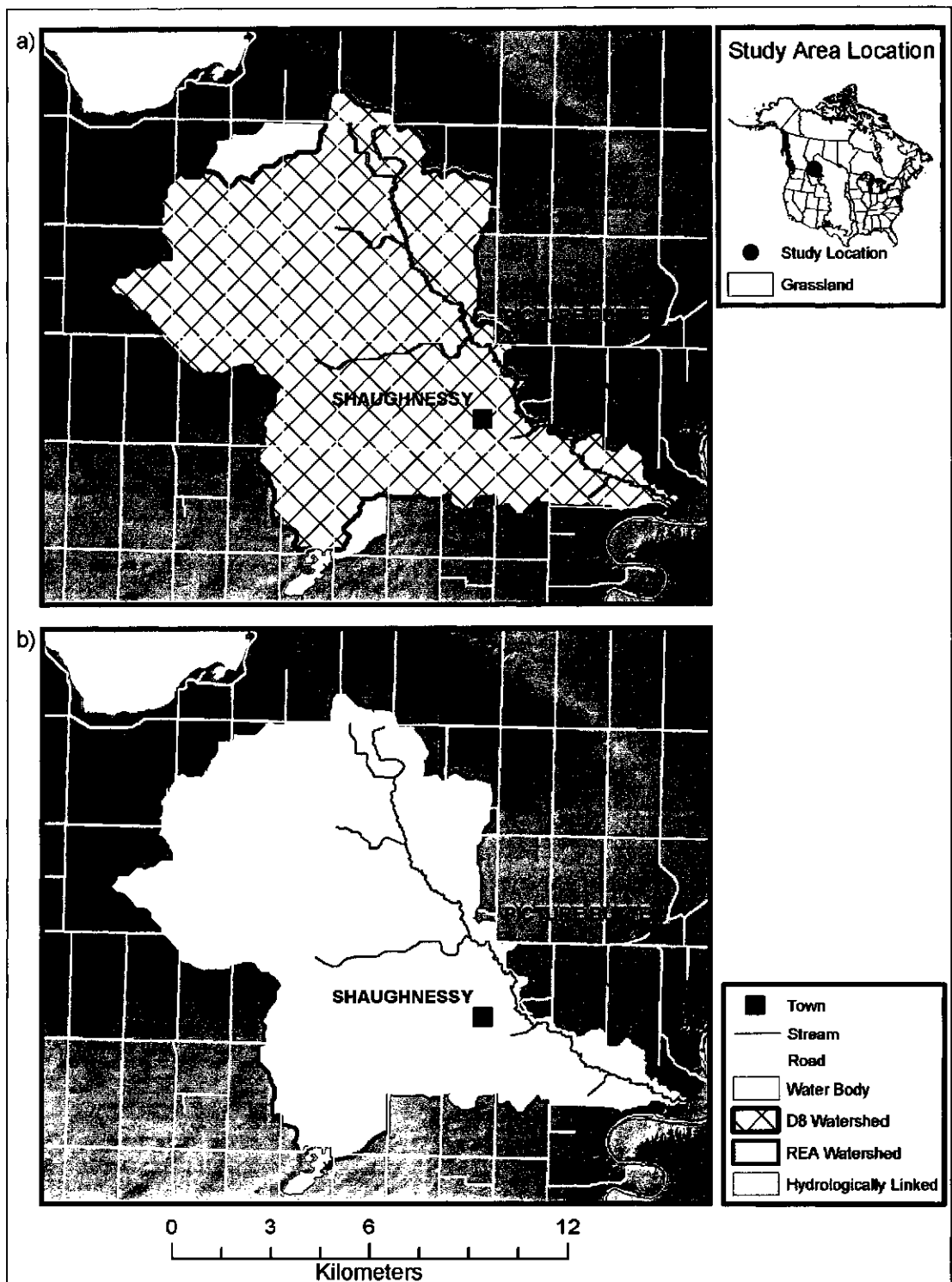
Figure 31 Delineated watersheds

a) Piyami Drain watersheds delineated with the REA and the D8 algorithm.
b) Piyami Drain hydrologically linked watershed.

87

Chapter 5

5 Overland Flow Path Modelling with Digital Elevation Models in Irrigated Landscapes

5.1 Introduction

Occasional contamination of raw water samples from the bacterial pathogens *E.Coli* and *Salmonella spp.* has prompted an investigation into land-use impacts on water quality in southern Alberta, Canada (Gannon et al., 2002; Hyland et al., 2003; Johnson et al., 2003). However, the irrigation distribution system of the Lethbridge Northern Irrigation District (LNID), and the relatively coarse elevation data set currently available for the province of Alberta (viz. 100-m regularly spaced point-elevations, plus elevation breaklines) makes watershed delineation with conventional grid-based algorithms prone to error. The canal enforcement algorithm (CEA) was, therefore, designed to enable the accurate delineation of watersheds to facilitate the investigation of watershed properties on surface water quality.

The accuracy of automated surface drainage derivation and watershed delineation is dependent upon the accuracy of the DEM and the conceptual accuracy of the flow direction algorithm implemented (Quinn and Beven, 1991; Garbrecht and Martz, 2000; Wise, 2000; Endreny and Wood, 2001). See Chapter 2 for a review of surface drainage derivation error due to the digital representation of terrain, and the choice of flow direction algorithm.

To minimize modelling error associated with DEM quality and resolution, and given the

restriction of data availability, several procedures have been developed that utilize

ancillary data to enforce flow directions along several landscape features, including:

- streams (Hutchinson, 1989, Saunders, 2000; Turcotte et al., 2001),

- tillage furrows and headlands (Souchere et al., 1998; Cerdan et al., 2001; Takken et al., 2001 [a, b, c]), and

- roads and ditches (Chapter, 4).

Similar to these procedures, the CEA overcomes drainage derivation inaccuracies by

enforcing known canal flow directions. However, irrigation canal networks present the

additional problem of split flow, therefore, extra steps are required to accurately model

overland flow in irrigated landscapes.

Irrigation canals divert surface runoff from its natural pathway because the orientation of

canals often does not coincide with the orientation of the naturally occurring topographic

slope. In fact, canals are often constructed to route water across topographic ridges in

order to maximize the hydraulic head for further distribution and irrigation. Naturally,

these ridges form watershed boundaries, however, the construction of irrigation canals

results in inter-basin water transfers creating highly modified overland flow drainage

patterns. Because water within irrigation canal segments diverges, multiple overland

flow paths can link two locations in the landscape. Irrigation canals can dramatically

change watershed boundaries and the hydrological and biophysical processes operating

within the watershed (Snaddon et al., 1998). Studies intending to identify contaminant

pathways and/or delineate watershed boundaries must explicitly account for the divergent

(or split) flow patterns that occur within an irrigation network. This paper presents an automated grid-based watershed delineation methodology that enforces flow directions along irrigation canals, and accounts for split flow within canal networks.

5.2 Methodology

5.2.1 The Canal Enforcement Algorithm

The algorithm, a stand-alone program written in Microsoft Visual Basic, is referred to as the canal enforcement algorithm (CEA). Appendix 9.3 contains several snippets of code from the CEA. The CEA defines a flow direction matrix for the cells that comprise an irrigation canal and stream network, and imposes these matrices on a DEM-derived flow direction matrix created using conventional grid-based processing. The DEM-derived flow direction matrix is defined using the D8 flow direction algorithm (e.g., Jensen and Domingue, 1988) as implemented in ESRI's ArcView, ArcGIS, and ArcInfo. Alternate flow direction values are stored for individual grid cells that represent irrigation canal intersections. An iterative watershed delineation routine subsequently defines the upstream contributing area to a specified outlet grid cell taking into consideration the alternate flow directions within the canal network, thereby accounting for divergence.

5.2.2 Conceptual Model of Canals

In nature, runoff water flows convergently from hillslopes to valleys forming progressively larger open channel drainage networks (Figure 32). Several authors have made the distinction between hillslope processes, that are more accurately modeled with

90

multiple flow direction algorithms, and channel process that are more accurately modeled with single flow direction algorithms (Freeman, 1991; Quinn et al., 1991; Costa-Cabral and Burges, 1994; Desmet and Govers, 1996; Gallant and Wilson, 1996; Tarboton, 1997). However, irrigation canals are concentrated flow systems with divergent flow patterns (Figure 33). Accurately modelling overland flow within an irrigated landscape, therefore, requires a single flow direction algorithm that supports divergent flow.

Occasionally, open channel irrigation canals are also routed underneath or overtop drainage courses via siphons and flumes to facilitate the natural progression of runoff and stream flow (Figure 34). Analogous to a bridge, the cross-flow patterns illustrated in Figure 34 add the complexity of a third dimension to overland flow modelling in irrigated landscapes.

In addition to flumes and siphons, canal pipelines also add the complexity of a third dimension to overland flow modelling in irrigated landscapes. A canal pipeline can convey water in a direction different from that defined by the overlying topography. Thus, if a pipeline supplies return flow to a watershed outlet, the drainage area for that watershed also includes the runoff contributing area for the most upstream point in the pipeline.

5.2.3 Data Requirements of the Canal Enforcement Algorithm

The CEA requires input files in ESRI ArcView / ArcInfo grid ascii format (Appendix 9.2). The model requires ten input data layers that are described in Table 2.

91

Table 2 Required data layers for input into the CEA

Layer Name	Layer Description
Topographically defined flow direction matrix	ESRI's D8 format (flow direction command)
Topographically defined stream matrix	Threshold flow accumulation value
Stream outlet	A value of 1 specifies the most downstream location in the stream
Streams	A value of 1 specifies cells that represent streams
Canal order	Used to encode canal segment flow directions
Canal identification	Used to define canal segments
Canal entry	A value of 1 specifies the most upstream location in the irrigation canal distribution system
Canal looping	Used to encode circular flow paths within the irrigation canal distribution system
Canal-stream crossing locations	A value of 1 specifies flume and siphon structure locations
Watershed outlet	A value of 1 specifies the point whose upstream contributing area is required

5.2.4 Calculation of the Flow Direction Matrix

Step 1: Enforce stream drainage pattern

Starting with the stream outlet grid cell, all cells in the stream data layer are routed to the

stream outlet. Enforcing the known stream locations has the same effect as lowering the

elevation of the DEM cells along known watercourses. This process, often referred to as

"stream burning" has been shown to significantly improve DEM-derived drainage

networks (Saunders, 2000).

Step 2: Enforce canal drainage network

Starting with the canal entry grid cell, all cells are routed downstream from lower to

higher order canals. As each canal junction is identified, alternate flow directions are

determined that route flow into the higher order canal segments. A log file is created

containing the row and column coordinates for each junction as well as the secondary (or

alternate) flow direction(s). The algorithm progresses downstream until all canal grid

92

cells for a particular canal segment (or ID) have been processed and one of the following three conditions is met:

- the canal ends but is linked to another canal,

- the canal ends but is linked to a stream, or

- the canal ends without a canal or stream linkage.

If the canal ends without linking to either a canal or a stream (i.e., within one row and one column) the grid cell is flagged as a dead end canal grid cell (Figure 35: 'A'). If the canal ends but is linked to a stream, a flow direction is assigned into the stream (Figure 35: 'B'). Canal-to-stream linkages support return flows within an irrigation canal network. If the canal ends but is linked to a canal of equal or lower order, a flow direction is assigned into the adjacent canal (Figure 35: 'C'). Similar to the process of enforcing known stream locations in step one, step two enforces the location of canals into the flow direction matrix.

Step 3: Combine flow direction grids

The enforced stream and canal drainage networks are imposed onto the DEM-derived (D8) drainage pattern, creating a single flow direction matrix. Following the compilation of the three flow direction matrices a check is performed to ensure cross-flow patterns are not produced. Cross-flow patterns result when attempting to enforce flow along linear features that do not include cardinal neighbours in the raster representation (Figure 36a). Cross-flow patterns would result in overland flow progressing from the natural landscape across grid cells representing irrigation canal segments. Thus, the cross-flow check ensures irrigation canal segments capture overland flow from adjacent cells (Figure 36b).

93

Step 4: Assign canal network dead end grid cell flow directions

The grid cells representing dead ends in the canal network are temporarily assigned a

flow direction from the DEM-derived (D8) flow direction matrix. A check is performed

to determine whether the DEM-derived flow direction introduces a circular flow pattern.

Circular flow patterns are not permitted in grid-based modelling because all grid cells

must drain to the edge of the DEM matrix (Jensen and Domingue, 1988). If a circular

flow pattern is identified, the algorithm steps back, one grid cell at a time, starting with

the terminus grid cell and locates the first DEM-derived flow direction that does not

produce circular flow. After this grid cell has been identified all of the flow from the

canal segment is re-routed out of the canal through this grid cell. This process can

produce flow patterns within a canal segment that are in the wrong direction. However,

the restriction of a continuous flow direction matrix in grid-based hydrological modelling

necessitates this compromise. Following the completion of step four, a continuous flow

direction matrix is produced with the stream and canal network enforced.

Step 5: Create cross-flow patterns at canal-stream crossing locations.

At each canal-stream crossing location, the flow directions are manipulated to create a

cross-flow pattern, thereby simulating a siphon or flume structure. Cross-flow drainage

patterns facilitate the natural progression of runoff in drainage courses defined by the

DEM while maintaining the enforcement of the canal segment.

94

Step 6: Delineate watershed

The model delineates the upstream contributing area for the grid cell representing the watershed outlet. In contrast to conventional automated watershed algorithms, the CEA takes into account multiple flow directions at canal junction points. Thus, the watershed produced is representative of the multiple overland flow pathways within the irrigation canal network.

5.3 Results

The CEA was tested on the Piyami Drain watershed located in southern Alberta, Canada (Figure 37). Prior to anthropogenic disturbances Piyami Creek drained approximately 110 km^2 to the Oldman River that runs through the city of Lethbridge (Figure 37). The topography is comprised of gently rolling hills near Piyami Creek, as well as extensive flat areas around the outer edges of the watershed. The total relief of the natural watershed is 204 meters, with an average basin slope of 2.5%. Agriculture within the Piyami Drain watershed is irrigated by the distribution system of the Lethbridge Northern Irrigation District (LNID) (Figure 37). Approximately 600 km of irrigation canals comprise the LNID (Morris, pers. com.).

The DEM for the study area was interpolated from point-elevation data using the TOPOGRID command within ArcInfo that uses the 1996 version of ANUDEM (Australian National University Digital Elevation Model) developed by Hutchinson (1989). The elevation data were provided by AltaLIS (Calgary, Alberta) (See section

3.1.3 Which data are available to model flow pathways in the study area?). The DEM

was interpolated to a 20-m grid cell size.

Irrigation canal segments were categorized into pipeline, open channel, or return flow

(i.e., drainage) channels. Because pipelines do not impact overland flow drainage

patterns they were not enforced into the flow direction matrix. The canal segments

categorized as return flow canals were merged with a stream data layer and enforced

according to step number 1 (See Section 5.2.4). The flow directions in the open channel

canal segments were determined and used to create the canal order data layer. The open

channel canal segments were enforced according to steps 2 to 4 (See Section 5.2.4).

Additionally, sixteen canal-stream crossing structures (i.e., flumes and siphons) were

input into the model. The operations manager at the LNID identified eleven of the

sixteen canal-stream crossing locations (Morris, pers. com.). However, Morris (pers.

com.) also stated that because the existing siphons and flumes had never been input into

their database, several additional structures were presumably installed. Because the canal

mainline does not typically intercept runoff (Morris, pers. com.), it was assumed all

locations with channelized flow patterns perpendicularly orientated to the canal mainline

included either a siphon or a flume. Thus, five additional canal-stream crossing locations

were included along the canal mainline. The additional canal-stream crossing locations

were selected by analyzing air photos, a DEM-derived channel network, and a hillshade

surface derived from the DEM. The cross-flow patterns at each of the sixteen canal-

stream crossing locations were enforced into the flow direction matrix according to step

number 5 (See Section 5.2.4).

96

5.3.1 Field Scale Results

Significant discrepancies between the DEM-derived drainage patterns and the true canal flow directions indicated that many open channel irrigation canals were not adequately represented in the DEM. Because of this information loss within the DEM, the conventional D8 flow direction algorithm failed to accurately model overland drainage patterns. Figure 38a shows a portion of the DEM-derived drainage pattern overlaid with several canal segments. The drainage patterns progress across the canal towards the bottom of the image. In contrast, the CEA-derived drainage patterns coincided precisely with the known canal flow directions (Figure 38b). Instead of proceeding across the canal, runoff from the top of the image is captured by the canal mainline that runs from the west to the east side of Figure 38. Through the implementation of the CEA, irrigation canals, usually not represented in the DEM, intercept overland flow.

5.3.2 Watershed Scale Results

5.3.2.1 Final Watershed Areas

The watershed boundaries delineated using the conventional D8 flow direction algorithm (DEM-derived) and the CEA are shown in Figure 39. The DEM-derived watershed comprised 226 km^2, whereas the CEA-derived watershed comprised 6,042 km^2. The D8 and CEA-derived watersheds were also compared quantitatively using a percent agreement statistic (Equation 3). A percent agreement of 3.7% was attained between the DEM and CEA-derived watersheds.

97

$$XPA = \frac{WB}{WD8 + WCEA + WB} \times 100\%$$ (Equation 3)

Where:
XPA	= watershed % agreement
WB	= area delineated by both the D8 and the CEA algorithms
WD8	= area delineated by the D8 algorithm only
WCEA	= area delineated by both the CEA algorithm only

5.3.2.2 Irrigation Siphon and Flume Structures

The impact of introducing cross-flow patterns at canal-stream crossing locations is illustrated in Figure 40. The locations labeled 'A' in Figure 40 represent flume or siphon structures that facilitate the progression of runoff across an irrigation canal segment. The upstream contributing areas from these locations do not contribute runoff to the outlet of Piyami Drain. In contrast, the upstream contributing areas of canal-stream crossing locations situated within the natural stream channel of Piyami Drain (labeled 'B') remain in the delineated watershed. Runoff originating in the areas labeled 'C' in Figure 40 is intercepted by an open channel irrigation canal, and thus contributes runoff to Piyami Drain. Whereas the upstream contributing areas of the points labeled 'A' were not included in the watershed, the areas labeled with a 'C' were included because evidence of concentrated (or channelized) flow patterns in the pre-assessment was not prominent, and thus did not suggest the presence of a siphon or flume structure that would have facilitated the natural progression of runoff. Although berms are usually present adjacent to the canal mainline to prevent this type of runoff interception, drainage culverts are often installed through berms in areas that accumulate runoff. Therefore, the inclusion of these areas in the watershed is conceptually accurate. Field validation was not, however, carried out at this time due to limited in-field access.

Figure 41 shows the CEA-derived watershed without taking siphon/flume structures into consideration. Failing to account for canal-stream crossing structures resulted in the erroneous capture of each siphon and/or flume structures upstream contributing area. Thus, thirteen additional runoff contributing areas totaling 2,547 km^2 were included in the watershed. By failing to account for cross-flow patterns the percent agreement between the D8 and CEA-derived watersheds decreased from 3.7 to 2.6%, and the total watershed delineation error increased by 30%.

5.3.2.3 Irrigation Canal Pipelines

Following the initial watershed delineation, the locations of canals categorized as pipelines were analyzed to determine whether they influence the contributing area of Piyami Drain. Although several canal pipelines were contained in the watershed, the segment illustrated in Figure 42 was the only pipeline that intersected the watershed boundary. Within the conceptual view of canals (See Section 5.2.2), accurately delineating the Piyami Drain watershed required identifying and including the drainage area for the origin (or intake) of the canal pipeline. Thus, the runoff contributing area of the most upstream point for the pipeline was determined using the CEA and added to the initial watershed delineation. Accounting for this canal pipeline added an additional 3.3 km^2 to the total watershed area.

99

5.3.2.4 Final Watershed Areas within the LNID

To evaluate the consequence of runoff capture within the LNID, the conventional D8-derived watershed was compared with the CEA-derived watershed including only the contributing area downstream of the diversion in the Oldman River (Figure 43). The DEM-derived watershed comprised 226 km^2 while the CEA-derived watershed comprised 682 km^2 with a percent agreement of 50.3%.

5.4 Discussion

Due to generalization within the DEM and the inability of the conventional D8 flow direction algorithm (or others) to account for canal induced divergent flow patterns, the DEM-derived (D8) watershed is not an accurate representation of Piyami Drain's drainage area. In contrast, the watershed derived using the CEA was conceptually much more accurate due to the following:

- The CEA-derived watershed included the headwaters of the Oldman River.

- The CEA-derived watershed included areas that contribute runoff through interception by open channel irrigation canals.

- The drainage network used to derive the watershed accurately modeled siphon and flume structures.

- The CEA-derived watershed included areas that contribute runoff to Piyami Drain via pipelines.

- The drainage network for the cells representing irrigation canals coincided with the known canal flow directions.

100

Modelling the complex drainage structure within the LNID distribution system also introduced several conspicuous features to the boundary of the watershed that are atypical of watersheds in undisturbed landscapes, including:

- narrow peninsula-type features due to runoff interception by open channel irrigation canals,

- one grid cell wide segments that represented irrigation canals, and

- areas entirely contained in the watershed that did not contribute runoff to the watershed outlet.

The large differences between the D8 and CEA methodologies indicate that conventional grid-based flow direction algorithms do not accurately model flow in irrigated landscapes. Therefore, investigating the relationships between pathogen occurrence and the spatial characteristics of the Piyami Drain watershed, derived using conventional grid-based algorithms, would have been erroneous.

The large discrepancies between the watersheds derived using the conventional approach (i.e., D8) and the CEA may raise some doubt as to the accuracy of the CEA. However, the watershed boundaries are considered accurate because the CEA enforces known canal flow directions. A DEM interpolated from point-elevation data with a very small sampling interval could be used to verify these watersheds, however, such a data set does not exist.

5.5 Conclusions

The conceptual accuracy of conventional grid-based flow direction algorithms is considered adequate to successfully implement hydrological models for many applications (e.g., Moore et al., 1991). However, if the study area is partly or fully contained within an irrigation district conventional grid-based routing algorithms fail to simulate drainage patterns accurately. A new grid-based overland flow routing algorithm, called the canal enforcement algorithm (CEA), was described that improves overland flow routing in irrigated landscapes. The CEA improves modeled overland flow directions by:

- enforcing the flow directions within canals,

- accounting for divergent (split) flow at canal intersections, and

- enabling streams to cross canals without runoff capture into the irrigation canal network.

The differences between the conventional D8 (DEM-derived) watershed and the CEA-derived watershed presented in this study indicate that the consequences irrigation canals impose on overland flow directions are significant. The discrepancies between the D8 and the CEA-derived watersheds also infers that the biophysical processes modeled within the watershed would also differ significantly from those modeled using a conventional flow direction algorithm (e.g., D8). Hydrological models that rely on conventional DEM-derived flow direction matrices in similar landscapes are, therefore, potentially inaccurate. The CEA provides a means to overcome erroneous flow direction derivation and watershed delineation that results from DEM generalization, and the restrictions of conventional grid-based overland flow routing algorithms.

102

Figure 32 Natural drainage topology
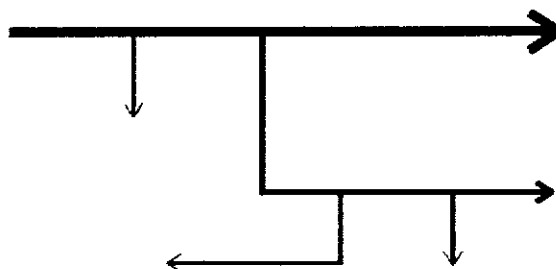
Figure 33 Drainage topology within irrigation networks

━━ Canal Segment
- - - - River Network
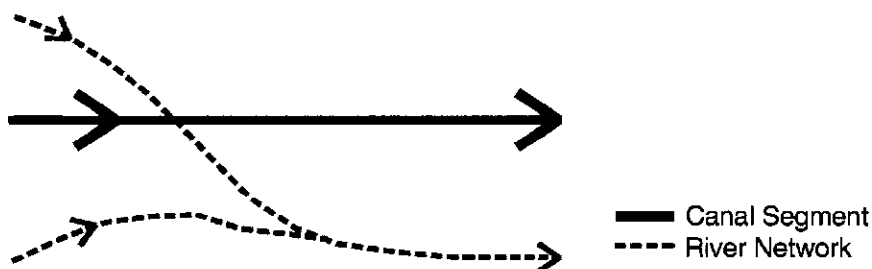
Figure 34 Irrigation canal cross-flow drainage pattern

■ Canal Segment Terminus
—— Canal Segment
- - - River Network
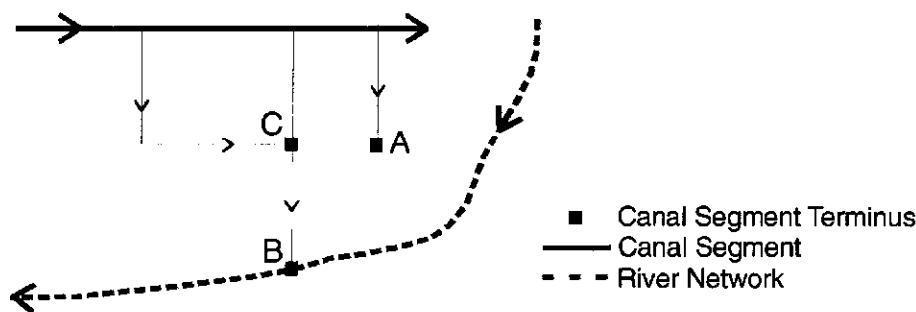
Figure 35 Canal segment links
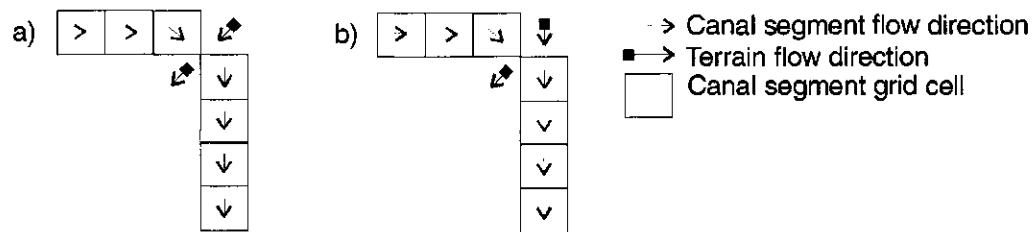
Figure 36 Cross-flow pattern drainage patterns

a) before processing CEA step three, and b) and after step three
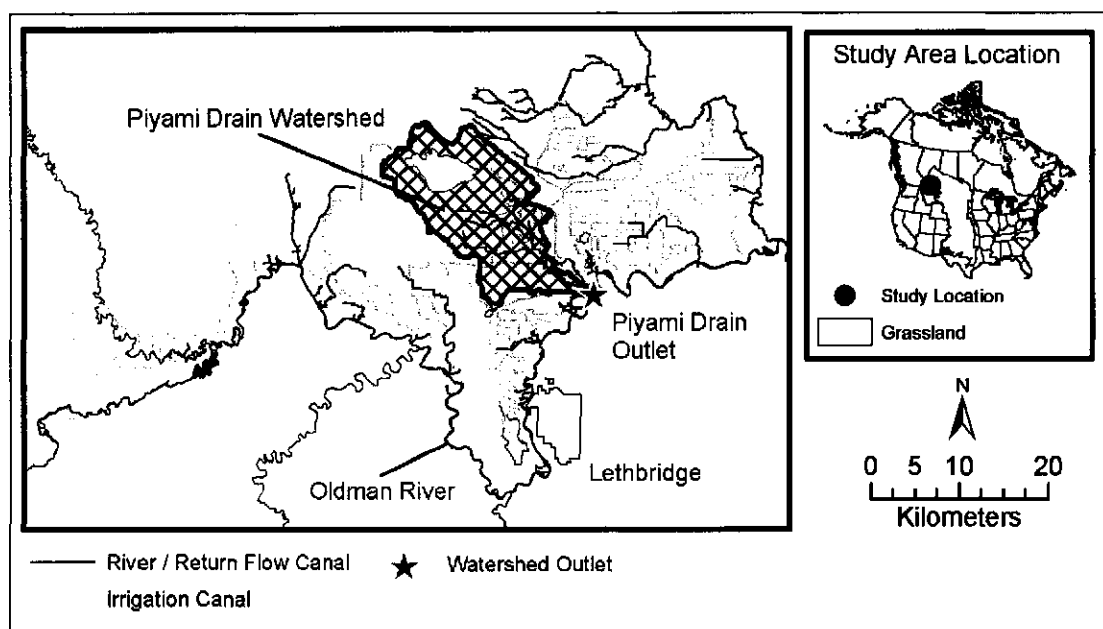
Figure 37 CEA Piyami Drain watershed study area
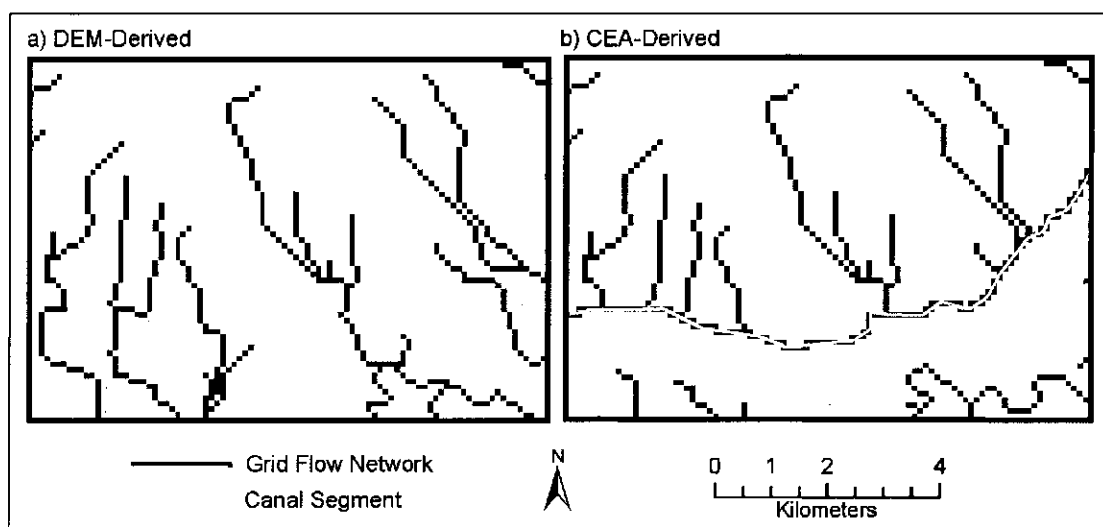
Figure 38 Overland flow networks

104

a) DEM-derived, and b) CEA-derived network
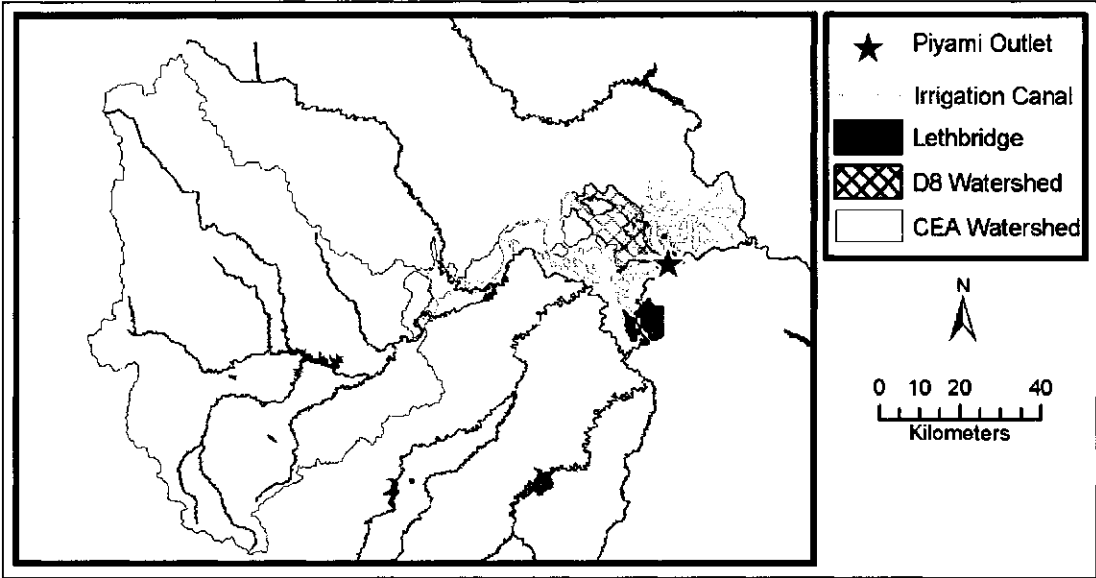
Figure 39 DEM and CEA-derived watersheds
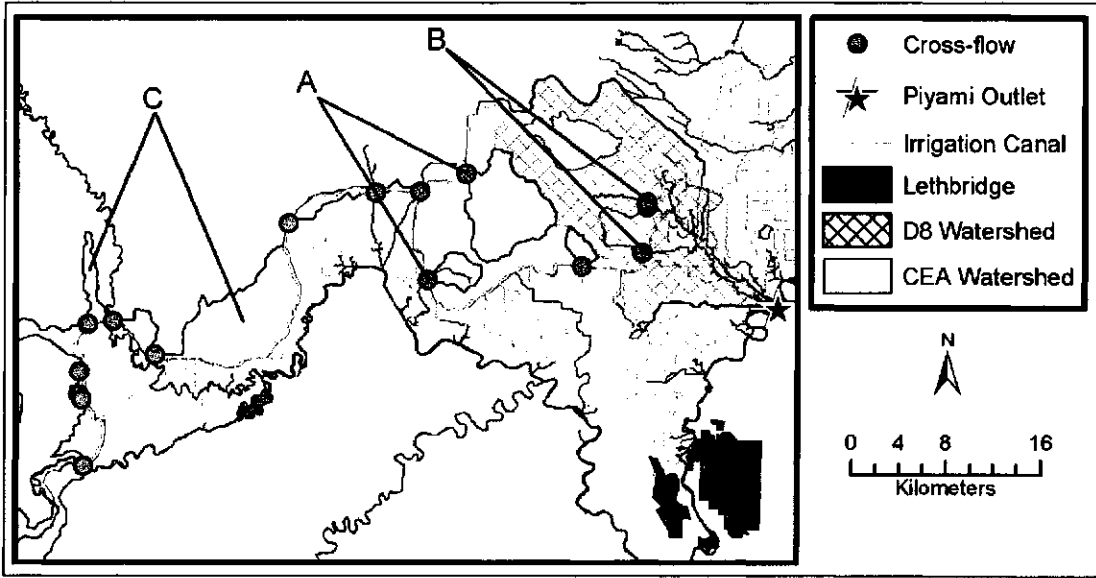
Figure 40 Canal-stream cross-flow patterns within the Piyami Drain watershed

A) cross-flow structure enabling the flow of runoff out the watershed
B) cross-flow structure on the natural stream channel of Piyami Drain
C) runoff source areas intercepted by irrigation canals due to the lack of a cross-flow structure
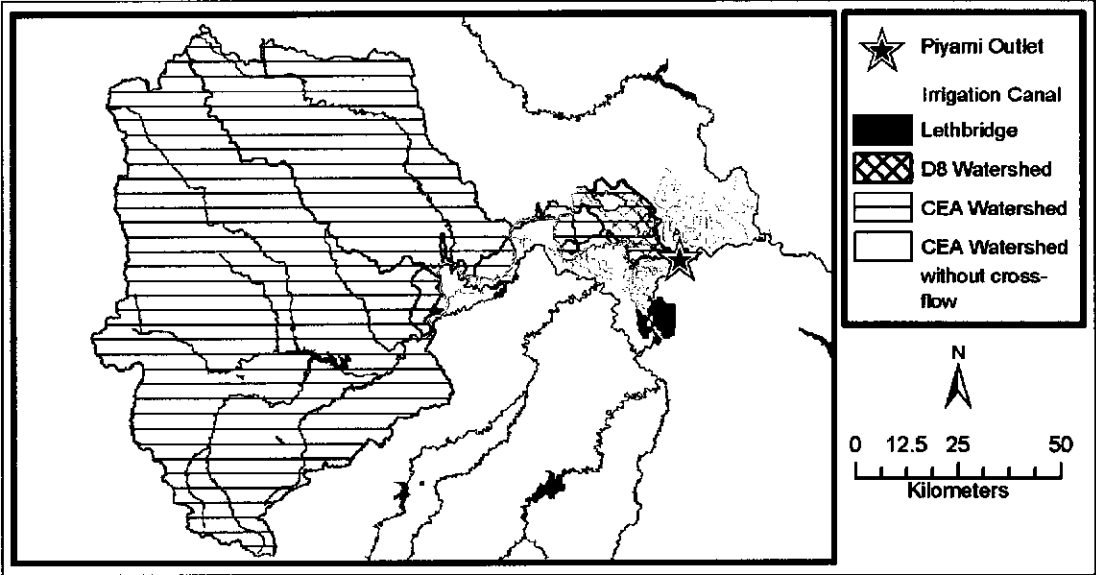
Figure 41 DEM-derived and CEA-derived watershed without cross-flow patterns at canal-stream crossings
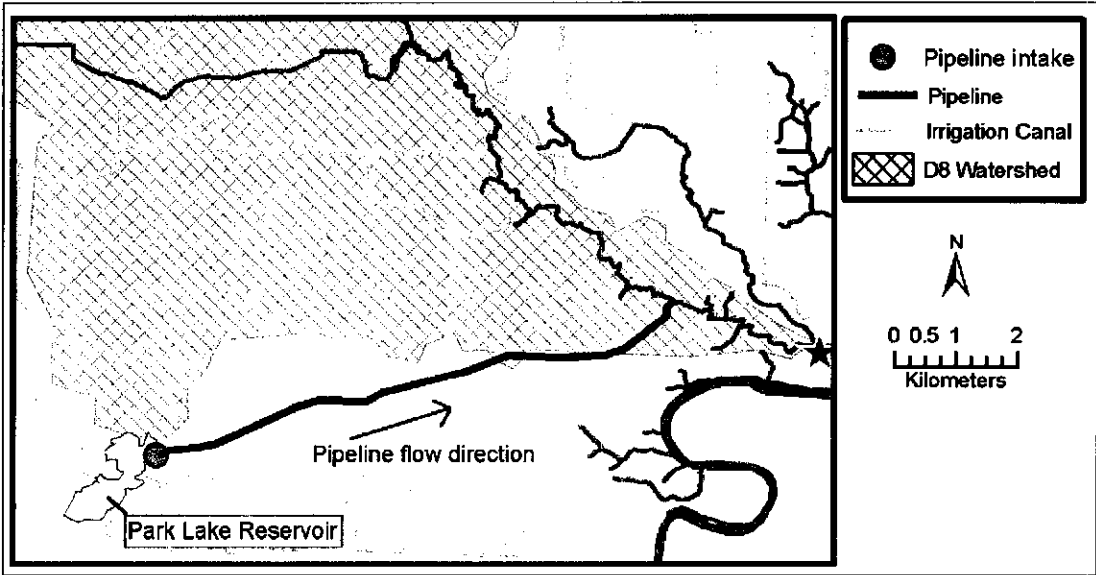
Figure 42 Piyami Drain irrigation canal pipeline
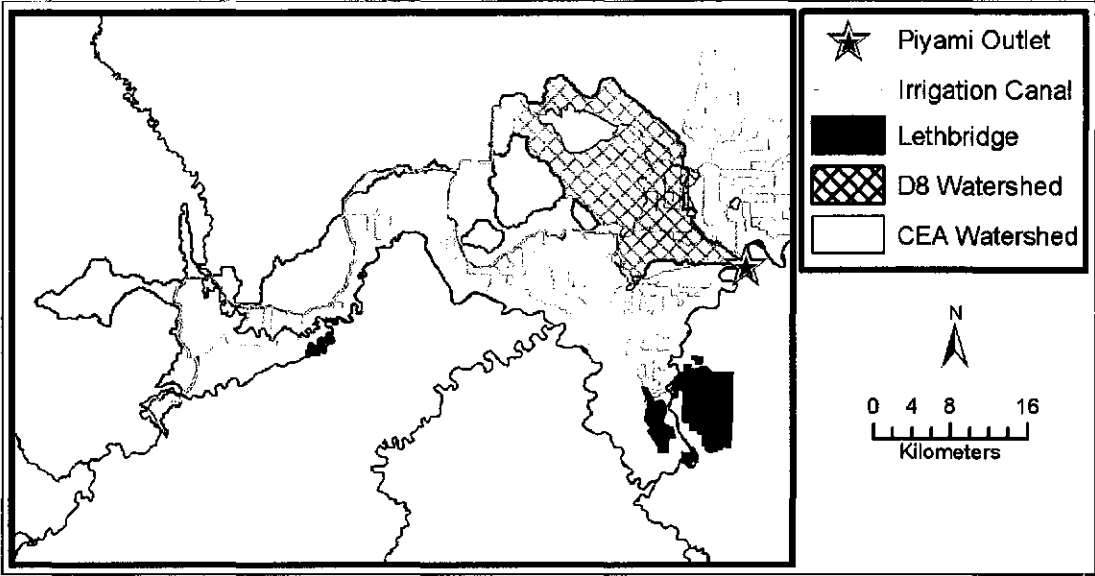
Figure 43 DEM-and CEA-derived watersheds downstream of the irrigation canal diversion

Chapter 6

RIDEM: a Grid-Based Model to Downscale Flow Paths in Landscapes with Rural Infrastructure

6.1 Introduction

Although several studies have found positive correlations between livestock densities and poor water quality at the watershed scale (e.g., Crowther et al., 2002; Guenette, 2002; Tian et al., 2002; Tong and Chen, 2002), stating a similar relationship in southern Alberta is more complicated because runoff flow paths have been highly altered by the construction of roads, ditches, culverts, and irrigation canals (Chapter 4 and 5). As a result, these features, which disturb natural flow paths, make defining watershed boundaries exceedingly difficult. The investigation of the spatial and temporal influence of watershed properties on surface water quality requires the accurate delineation of runoff transport pathways and watershed boundaries. To accomplish this task, a watershed delineation procedure that accounts for roads, ditches, culverts, and irrigation canals is required.

The best method to delineate watersheds accurately is to use a digital elevation model (DEM) and a flow direction algorithm (See section 2.2.2 Grid-Based Flow Direction Algorithms). However, poor landscape representation in DEMs frequently causes the derivation of over-simplified drainage patterns in grid-based models (Moore et al., 1991; Grayson et al., 1993; Band and Moore, 1995; Schneider, 2001). These inaccuracies are exacerbated in low-relief landscapes where rural infrastructure (e.g., roads) has significantly modified the landscape drainage patterns (Ludwig, 1996; Cerdan et al.,

2001; Takken et al., 2001 [a, b, c]; Chapter 4 and 5). For this study the regional elevation

data set, that was used to derive surface drainage patterns and thus delineate watersheds,

was sampled at a scale too large to resolve critical sources of landscape drainage

variability (viz. roads, ditches, culverts, and irrigation canals). If a conventional grid-

based flow direction algorithm (e.g., D8, DEMON, Flux Decomposition, D8-TOPAZ, D-

Infinity, D8-LTD) were used to delineate watersheds, the drainage patterns would be

grossly simplified. Therefore, the scale of model output would not be adequate to

investigate interactions between land use and water quality in the study area. Beven

(1995) described this as the "scale problem", where information gained at one scale is

used to make predictions at a different scale.

Several studies have documented the effects rural infrastructure and agricultural field

operations impose on hydrological processes at different spatial scales, including:

- tillage furrows,

- roads, ditches, culverts,

- and irrigation canals.

At the field scale, tillage furrows and ditches have been shown to modify flow directions

significantly. At a larger scale, roads concentrate and divert surface runoff, and also

change the patterns of soil erosion as well as the size and shapes of watersheds (See

section 2.4.1 Anthropogenic Terrain Features).

Rural infrastructure can also influence the hydrological processes operating at regional

scales. Although the effect irrigation canals have on watersheds derived in a grid-based

environment has not been well researched, Nyssen (2002) stated that the linear features that cause divergent flow patterns are significant, but are, however, difficult to model. Chapter 5 of this thesis demonstrated that the boundaries of watersheds containing irrigation infrastructure hardly resemble those that occurred naturally. In addition to the hydrological implications of inter-basin water transfers (IBT's) that result from irrigation, Snaddon et al. (1998) concluded that IBT's can also have disastrous consequences on the ecological and sociological processes within a region.

This paper presents the model RIDEM (Rural Infrastructure Digital Elevation Model). RIDEM enables the delineation of watersheds in low-relief areas where drainage patterns have been altered by the construction of roads and irrigation canals through the implementation of the road enforcement algorithm (REA) (Chapter 4), and the canal enforcement algorithm (CEA) (Chapter 5). Both algorithms incorporate ancillary data to take into account anthropogenic landscape features that influence drainage patterns, but are not resolved following the interpolation of a grid-based DEM. The CEA algorithm also resolves the inability of single flow direction algorithms to model the divergent (or split) flow paths that occur within irrigation distribution systems. Because RIDEM considers only elevation values as well as the spatial location of roads, irrigation canals, culverts, and siphon / flume structures, RIDEM is implemented solely for the delineation of gross watersheds and dead drainages. RIDEM was programmed as a stand-alone application in Microsoft Visual Basic. Appendix 9.3 contains several snippets of Visual Basic code from RIDEM.

6.2 Methodology & Study Area

Using a DEM with a 20-m grid cell size, watersheds were delineated for three water quality sampling locations located within the Lethbridge Northern Irrigation District (LNID), including: Sientza Drain, Piyami Drain, and Battersea Drain (Figure 44). The drainage channel for each watershed is used to convey irrigation return flow to the Oldman River. Prior to anthropogenic disturbances, the runoff contributing areas of Sientza, Piyami, and Battersea Drain were approximately 21, 258, and 63 km^2 respectively. Although the LNID diverts water into its distribution system from the Oldman River, the study area was limited to the area downstream of the diversion. Therefore, the study area did not include the headwaters of the Oldman River, even though this area comprises a significant portion of each watershed (Chapter 5). The remaining study area extends from the forested Porcupine Hills situated east of the Rocky Mountains, to the flat prairie grasslands northeast of Lethbridge.

Field observations during a significant precipitation event in June, 2002, in which 140-mm of rain fell within three consecutive days (Gallant, 2002), made it clear that roads, ditches, culverts, and irrigation canals significantly influence overland flow pathways in southern Alberta (See section 3.1.1 Which features in the landscape impact overland flow paths?). Although the majority of research previously completed on the hydrological effects of roads was conducted in forested regions (e.g., Montgomery, 1994; Wemple et al., 1996; Jones et al., 2000; Tague and Band, 2001; La Marche and Lettenmaier, 2001), these observations indicate that the combination of roads, culverts, and irrigation canals

111

also influence the size and shapes of watersheds, and subsequently the stream water quantity, quality, and timing in the grasslands of southern Alberta.

6.2.1 Model Steps

The steps taken to implement and verify the watersheds derived with the RIDEM model are outlined as a flow-chart in Figure 45.

Step 1: Conventional flow direction routing (D8-TOPAZ)

Landscape drainage patterns were derived using the conventional grid-based approach. This process involved filling local sinks in the DEM, and subsequently deriving for each cell in the grid matrix the local flow direction. The D8 flow direction algorithm was used for this process as implemented in TARDEM, a suite of programs for the analysis of digital elevation data (Tarboton, 2000). TARDEM's implementation of the D8 algorithm is identical to the original D8 algorithm introduced by O'Callaghan and Mark (1984) for grid cells with a neighbouring cell at a lower elevation. However, the algorithm uses the approach introduced by Garbrecht and Martz (1997) for cells that lack a downslope neighbour. From this point on, the implementation of the D8 algorithm in TARDEM is referred to as D8-TOPAZ.

Step 2: REA

The flow direction matrix output from the conventional process described in step one was manipulated by enforcing typical road cross-sectional profiles using the REA model (e.g., Chapter 4). Approximately 1,032-km of gravel roads and paved secondary highways,

112

comprising 440 segments within a GIS vector layer, were classified into one of three

categories, as follows:

- flat roads,

- raised roads, and

- roads with a ditch (Chapter 4) (Figure 46).

Fifty-two road cross sections were surveyed with a theodolite to determine the average

ditch-to-road and ditch-to-field height within each road category (Figure 47). Appendix

9.1 contains each of the 52 surveyed road cross-sections. Because the study area

contained different road classes, which have different construction templates (Alberta

Transportation and Utilities, 1996), the roads were categorized into four individual

classes, including:

- secondary highway (raised road)

- secondary highway (road with ditch)

- local road (raised road)

- local road (road with ditch).

The mean ditch-to-field and ditch-to-road height for each category was then used to

manipulate the conventional flow direction matrix with the REA (Table 3). Categorizing

the roads into the four classes was intended to minimize the variation of ditch-to-road and

ditch-to-field heights within each category. Therefore, the error associated with

enforcing a single road cross-sectional profile over the length of an entire road segment

was minimized.

Table 3 Summary statistics of surveyed ditch-to-road and ditch-to-field heights

		Secondary highway		Local (gravel) road	
		Measured Heights (m)		Measured Heights (m)	
		Ditch to Field	Ditch to Road	Ditch to Field	Ditch to Road
Raised Roads	Average	--	--	**0.034**	**0.919**
	Standard deviation	--	--	0.153	0.462
	Minimum	--	--	-0.250	0.233
	Maximum	--	--	0.395	2.050
Road with Ditch	Average	**0.762**	**1.581**	**0.471**	**1.079**
	Standard deviation	0.452	0.249	0.262	0.374
	Minimum	0.080	0.895	0.015	0.340
	Maximum	1.930	2.010	1.006	1.773

A total of 206 culverts located at road intersections were also mapped and used as an input parameter in the REA model (Figure 46). Drainage culverts installed at road intersections were included to enable the REA model to simulate the hydrological linkages between ditch segments more accurately (Chapter 4).

Step 3: CEA

The flow direction matrix output from the REA was subsequently manipulated with the CEA to account for the distribution system of the LNID (e.g., Chapter 5). This process consisted of enforcing the known flow directions within each canal segment, incorporating cross-flow patterns associated with flume and siphon structures, and incorporating divergent flow patterns at canal junctions. Approximately 682-km of irrigation canals were enforced along with 16 cross-flow structures (Figure 48).

Step 4: Model Verification

Verifying the drainage patterns and watersheds delineated with the RIDEM model was a difficult undertaking because:

- A more accurate data set of elevations or watershed boundaries did not exist.

- The extent of the study area was relatively large (approx. 1400 km^2), prohibiting

  direct field verification of watershed boundaries.

- Infield flow direction determination in some areas was uncertain because the terrain

  in the study area was relatively flat. The average slope in the study area was 2.4 %.

However, verifying the locations where runoff was predicted to cross a road assessed the

accuracy of the REA component of RIDEM. Because these locations correspond to

topographic depressions where runoff concentrates, it was hypothesized that these

locations should contain a drainage culvert to facilitate the progression of runoff. The

predicted culvert locations were considered accurate if any one of the following features

was located at each location, including:

- a culvert,

- road-side cattails (*Typha latifolia*),

- runoff ponding,

- dead vegetation due to the prolonged spring precipitation event in the spring of

  2002,

- a prominent topographic depression, or

- an irrigation canal.

The model was considered in error when the predicted culvert location was not located in

a depression, but located on a ridge or along a side slope. The CEA component of

RIDEM was assumed accurate because the flow directions for each segment coincided

with the known flow directions.

115

Step 5: Delineation of dead drainages.

Ludwig et al. (1995) states that areas with high infiltration capacities or high surface water storage break the hydrological connection between an area in a watershed and the outlet. In southern Alberta, runoff almost never flows overtop of local roads, even in the most extreme precipitation event. Therefore, the upstream contributing area (or watershed) of each predicted runoff road crossing location that did not contain a culvert was considered a dead drainage. Because the objective of this study was to determine areas likely to contribute runoff, and thereby influence water quality, these areas were extracted from each watershed. The remaining watershed represents the gross watershed boundaries, excluding dead drainages caused by the construction of roads. The area that remains in each watershed is, therefore, linked to the watershed outlet by a direct drainage pathway. Dead drainage extraction from gross watershed boundaries has been implemented previously to determine effective watershed boundaries (PFRA, 1983), estimate erosion patterns (Ludwig et al., 1995), and for the development of the third version of the digital atlas of the world water balance (Asante, 1996).

6.3 Results

6.3.1 Gross watershed boundaries

The gross watersheds derived using RIDEM differed significantly from those derived with the D8-TOPAZ algorithm. RIDEM significantly impacted the shape and spatial arrangement of the gross watershed boundaries (Figures 49-51). The greatest similarity between the conventional D8-TOPAZ and RIDEM watershed delineation methodologies

116

occurred in Piyami Drain, yet less than half the grid cells (or 49.4%) were common to

both watersheds (Table 4). The area comparisons (or percent agreement) listed in Table

4 were calculated using the percent agreement statistic (Equation 4).

Table 4 RIDEM watershed area comparisons

Watershed Name	Watershed Area (square km)		Percent Agreement (%)
	D8-TOPAZ	RIDEM	
Szeitna Drain	21.5	207.0	10.0
Piyami Drain	257.9	504.7	49.4
Battersea Drain	63.0	405.1	15.3

$$XPA = \frac{WB}{WD8 + WH + WB} \times 100\%$$ (Equation 4)

Where:

XPA = watershed % agreement
WB = area delineated by both the D8-TOPAZ and the RIDEM algorithms
WD8 = area delineated by the D8-TOPAZ algorithm only
WH = area delineated by the RIDEM algorithm only

6.3.2 Dead drainages

RIDEM predicted 647 locations where runoff would theoretically cross a road (Figure

52). Of these 647 predicted culvert locations 275 (43%) contained a culvert or irrigation

canal, 495 (77%) showed direct evidence for model verification, 70 (11%) locations

showed neither evidence to confirm the model nor evidence to suggest model error, and

82 (13%) were considered erroneous. The uncertainty of the 70 locations was due to the

presence of extremely flat terrain, making it difficult to judge the appropriateness of the

predicted culvert location.

117

Extracting road induced dead drainages significantly reduced the watershed area for each

water quality sampling station (Table 5). Additionally, the hydrologically linked

watersheds became convoluted and patchy (Figures 53–55).

Table 5 RIDEM hydrologically linked watershed areas

Watershed Name	Watershed Area (Square km)		% of Gross Watershed
	Gross Watershed	Hydrologically Linked	Hydrologically Linked
Szeitna Drain	207.0	138.1	66.7
Piyami Drain	504.7	322.3	63.9
Battersea Drain	405.1	265.0	65.4

6.4 Discussion

The differences between the gross watershed areas derived using the conventional D8-

TOPAZ approach and RIDEM indicates that rural infrastructure (viz. roads, ditches,

culverts, irrigation canals, and siphons/flumes) significantly influences the size and shape

of watersheds in the study area. In fact, the watershed area discrepancies are much larger

than those reported here because the area comparisons did not include the headwaters of

the Oldman River, which is the source of irrigation water in the LNID (e.g., Chapter 5).

The results also suggest that rural infrastructure influences watersheds with small

drainage areas (i.e., Szeitna Drain and Battersea Drain) to a greater extent than larger

ones (i.e., Piyami Drain). As a result, the errors associated with conventional watershed

delineation processes are presumably very large for locations with small upstream

contributing areas.

The characteristics of the gross watershed boundaries delineated with RIDEM became

atypical of prairie watersheds unaffected by anthropogenic disturbances. Instead of

118

forming shapes similar to water drops, the watersheds became comprised of several

fragmented areas linked by the irrigation canal network. The watershed boundaries

derived using the conventional D8-TOPAZ flow direction algorithm (Figures 49-51) are,

however, likely to coincide with the watershed boundaries prior to the construction of

roads and irrigation canals for two reasons:

- The sampling interval of the elevation points used to interpolate the DEM was too

    coarse to resolve anthropogenic terrain features (or rural infrastructure). Therefore,

    the DEM was more indicative of the landscape terrain prior to the construction of

    roads, ditches, culverts, and irrigation canals.

- The conventional grid-based flow direction algorithm D8-TOPAZ has not been

    designed to model the divergent flow patterns that occur within the distribution

    system of the LNID. Therefore, the D8-TOPAZ algorithm is conceptually

    inaccurate in irrigated landscapes, but would be representative of flow paths in a

    natural setting.

While irrigation canals affected the gross watershed boundaries, roads influenced intra-

watershed transport, significantly affecting the portion of the gross watersheds linked to

the outlet by a direct drainage pathway. The consistency between the predicted runoff

road crossing locations, and observations made in the field, verified the accuracy of the

drainage modifications made by the REA. The hydrologically linked areas of the gross

watersheds following the extraction of road induced dead drainages were convoluted, and

contained regions that would not contribute runoff to the watershed outlet (Figures 53-

55). Additionally, because a portion of the canal mainline was common to each

watershed, and the topography in each watershed is similar, the proportion of each gross watershed linked to the outlet was nearly equal. The hydrologically linked watershed maps also indicate that even remote areas of the watershed are adequately linked to the watershed outlet to potentially influence water quality. In contrast, areas directly adjacent to the watershed stream channel may be disconnected from the outlet by the presence of roads that act as barriers to overland flow. Consequently, remote areas of the watershed may be as much of a pollution problem as areas immediately adjacent to watershed outlets.

The sensitivity of the watersheds to small-scale terrain features (e.g., ditches) indicated that the scale of the DEM was insufficient to delineate the watersheds accurately using a conventional grid-based flow direction algorithm. This conclusion supports the statements made previously regarding the tendency of grid-based runoff routing models to produce grossly simplified drainage patterns (Moore et al., 1991; Grayson et al., 1993; Band and Moore, 1995). However, the incorporation of ancillary data effectively reduced the scale of runoff transport pathways modeled below the scale governed by the DEM alone. Additionally, RIDEM improved the conceptual accuracy of the conventional grid-based flow direction algorithm D8-TOPAZ by modelling divergent flow at canal intersections. Implementing RIDEM would, therefore, significantly affect the results of analyzing overland flow paths and the distance of suspected pollution areas to streams. This type of spatial analysis has been used previously to provide insights into runoff fate and land-use impacts on water quality (e.g., Cluis et al., 1996; Tian et al., 2002; Endreny, 2002).

120

Band and Moore (1995) described the development of fully distributed parameter hydrological models as little more than "academic exercises" because of the difficulty collecting terrain data (among others) of sufficient detail to characterize a watershed. The flow direction matrices derived using RIDEM could, however, be incorporated into existing grid-based models to enhance the scale of runoff transport process. Models such as ANSWERS (Areal Nonpoint Source Watershed Environment Response Simulation) (Bouraoui and Dillaha, 2000), TOPLATS (Topographically-Based Land-Atmosphere Transfer Scheme) (Endreny and Wood, 1999), or GRISTORM (Grid-Based Variable Source Area Storm Runoff Model) (Kim and Steenhuis, 2001) could be used to determine event-based effective watershed areas. Alternatively, much simpler models that utilize grid-based flow direction matrices such as the Contributing Area-Dispersal Area (CADA) Export Coefficient (EC) model (Endreny, 2002) could be implemented to determine locations where pollutant loads enter local receiving waters unfiltered. Models such as the fecal coliform model presented by Tian et al. (2002) could also be used to assess biological pathogen transport.

The accuracy of drainage patterns derived with the RIDEM model is dependent upon the quality of the DEM. The increasing availability of high resolution DEMs will improve the results conventional grid-based flow direction algorithms produce, as well as the results of the RIDEM model. However, the inadequacy of the grid-data structure to represent hydrologically significant terrain features (Schneider, 2001) ensures ancillary

121

data models such as RIDEM provide superior results to conventional grid-based routing algorithms.

6.5 Conclusion

The results of this study show that RIDEM can be used to downscale grid-based drainage patterns. Because the model incorporates commonly available ancillary data (viz. roads, ditches, culverts, irrigation canals, and siphons/flumes) the implementation of RIDEM is both practical and cost effective. The application potential of RIDEM, therefore, extends beyond the identification of potential water pollution source areas. The model could also be used to aid erosion prediction, soil moisture modelling, and insect forecasting, among others.

Based on the differences between the gross watersheds derived using the conventional D8-TOPAZ flow direction algorithm and RIDEM two major conclusions were made:

- When regional scale DEMs do not represent rural infrastructure, overland flow patterns derived with conventional grid-based flow direction algorithms are over-simplified.
- The D8-TOPAZ flow direction algorithm fails to predict watershed structure accurately in irrigated landscapes.

Although some would argue that the inadequate representation of rural infrastructure within the DEM was due to an insufficient horizontal grid cell size, in actuality, it was the original photogrammetric sampling interval of the elevation points that ultimately restricted the landscape features that were expressed in the DEM (Zhang and

Montgomery, 1994; Gao, 1998; Huang, 2000; Gong et al., 2000; Kienzle, 2004).

Therefore, incorporating ancillary data to accurately derive overland flow paths at the

desired scale was a necessity.

Field observations showed that several small ditches and return flow channels were

located in the study area, but not included in the LNID database. Considering the effect

irrigation canals imposed on the landscape drainage patterns, these features need to be

incorporated into the canal database to maximize the accuracy of the simulated drainage

paths. Several authors have criticized discretized flow direction algorithms including D8-

TOPAZ, claiming algorithms supporting dispersion are more realistic on hillslopes

(Quinn et al., 1991; Freeman, 1991; Desmet and Govers, 1996; Tarboton, 1997). We,

however, suspect that at the regional scale, the extent of watersheds in this study area is

overwhelmingly more sensitive to rural infrastructure than the selection of grid-based

flow direction algorithm. Research is currently underway to test this hypothesis. Errors

associated with the prediction of road crossing culvert locations also suggested that some

terrain variation was not represented in the DEM. As a result, an point-elevation data set

collected at a sampling interval less than 100-m would enable the RIDEM model to

capture smaller scale landscape transitions.
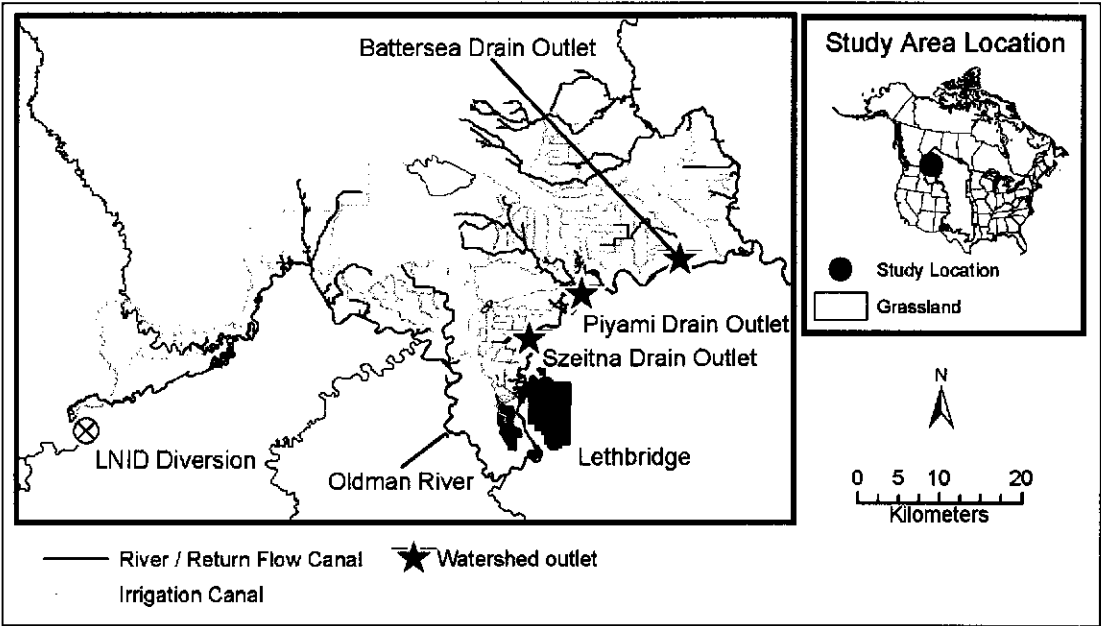
Figure 44 RIDEM study area overview
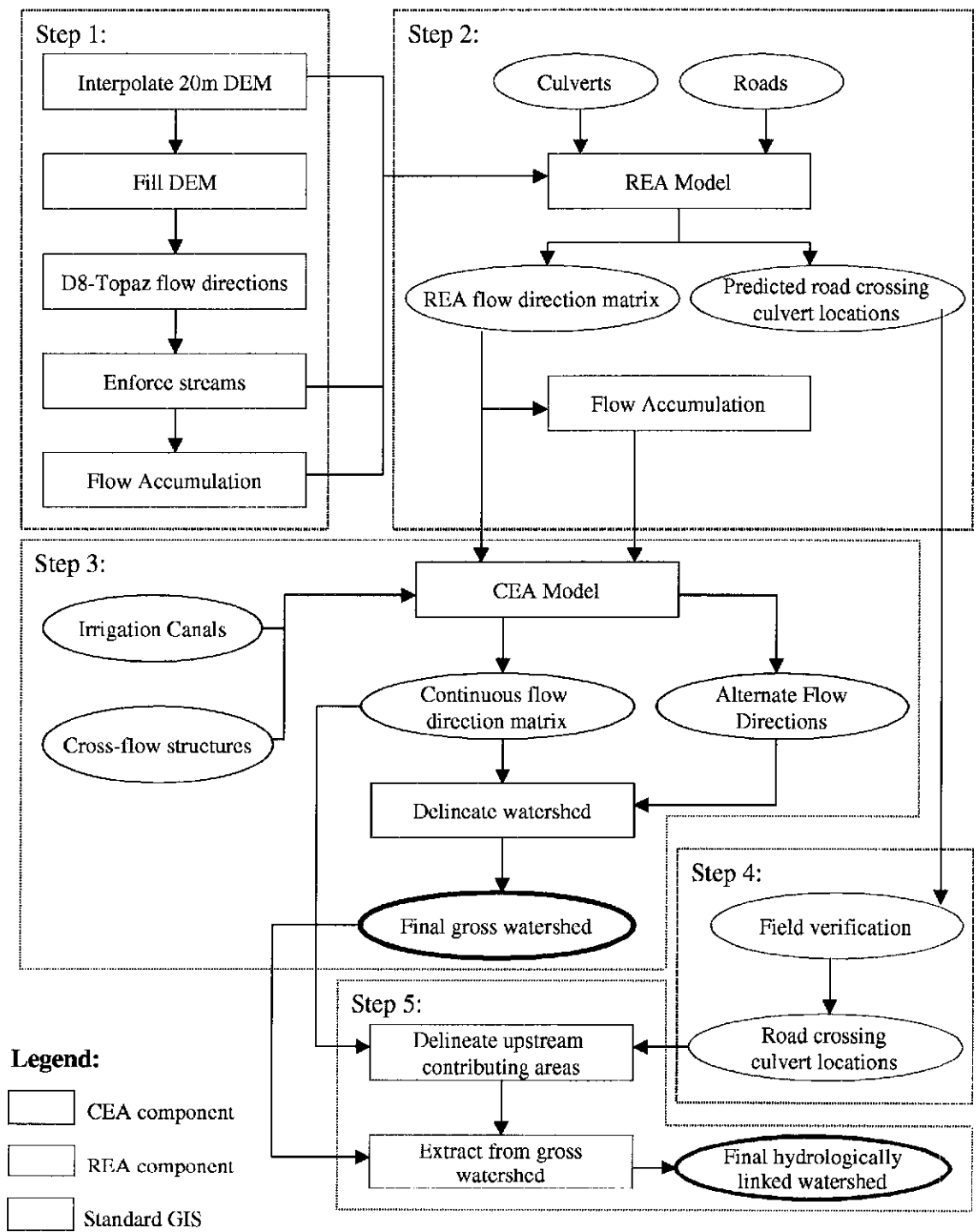
Figure 45 RIDEM methodology flow chart

125
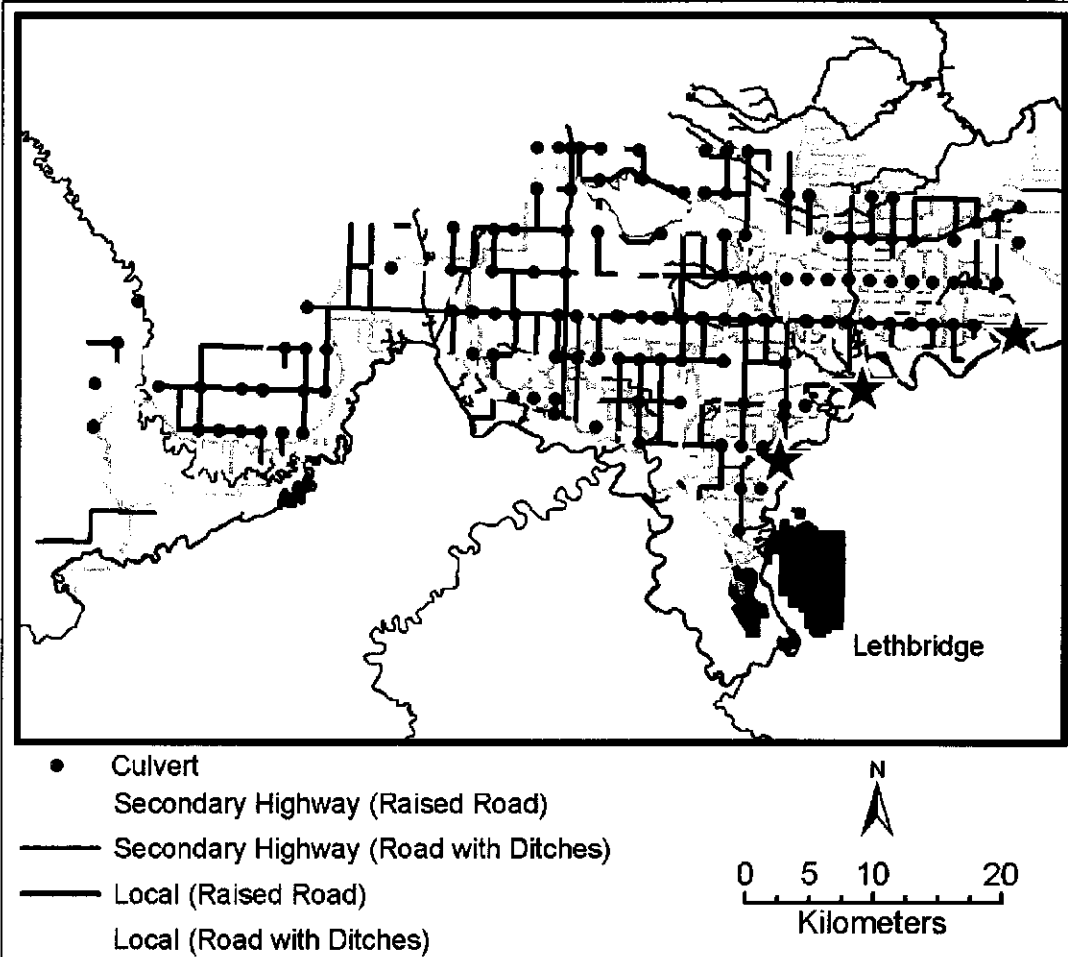
Figure 46 REA input parameters
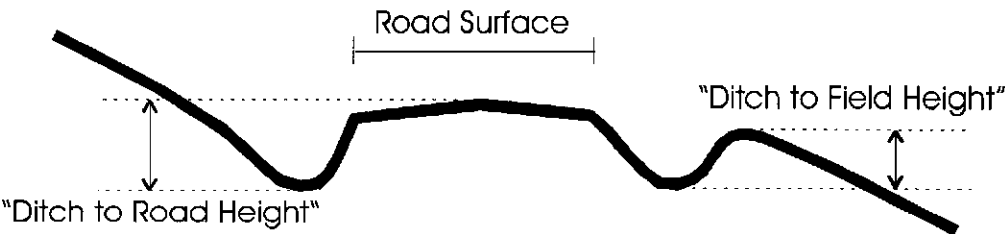
Figure 47 Conceptual diagram of a road cross-sectional profile used for the REA.

126
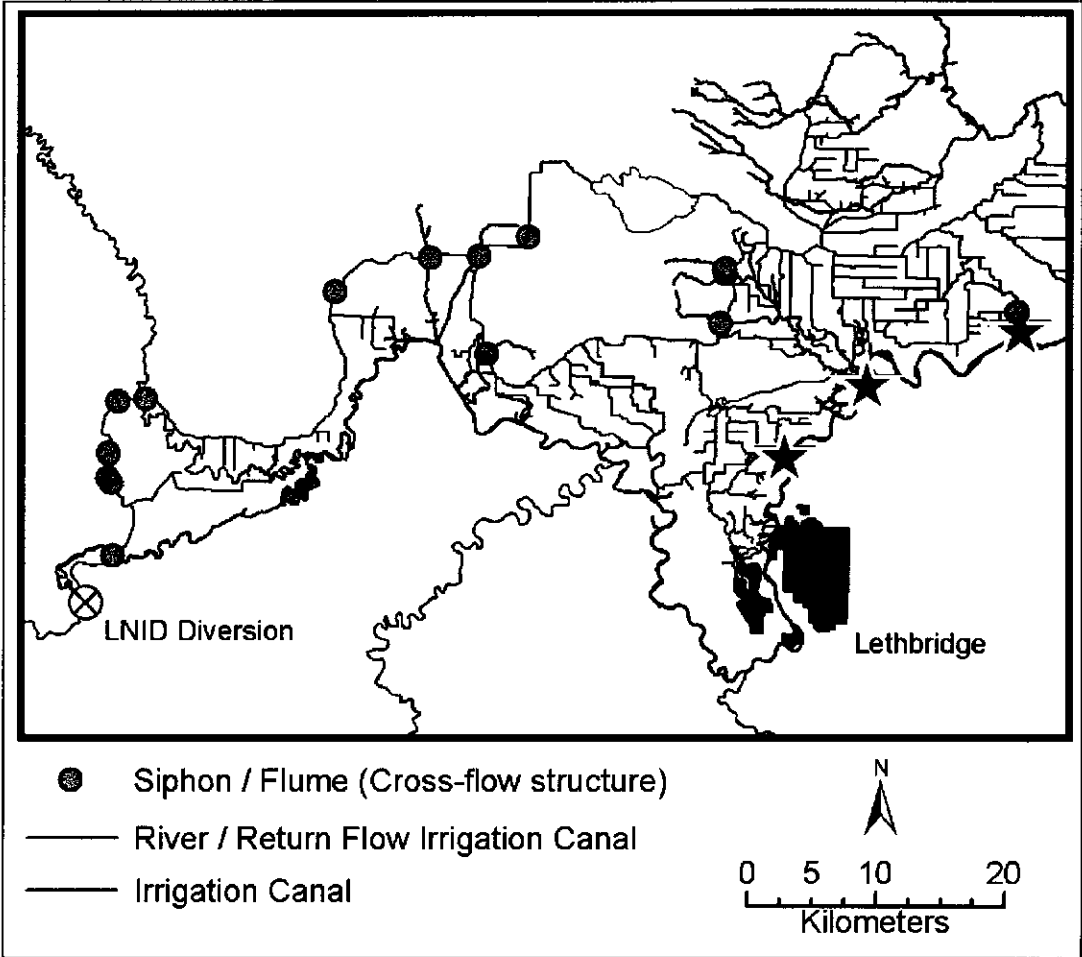
Figure 48 CEA input parameters.

127
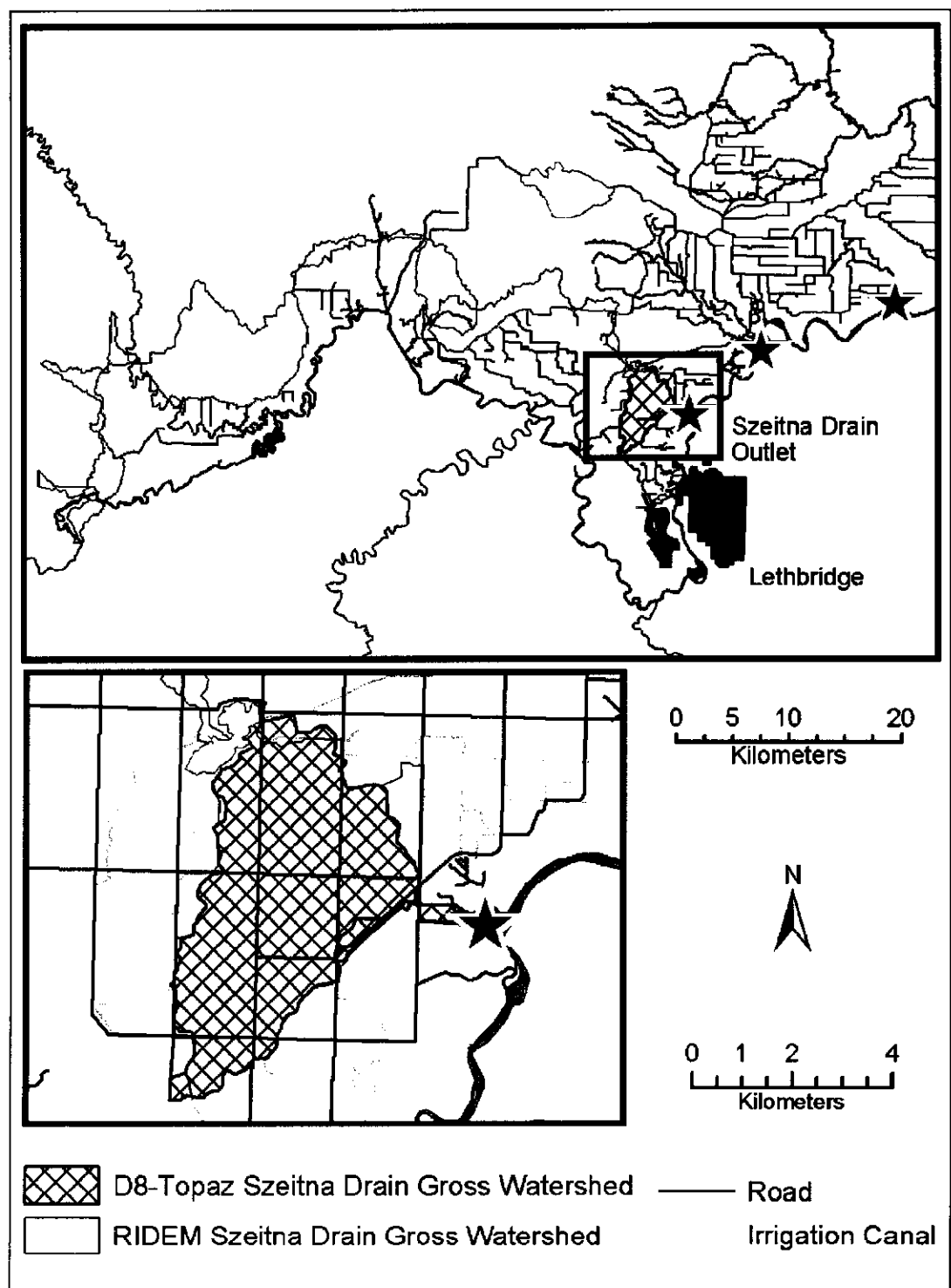
Figure 49 Szeitna Drain gross watershed areas derived using the D8-TOPAZ and the RIDEM models

The overview map (top image) shows the complete watershed. The extent of the inset map (lower image) is limited to the area of the conventional D8-TOPAZ derived watershed that shows the effects of roads on the watershed boundary.
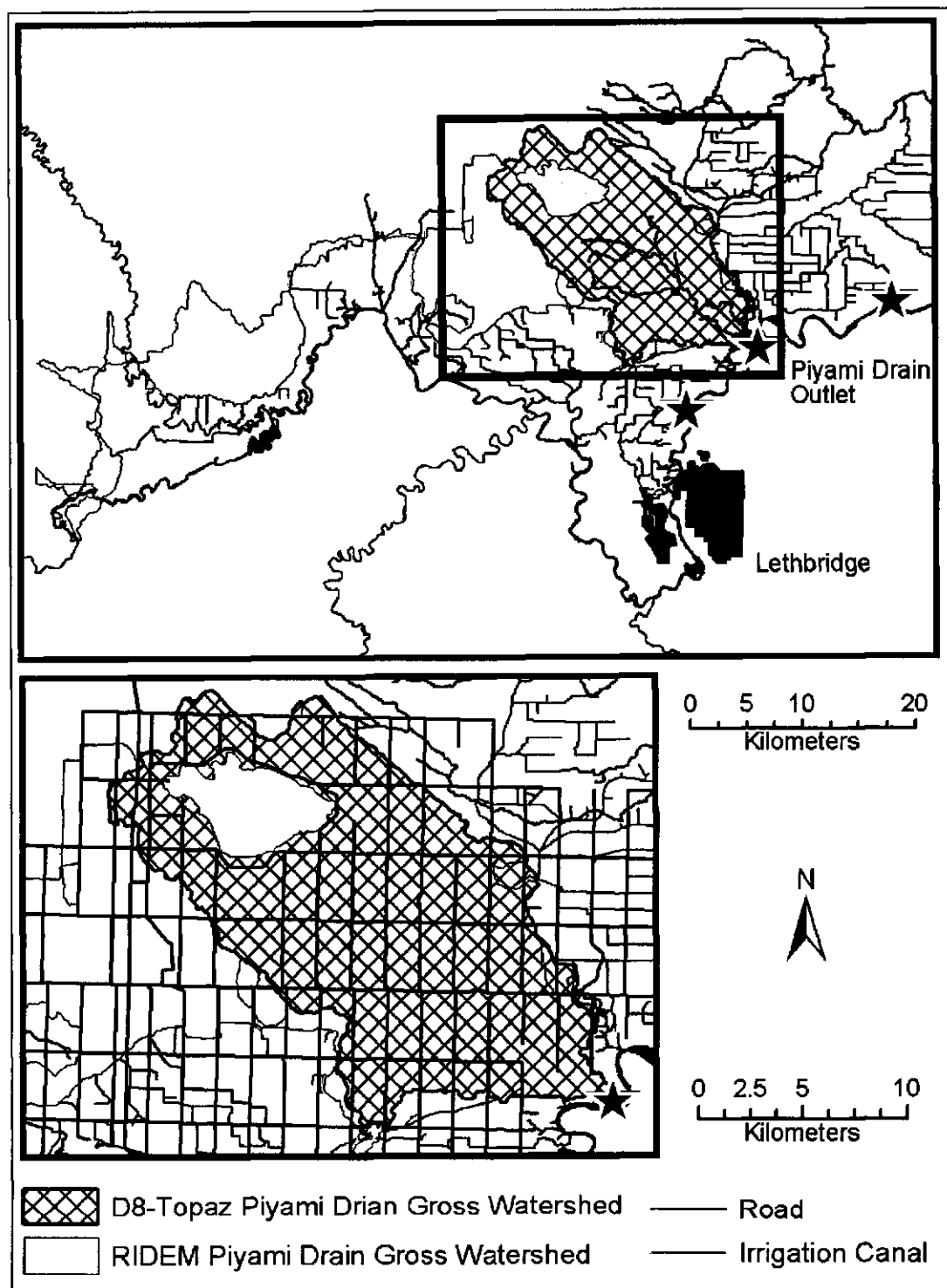
Figure 50 Piyami Drain gross watershed areas derived using the D8-TOPAZ and the RIDEM models

The overview map (top image) shows the complete watershed. The extent of the inset map (lower image) is limited to the area of the conventional D8-TOPAZ derived watershed that shows the effects of roads on the watershed boundary.

129
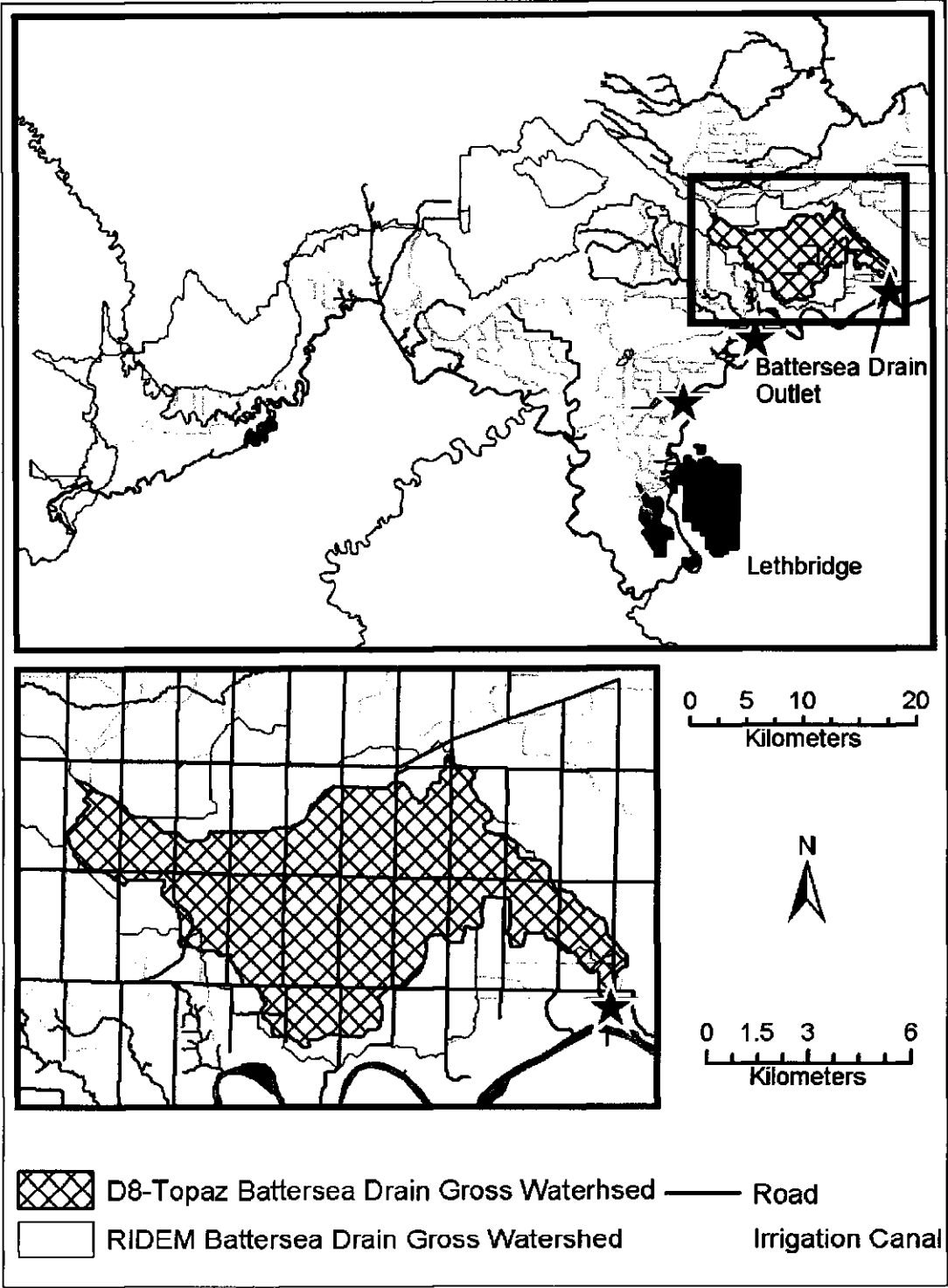
Figure 51 Battersea Drain gross watershed areas derived using the D8-TOPAZ and the RIDEM models

The overview map (top image) shows the complete watershed. The extent of the inset map (lower image) is limited to the area of the conventional D8-TOPAZ derived watershed that shows the effects of roads on the watershed boundary.

130
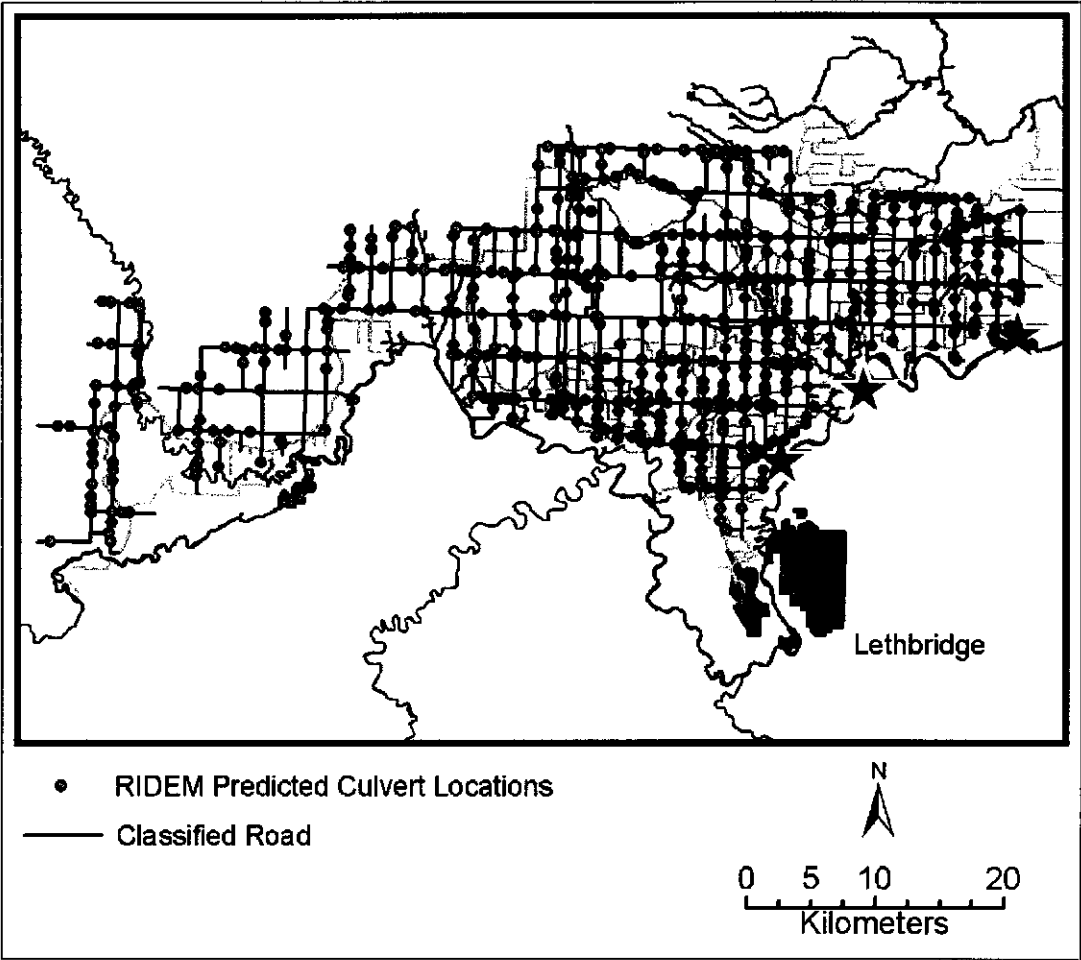
Figure 52 Predicted runoff road crossing culvert locations
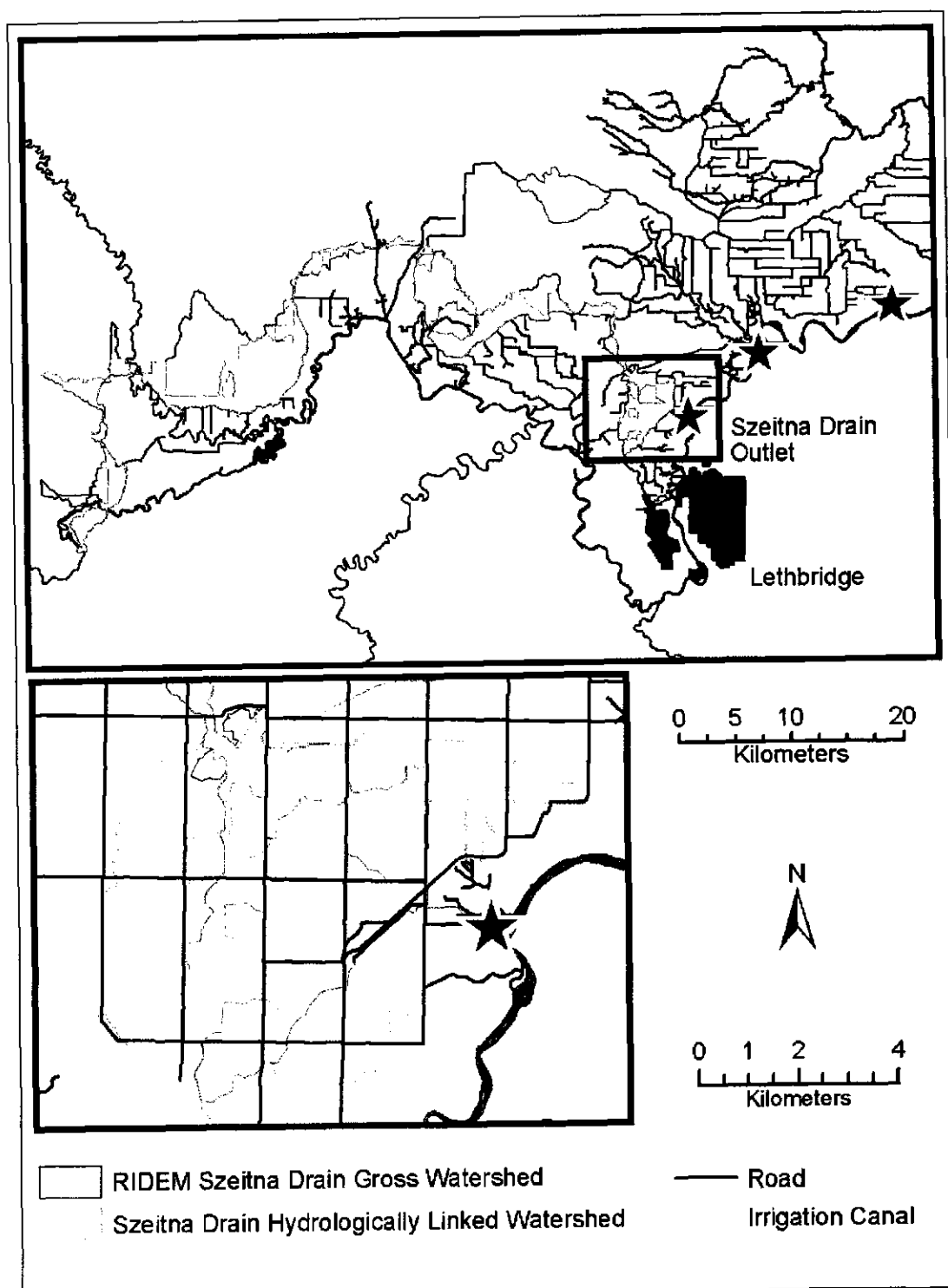
Figure 53 Szeitna Drain hydrologically linked watershed

132
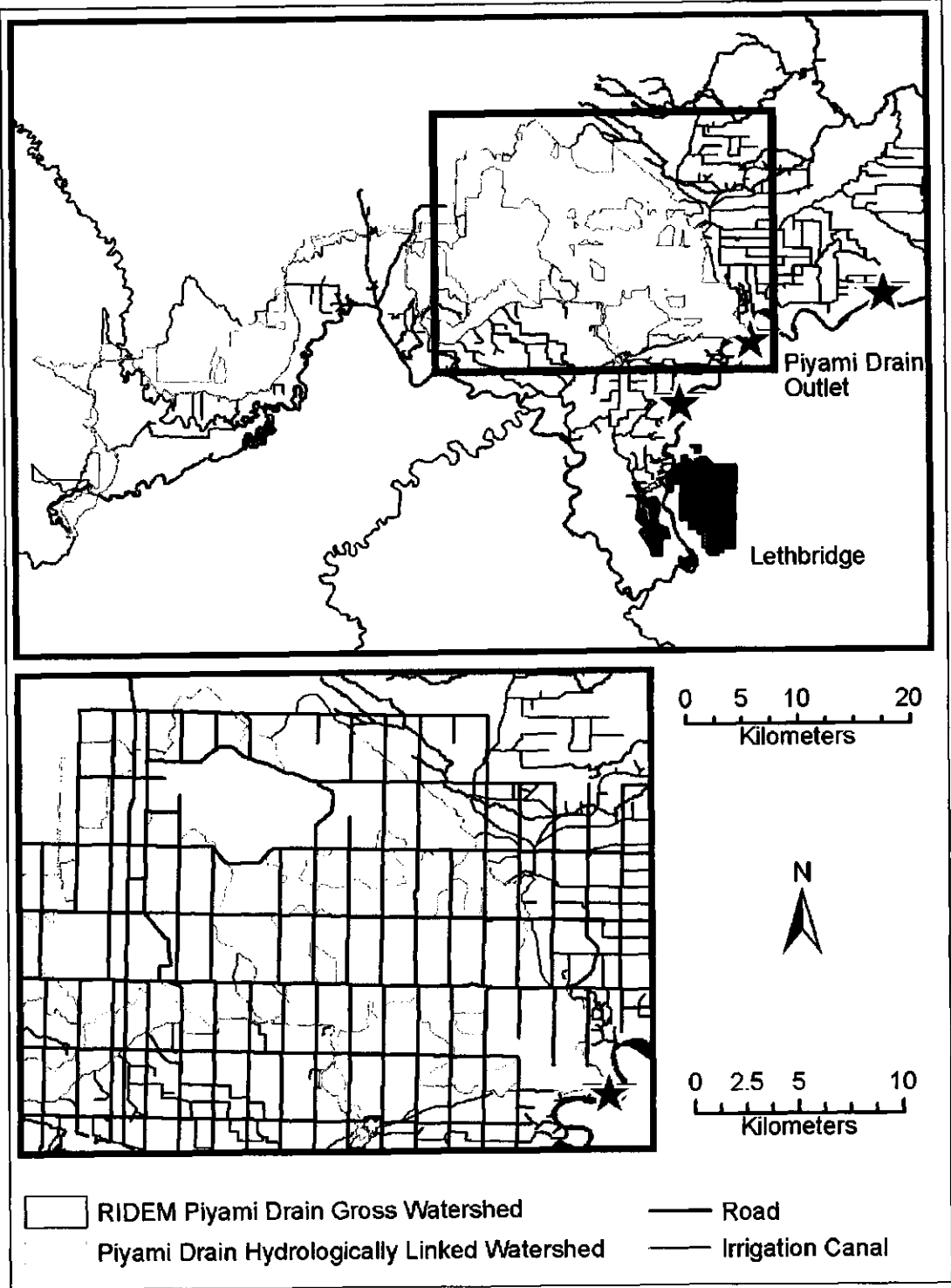
Figure 54 Piyami Drain hydrologically linked watershed
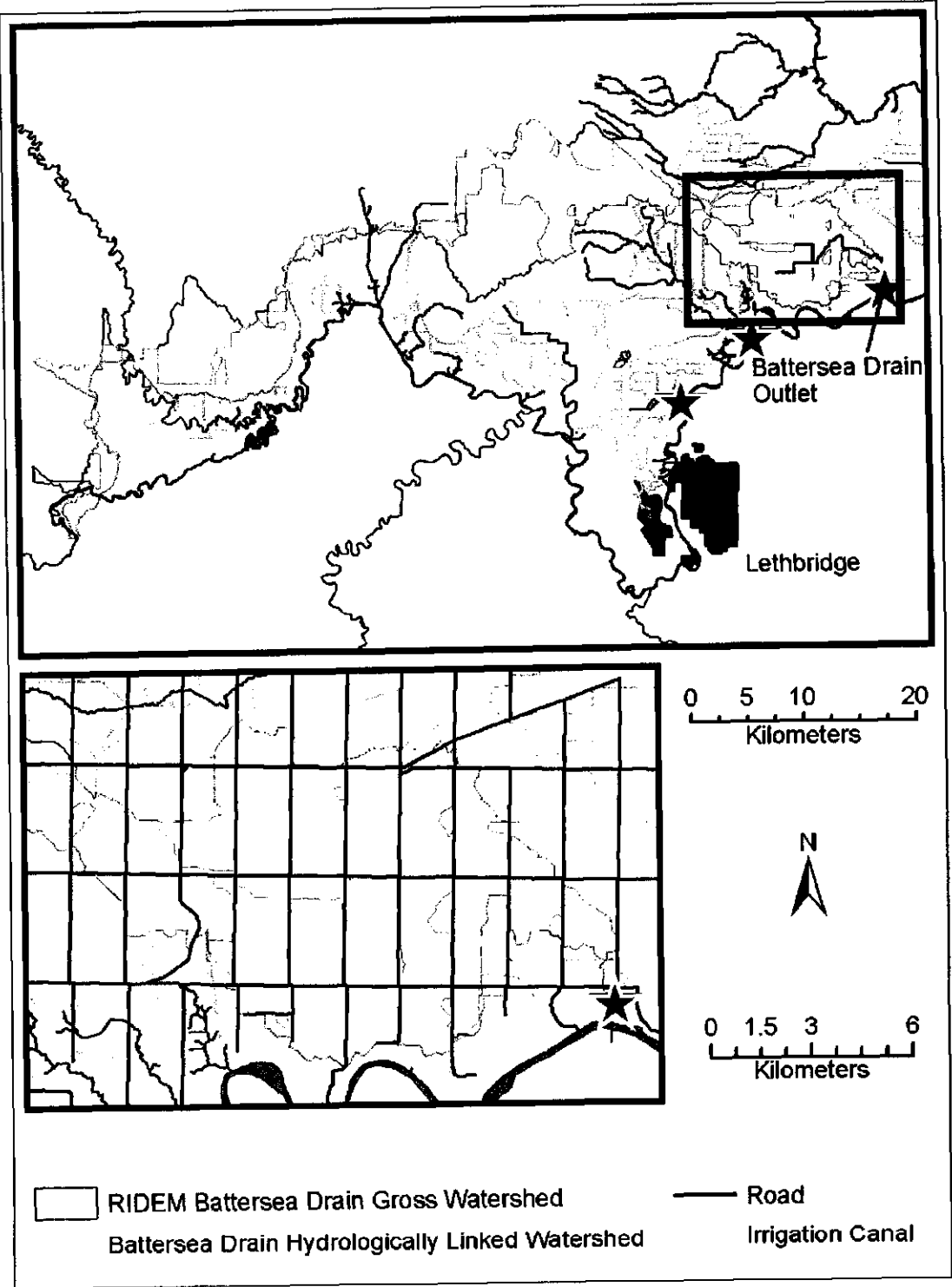
Figure 55 Battersea Drain hydrologically linked watershed

Chapter 7

7 Conclusion

7.1 Summary

The effect of rural infrastructure on runoff transport pathways was studied in a grassland

region of southern Alberta, Canada, where the quality of local surface water quality has

been degraded. The area is highly fragmented by a network of roads and irrigation canals

that have significantly modified runoff transport pathways. Because these features are

too small to be represented in standard point-elevation data sets, they could not be

accounted for with conventional grid-based runoff routing procedures. As a result,

previous attempts to delineate the runoff contributing areas for several water-quality

monitoring stations were inaccurate. These inaccuracies lead researchers to question the

predicted associations between land use and water quality that were based on these

preliminary watersheds. In a study seeking associations between *Escherichia coli*

O157:H7 and *Salmonella spp.* Johnson et al. (2003) stated that the predictive capability

of their model was limited because it did not account for runoff transport pathways.

By incorporating commonly available ancillary data to modify grid-based drainage

networks, RIDEM, a computer model created during the completion of this research,

downscaled the grid-based drainage paths, thereby enabling the accurate delineation of

watershed boundaries. Because the accuracy of the runoff flow paths created with

RIDEM were significantly more accurate than those created using conventional

processes, RIDEM may also benefit studies that attempt to predict: soil moisture, soil

135

salinization, erosion potential, sedimentation rates, catchment runoff response, non-point source pollution, optimal fertilizer and pesticide application rates, and biological productivity.

7.1.1 Roads, Ditches, and Culverts

Landscape drainage patterns that resulted from elevation changes and drainage culverts installed during the construction of roads was modeled. A case study revealed that 94% of the Piyami Drain watershed delineated with the conventional D8 flow routing algorithm, and the Piyami Drain watershed delineated with the road enforcement algorithm (REA), coincided. This result indicated that roads have a moderate capacity to affect watershed boundaries at the regional scale. At the field scale, however, runoff patterns between these two methodologies differed significantly. Runoff was predicted to flow across 74% of all grid cells representing roads with the conventional D8 flow direction algorithm. After accounting for roads, ditches, and culverts at road intersections with the REA, this proportion decreased to less that 1%. Although roads affected the gross watershed boundaries, the impact of road construction on runoff transport pathways was, therefore, much more pronounced within each watershed.

7.1.2 Irrigation canals, and Siphon / Flume Structures

The construction of irrigation canals has created highly modified drainage patterns that are not accurately simulated with conventional grid-based flow routing procedures. The results of implementing the canal component of RIDEM, the canal enforcement

algorithm (CEA), showed that irrigation canals and siphon/flume structures altered both intra and inter-watershed runoff patterns significantly. A case study revealed that less than 4% of the Piyami Drain watershed delineated with a conventional grid-based flow direction algorithm, and the CEA, coincided. Thus, in irrigated landscapes conventional grid-based flow direction algorithms should not be implemented to simulate runoff flow patterns.

7.1.3 Rural Infrastructure

The RIDEM model, which integrates the REA and CEA, was used to delineate the watersheds for three water quality monitoring stations (viz. Szietna, Piyami, and Battersea Drain). Considering only the watershed areas downstream of the LNID diversion, the watershed areas common to both the conventional grid-based flow direction algorithm and RIDEM ranged from 10-49%. These differences indicate that the scale of this study was not within the range of scales at which the DEM is adequate to delineate watersheds using conventional methods. Thus, the runoff flow patterns derived from the regional scale DEM were grossly simplified, supporting the warnings of potential scale mismatch made earlier by Moore et al. (1991), Grayson et al. (1993), and Band and Moore (1995). It was also concluded that approximately one third of the gross watershed areas were unlikely to reach the watershed outlet due to road induced dead drainages. Contaminants originating upstream of these dead drainage locations would not, therefore, effect the water quality at the watershed outlets via runoff. The differences between the runoff flow networks produced by RIDEM and the conventional

137

grid-based routing algorithm indicate that all biophysical processes modeled, that rely on

runoff flow directions, would also differ significantly between these two methodologies.

7.2 Future Research

The ability of RIDEM to produce realistic runoff flow patterns, where conventional grid-

based flow routing failed, enables the completion of smaller scale runoff studies.

Therefore, RIDEM improves on the previous attempts to delineate watersheds for several

water-quality monitoring stations in the Oldman River watershed. However, foregoing

studies and field observations made during the completion of this thesis indicate that

three additional sources of drainage variation need to be researched, including:

- small-scale ditches at field boundaries,

- alternate flow direction algorithms, and

- elevation uncertainty in the DEM.

Field observations indicated that several small-scale ditches at field boundaries (i.e.,

irrigation canals and return flow channels) were located in the study area but not included

in the LNID database (Figure 56). Considering the effect irrigation canals imposed on

the landscape drainage patterns, these ditches need to be incorporated to maximize the

accuracy of the simulated drainage paths.

Although discretized flow direction algorithms including D8-TOPAZ have been

criticized (Quinn et al., 1991; Freeman, 1991; Costa-Cabral and Burges, 1994; Desmet

and Govers, 1996; Tarboton, 1997), results emanating from this research lead to the

138

conclusion that at the regional scale, the extent of watersheds in this study area is overwhelmingly more sensitive to rural infrastructure than the selection of the most appropriate grid-based flow direction algorithm. The two main reasons are:

- Roads, ditches, culverts, and irrigation canals are permanent features that are sufficiently large to convey runoff. Therefore, the drainage network these features create overrides the flow directions defined by the naturally occurring topographic slope.

- The road network is relatively dense, therefore, the area in which discrepancies would arise from the selection of flow routing algorithm is limited.

However, coupling the enforced drainage network produced with RIDEM, along roads and within irrigation canals, with a multiple flow direction algorithm that minimizes dispersion, such as D-Infinity (Tarboton, 1997), could be an effective method to improve the simulation of both concentrated and hillslope processes. Additionally, new algorithms such as the D8-LTD (Orlandini et al., 2001) may significantly improve the accuracy of runoff flow paths on hillslopes that are not aligned with the grid cell matrix, while avoiding the complexities and inaccuracies introduced through dispersion.

Similar to all hydrological models, the scale of the data input into RIDEM determines the scale of the output results. Improving the sampling interval of the point-elevation dataset in the study area would enable the creation of a DEM that captures high frequency terrain variation that significantly impacts runoff transport in the grasslands of southern Alberta. Similarly, the propagation of errors due to vertical inaccuracies in the DEM introduces uncertainty to DEM-derived runoff transport pathways (Endreny and Wood, 2001).

139

Stochastic modeling approaches that attempt to capture this component of uncertainty could be implemented to create probability maps quantifying the likelihood of runoff contribution (e.g., Endreny and Wood, 2001). Ancillary data models, such as RIDEM will, however, continue to produce runoff flow patterns more effectively than current grid-based processes due to the inadequacy of the grid-data structure and conceptual inaccuracies of grid-based flow direction algorithms.

a)
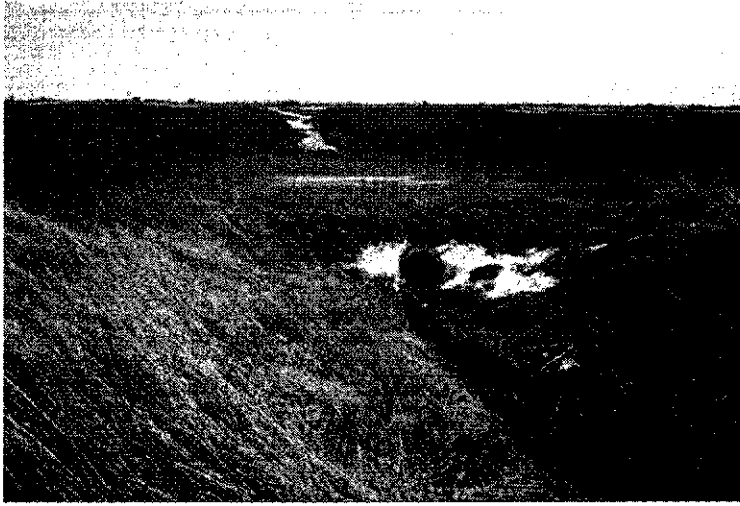
b)

Figure 56 Small-scale ditches within the LNID

141

8 References

Alberta Transportation and Utilities. (1996) Highway geometric design guide, http://www.trans.gov.ab.ca (July 1, 2002).

Alberta Agriculture, Food and Rural Development, Irrigation and Resource Management Division Irrigation Branch. 1997. Irrigation districts and major irrigation works within southern Alberta. Map.

Alberta Agriculture, Food and Rural Development. (2003) September estimate of production of 2002 principal field crops in Alberta, http://www1.agric.gov.ab.ca/$department/deptdocs.nsf/all/sdd5529?opendocument (April 25, 2003).

Asante, K., Olivera, F., Maidment, D., Famiglietti, J. (1999) Digital atlas of the world water balance, Version 3.0. Center for Research in Water Resources, The University of Texas at Austin, http://www.crwr.utexas.edu/gis/gishydro99/atlas/atlas.htm (June 6, 2003).

Band, L. E. (1986) Topographic partition of watersheds with digital elevation models. Water Resources Research, 22, 15-24.

Band, L. E., Moore, I. D. (1995) Scale: landscape attributes and geographical information systems. In: Scale issues in hydrological modelling, edited by J. D. Kalma and M. Sivapalan, pp. 159-179. Toronto, Ontario: Wiley.

Beven, K. (1995) Linking parameters across scales: subgrid parameterization and scale dependent hydrological models. Hydrological Processes, 9, 507-525.

Bouraoui, F., Dillaha, T. A. (2000) ANSWERS-2000: non-point-source nutrient planning model. Journal of Environmental Engineering, 126, 1045-1055.

Brasington, J., Richards, K. (1998) Interactions between model predictions, parameters and DTM scales for TOPMODEL. Computers & Geosciences, 24, 299-314.

Burrough, P. A., McDonnell, R. A. (1988) Principles of geographical information systems. New York, New York: Oxford.

Cerdan, O., Souchere, V., Lecomte, V., Couturier, A., Le Bissonnais, Y. (2001) Incorporating soil surface crusting processes in an expert-based runoff model: sealing and transfer by runoff and erosion related to agricultural management. Catena, 46, 189-205.

Chicalo, G. M. (2002) The Chicalo Archives - A Journey Through Time. http://www.chicalo.com/chicalo/subpages/canada_free_land.htm (September 17, 2003).

Cluis, D., Martz, L., Quentin, E., Rechatin, C. (1996) Coupling GIS and DEM to classify the hortonian pathways of non-point sources of the hydrographic network. Proceedings of the HydroGIS 96: Applications of Geographic Information Systems in Hydrology and Water Resources Management held in Vienna, Austria, in April 1996, no. 235.

Cooke, S. E., Mitchell, P., Roy, L., Gammie, L., Olson, M., Shepel, C., Heitman, T. L., Hiltz, M., Jackson, B., Stanley, S., Chanasyk, D. (2002) Relationship between beef production and waterborne parasites (Cryptosporidium spp. And Giardia spp.) in the North Saskatchewan River basin, Alberta, Canada. Alberta Agriculture, Food and Rural Development, Edmonton, Alberta, CABIDF Project No. 97AB080.

Costa-Cabral, M. C., Burges, S. J. (1994) Digital elevation model networks (DEMON): a model of flow over hillslopes for computation of contributing and dispersal areas. Water Resources Research, 30, 1681-1692.

Crowther, J., Kay, D., Wyer, M. D. (2002) Faecal-indicator concentrations in waters draining lowland pastoral catchments in the UK: relationships with land use and farming practices. Water Research, 36, 1725-1734.

De Roo, A. P. J., Jetten, V. G. (1999) Calibrating and validating the LISEM model for two data sets from the Netherlands and South Africa. Catena, 37, 477-493.

Desmet, P. J. J., Govers, G. (1996) Comparison of routing algorithms for digital elevation models and their implications for predicting ephemeral gullies. Geographical Information Systems, 10, 311-331.

Desmet, P. J. J., Poesen, J., Govers, G., Vandaele, K. (1999) Importance of slope gradient and contributing area for optimal prediction of the initiation and trajectory of ephemeral gullies. Catena, 37, 377-392.

Dijck, S. V. (2000) Effects of agricultural land use on surface runoff and erosion in a Mediterranean area. Netherlands: University of Utrecht.

Dingman, S. L. (2002) Physical Hydrology second edition. New Jersey, New York: Prentice-Hall, Inc.

Endreny, T. A., Wood, E. F. (1999) Distributed watershed modeling of design storms to identify nonpoint source loading areas. Journal of Environmental Quality, 28, 388-397.

Endreny, T. A., Wood, E. F. (2001) Representing elevation uncertainty in runoff modelling and flowpath mapping. Hydrological Processes, 15, 2223-2236.

Endreny, T. A. (2002) Forest buffer strips mapping the water quality benefits. Journal of Forestry, January/February, 35-40.

Environment Canada. (1998) Canadian daily climate data, CDCD V1.01, Climate Information Brach, Atmospheric Environmental Service. Ottawa, Ontario.

Fairchild, J., Leymarie, P. (1991) Drainage networks form grid digital elevation models. Water Resources Research, 27, 709-717.

Finke, P. A., Bierkens, M. F. P. (2002) Choosing appropriate upscaling and downscaling methods for environmental research. Proceedings of the international conference on agricultural effects on ground and surface waters: research at the edge of science and society held in Wagenengen, Netherlands, on October 1 – October 4 2000, pp. 405-409.

Freeman, T. G. (1991) Calculating catchment area with divergent flow based on a regular grid. Computers & Geosciences, 17, 413-422.

Gallant, J. C., Wilson, J. P. (1996) TAPES-G: a grid-based terrain analysis program for the environmental sciences. Computers & Geosciences, 22, 713-722.

Gallant, S. (2002) Waters haven't yet peaked. Lethbridge Herald, June 10. Lethbridge, Alberta, pp A1.

Gannon, V. P. J., Graham, T. A., Read, S., Ziebell, K., Muckle, A., Mori, J., Thomas, J., Selinger, B., Townsend, I., Byrne, J. (2002) Bacterial pathogens in rural water supplies in southern Alberta. Proceedings of the First International Conference on Water and Health – ICWH held in Ottawa, Ontario, in Sept 2002.

Gao, J. (1998) Impact of sampling intervals on the reliability of topographic variables mapped from grid DEMs at a micro-scale. Geographical Information Science, 12, 875-890.

Garbrecht, J., Martz, L. W. (1996) Comment on "Digital elevation model grid size, landscape representation, and hydrologic simulations" by Weihua Zhang and David R. Montgomery. Water Resources Research, 32, 1461-1462.

Garbrecht, J., Martz, L. W. (1997) The assignment of drainage direction over flat surfaces in raster digital elevation models. Journal of Hydrology, 193, 204-213.

Garbrecht, J., Martz, L. W. (2000) Digital elevation models issues in water resources modeling. In: Hydrologic and hydraulic modeling support, edited by Dr. D. Maidment and Dr. D. Djokic, pp. 1-27. Redlands, California: ESRI Press.

Garbrecht, J., Ogden, F. L., DeBarry, P. A., Maidment, D. R. (2001) GIS and distributed watershed models. I:data coverages and sources. Journal of Hydrological Engineering, November/December, 506-514.

144

Gong, J., Li, Z., Zhu, Q., Sui, H., Zhou, Y. (2000) Effects of various factors on the accuracy of DEMs: an intensive experimental investigation. Photogrammetric Engineering & Remote Sensing, 66, 1113-1117.

Goodwin, R. B., Martin, F. R. J. (1975) Calculation of gross and effective drainage areas for the prairie provinces. Proceedings of the Canadian Hydrology Symposium held in Winnipeg, Canada, pp. 5.

Grayson, R. B., Bloschl, G., Barling, R. D., Moore, I. D. (1993) Process, scale and constraints to hydrological modelling in GIS. Proceedings of the HydroGIS 93: Applications of Geographic Information Systems in Hydrology and Water Resources held in Vienna, Austria, in April 1999, no. 211.

Guenette, M. (2002) Haynes creek watershed study. Alberta Agriculture Food and Rural Development, http://www.agric.gov.ab.ca/sustain/water/wq11.html (June 10, 2003).

Gyasi-Agyei, Y., Willgoose, G., De Troch, F. P. (1995) Effects of vertical resolution and map scale of digital elevation models on geomorphological parameters used in hydrology. Hydrological Processes, 9, 363-382.

Henning, M. (pers. comm.) Highway Geomatics. Alberta Transportation and Utilities. Edmonton, Alberta.

Huang, Y. D. (2000) Evaluation of information loss in digital elevation models with digital photogrammetric systems. Phtotogrammetric Record, 16, 781-791.

Hutchinson, M. F. (1989) A new procedure for gridding elevation and stream line data with automatic removal of spurious pits. Journal of Hydrology, 106, 211-232.

Hyland, R., Byrne, J., Selinger, B., Graham, T., Thomas, J., Townsend, I., Gannon, V. (2003) Spatial and temporal distribution of fecal indicator bacteria within the Oldman River basin of southern Alberta, Canada. Water Quality Resources Journal, 38, 15-32.

James, D. 1980. United States fruit and vegetable harvest projections - 1990. USDA-1007. Washington, D.C.: GPO.

Jensen, J. R. (1996) Introductory digital image processing a remote sensing perspective 2nd edition. Upper Saddle River, New Jersey, New York: Prentice Hall.

Jensen, S. K., Domingue, J. O. (1988) Extracting topographic structure from digital elevation data for geographic information system analysis. Photogrammetric Engineering and Remote Sensing, 54, 1593-1600.

Johnson, J. Y. M., Thomas, J. E., Graham, T. A., Townshend, I., Byrne, J., Selinger, B. L., Gannon, V. P. J. (2003) Prevalence of *Escherichia coli* o157:H7 and *Salmonella spp.*

145

In surface waters of southern Alberta and its relation to manure sources. Canadian Journal of Microbiology, 49, 326-335.

Jones, J. A., Swanson F. J., Wemple, B. C., Snyder, K. U. (1999) Effects of roads on hydrology, geomorphology, and disturbance patches in stream networks. Conservation Biology, 14, 76-85.

Juracek, K. (2001) Estimation of potential runoff-contributing areas. Proceedings of the Seventh Federal Interagency Sedimentation Conference held in Reno, Nevada, in March, v. 2, p. VII-26 to VII-33.

Kienzle, S. W. (2004) The effect of DEM raster resolution on first order, second order and compound terrain derivatives. Transactions in GIS, 8, In Press.

Kim, S. J., Steenhuis, T. S. (2001) GRIDSTORM: grid-based variable source area storm runoff model. American Society of Agricultural Engineers, 44, 863-875.

Kumler, M. P. (1994) An intense comparison of triangulated irregular networks (TINs) and digital elevation models (DEMs). Catographica, 31, 1-99.

La Marche, J. L., Lettenmaier, D. P. (2001) Effects of forest roads on flood flows in the Deschutes river, Washington. Earth Surface Processes and Landforms, 26, 115-134.

Lea, N. L. (1992) An aspect driven kinematic routing algorithm. In: Overland Flow: Hydraulics and Erosion Mechanics, edited by A. J. Parsons and A. D. Abrahams. pp 393-407. New York, Chapman & Hall.

Luce, C. H., Wemple, B. C. (2001) Introduction to special issue on hydrologic and geomorphic effects of forest roads. Earth Surface Processes and Landforms, 26, 111-113.

Ludwig, B., Boiffin, J., Chadoeuf, J., Auzet, A. V. (1995) Hydrological structure and erosion damage caused by concentrated flow in cultivated catchments. Catena, 25, 227-252.

Ludwig, B., Daroussin, J., King, D., Souchere, V. (1996) Using GIS to predict concentrated flow erosion in cultivated catchments. Proceedings of the HydroGIS 96: Applications of Geographic Information Systems in Hydrology and Water Resources Management held in Vienna, Austria, in April 1996, no. 235.

Mark, D. M. (1988) Network models in geomorphology. In: Modeling Geomorphological Systems, edited by M. G. Anderson, 73-97. New York, New York: John Wiley & Sons Ltd.

Martz, L. W., Garbrecht, J. (1992) Numerical definition of drainage network and subcatchment areas from digital elevation models. Computers and Geosciences, 18, 747-761.

146

Martz, L. W., Garbrecht, J. (1998) The treatment of flat areas and depressions in automated drainage analysis of raster digital elevation models. Hydrological Processes, 12, 843-855.

Martz, L, W., Garbrecht, J. (1999) An outlet breaching algorithm for the treatment of closed depressions in a raster DEM. Computers & Geosciences, 25, 835-844.

Montgomery, D. R., Foufoula-Georgiou, E. (1993) Channel network source representation using digital elevation models. Water Resources Research, 29, 3925-3934.

Montgomery, D. R. (1994) Road surface drainage, channel initiation, and slope instability. Water Resources Research, 30, 1925-1932.

Moore, I. D., Grayson, R. B. (1991) Terrain-based catchment partitioning and runoff prediction using vector elevation data. Water Resources Research, 27, 1177-1191.

Moore, I. D., Grayson, R. B., Ladson, A. R. (1991) Digital terrain modeling: a review of hydrological geomorphological, and biological applications. Hydrological Processes, 5, 3-30.

Morris, K. (pers. comm.) Operations Manager. Lethbridge Northern Irrigation District. Lethbridge, Alberta.

Nyssen, J., Poesen, J., Moeyersons, J., Luyten, E., Veyret-Picot, M., Deckers, J., Haile, M., Govers, G. (2002) Impact of road building on gully erosion risk: a case study from the northern Ethiopian highlands. Earth Surface Processes and Landforms, 27, 1267-1283.

O'Callaghan, J. F., Mark, D. M. (1984) The extraction of drainage networks from digital elevation data. Computer Vision, Graphics, Image Processing, 28, 323-344.

Olivera, F., Maidment, D. (1999) Geographic information systems (GIS)-based spatially distributed model for runoff routing. Water Resources Research, 35, 1155-1164.

ORBWQI (2000) Oldman river basin water quality initiative progress summary report September 2000. Oldman River Basin Water Quality Initiative, Lethbridge, Alberta.

Orlandini, S., Moretti, G., Franchini, M., Aldighieri , B., Testa E. B. (2003) Path-based methods for the determination of nondispersive drainage directions in grid-based digital elevation models. Water Resources Research, 39, 1144.

Prairie Farm Rehabilitation Administration, Hydrology Division. (1983) The determination of gross and effective drainage areas in the prairie provinces. Hydrology Report #104. Regina, Saskatchewan.

Quinn, P., Beven, K., Chevallier, P., Planchon, O. (1991) The prediction of hillslope flow paths for distributed hydrological modelling using digital terrain models. Hydrological Processes, 5, 59-79.

Quinn, P., Beven, K. J. (1993) Spatial and temporal predictions of soil moisture dynamics, runoff, variable source areas and evapotranspiration for Plynlimon, Mid-Wales. Hydrological Processes, 7, 425-448.

Quinn, P. F., Beven, K. J., Lamb, R. (1995) The In(a/tanβ) index: how to calculate it and how to use it within the TOPMODEL framework. Hydrological Processes, 9, 161-182.

Quinn, P. (2002) Models and monitoring: scaling-up cause-and-effect relationships in nutrient pollution to the catchment scale. Proceedings of the Agricultural Effects on Ground and Surface Waters: Research at the Edge of Science and Society held in Wageningen, Netherlands, in October, pp. 397-403. IAHS Publication no. 273.

Raber, G. T., Jensen, J. R., Schill, S. R., Schuckman, K. (2002) Creation of digital terrain models using an adaptive lidar vegetation point removal process. Photogrammetric Engineering & Remote Sensing, 68, 1307-1315.

Rieger, W. (1998) A phenomenon-based approach to upslope contributing area and depressions in DEMs. Hydrological Processes, 12, 857-872.

Saunders, W. (2000) Preparation of DEMs for use in environmental modeling analysis. In: Hydrologic and Hydraulic Modeling Support with Geographic Information Systems, edited by D. Maidment and Dean Djokic, pp. 29-51. Redlands, Environmental Systems Research Institute Inc.

Schneider, B. (2001) Phenomenon-based specification of the digital representation of terrain surfaces. Transactions in GIS, 5, 39-52.

Snaddon, C. D., Wishart, M. J., Davies, B. R. (1998) Some implications of inter-basin water transfers for river ecosystem functioning and water resources management in southern Africa. Aquatic Health and Management, 1, 159-182.

Souchere, V., King, D., Daroussin, J., Papy, F., Capillon, A. (1998) Effects of tillage on runoff directions: consequences on runoff contributing area within agricultural catchments. Journal of Hydrology, 206, 256-267.

Souchere, V., Cerdan, O., Ludwig, B., Le Bissonnais, Y., Couturier, A., Papy, F. (2003) Modelling ephemeral gully erosion in small cultivated catchments. Catena, 50, 489-505.

Strahler, A., Strahler, A. (1996) Inroducing physical geography. Toronto, Ontario: John Wiley & Sons Inc.

148

Tague, C., Band, L. (2001) Simulating the impact of road construction and forest harvesting on hydrological response. Earth Surface Processes and Landforms, 26, 135-151.

Takken, I., Govers, G., Steegen, A., Nachtergaele, J., Guerif, J. (2001a) The prediction of runoff flow directions of tilled fields. Journal of Hydrology, 248, 1-13.

Takken, I., Jetten, V., Govers, G., Nachtergaele, J., Steegen, A. (2001b) The effect of tillage-induced roughness on runoff and erosion patterns. Geomorphology, 37, 1-14.

Takken, I., Govers, G., Jetten, V., Nachtergaele, J., Steegen, A., Poesen, J. (2001c) Effects of tillage on runoff erosion patterns. Soil & Tillage Research, 61, 55-60.

Tarboton, D. G., Bras, R. L., Rodriguez-Iturbe, I. (1991) On the extraction of channel networks from digital elevation data. Hydrological Processes, 5, 81-100.

Tarboton, D. G. (1997) A new method for the determination of flow directions and upslope areas in grid digital elevation models. Water Resources Research, 33, 309-319.

Tarboton, D. G. 2000. TARDEM, a suite of programs for the analysis of digital elevation data, http://www.engineering.usu.edu/cee/faculty/dtarb/index.html (June 10, 2003).

Tarboton, D. G. (pers. comm.) Professor, Civil and Environmental Engineering. Utah State University. Logan, Utah.

Tian, Y, Q., Gong, P., Radke, J. D., Scarborough, J. (2002) Spatial and temporal modeling of microbial contaminants on grazing farmlands. Journal of Environmental Quality, 31, 860-869.

Tong, S. T. Y., Chen, W. (2002) Modeling the relationship between land use and surface water quality. Journal of Environmental Management, 66, 377-393.

Tribe, E. (1991) Automated recognition of valley heads from digital elevation models. Earth Surface Processes and Landforms, 16, 33-49.

Turcotte, R., Fortin, J. -P., Rousseau, A. N., Massicotte, S., Villeneuve, J. -P. (2001) Determination of the drainage structure of a watershed using a digital elevation model and a digital river and lake network. Journal of Hydrology, 240, 225-242.

United States Geological Survey. (2003) Regional trends of biological resources: grasslands—past and present, http://www.npwrc.usgs.gov/resource/2000/grlands/pastpres.htm (April 25, 2003).

Van Bohemen, H. D., Van De Laak, W. H. J. (2003) The influence of road infrastructure and traffic on soil, water, and air quality. Environmental Management, 31, 50-68.

Veregin, H. (1997) The effects of vertical error in digital elevation models on the determination of flow-path direction. Cartography and Geographic Information Systems, 24, 67-79.

Walker, J. P., Willgoose, G. R. (1999) On the effect of digital elevation model accuracy on hydrology and geomorphology. Water Resources Research, 35, 2259-2268.

Waters, J. R., Sharp, J. C. M., Dev, V. J. (1994) Infection caused by E.Scherichia coli 0157:H7 in Alberta, Canada, and in Scotland: a five year review, 1987-1991. Clinical Infectious Diseases, 19, 834-843.

Wemple, B. C., Jones, J. A., Grant, G. E. (1996) Channel network extension by logging roads in two basins, Western Cascades, Oregon. Water Resources Research, 32, 1195-1207.

Wise, S. (2000) Assessing the quality of hydrological applications of digital elevation models derived from contours. Hydrological Processes, 14, 1909-1929.

Zhang, W., Montgomery, D. R. (1994) Digital elevation model grid cell size, landscape representation, and hydrologic simulations. Water Resources Research, 30, 1019-1028.

9 Appendices

9.1 Road Survey Data

Surveyed road cross-sectional profiles quantifying the Ditch-to-Field and Ditch-to-Road heights.
Secondary highway cross-section survey data.

Raised road*			Road with ditches		
Site Number	Measured Heights (m)		Site Number	Measured Heights (m)	
	Ditch to Field	Ditch to Road		Ditch to Field	Ditch to Road
N/A	N/A	N/A	1	1.010	1.490
			2	0.399	1.751
			3	0.140	1.255
			4	0.801	1.799
			5	0.880	1.770
			6	0.370	1.560
			7	0.728	1.377
			8	1.450	1.760
			9	0.380	1.910
			10	0.720	1.820
			11	1.600	1.810
			12	1.445	1.730
			13	0.710	1.710
			14	0.571	1.548
			15	0.595	1.630
			16	0.242	1.712
			17	0.080	0.895
			18	0.908	1.660
			19	0.520	1.830
			20	1.230	1.360
			21	0.481	1.237
			22	0.730	1.270
			23	1.930	1.430
			24	0.750	1.490
			25	0.440	1.615
			26	0.675	1.305
			27	1.170	2.010
			28	0.382	1.542

* No secondary highways with a raised road template were surveyed

Surveyed road cross-sectional profiles quantifying the Ditch-to-Field and Ditch-to-Road heights. Local (gravel) road cross-section survey data.

Raised Road			Road with Ditches		
Site Number	Measured Heights (m)		Site Number	Measured Heights (m)	
	Ditch to Field	Ditch to Road		Ditch to Field	Ditch to Road
1	0.110	0.695	1	1.006	1.580
2	0.073	1.163	2	0.243	1.502
3	-0.095	0.270	3	0.350	1.773
4	0.354	1.285	4	0.855	1.510
5	-0.130	0.610	5	0.606	1.532
6	0.081	0.233	6	0.445	0.760
7	0.150	0.650	7	0.809	1.490
8	-0.070	0.705	8	0.295	1.130
9	-0.080	1.310	9	0.440	1.530
10	0.050	1.490	10	0.710	0.980
11	0.395	1.040	11	0.190	1.155
12	0.070	0.520	12	0.600	0.840
13	0.020	0.680	13	0.225	1.040
14	-0.070	1.340	14	0.460	0.635
15	0.165	0.340	15	0.050	0.590
16	0.030	0.495	16	0.020	0.680
17	0.094	1.097	17	0.650	1.090
18	-0.055	0.380	18	0.165	0.340
19	-0.035	0.520	19	0.130	1.370
20	0.321	0.503	20	0.444	1.173
21	-0.090	0.710	21	0.489	1.516
22	-0.070	1.370	22	0.710	1.713
23	-0.170	1.320	23	0.545	1.475
24	0.030	0.675	24	0.170	0.585
25	0.350	1.030	25	0.795	1.271
26	-0.250	1.165	26	0.550	0.990
27	0.140	0.620	27	0.795	1.480
28	0.015	0.440	28	0.760	0.750
29	-0.040	1.490	29	0.575	1.030
30	0.115	0.555	30	0.400	1.230
31	-0.040	1.490	31	0.370	0.915
32	-0.022	1.648	32	0.670	1.110
33	-0.070	1.340	33	0.175	0.870
34	-0.130	2.050	34	0.110	0.910
			35	0.015	0.440
			36	0.460	1.290
			37	0.115	0.555
			38	0.730	0.910
			39	0.750	1.271
			40	0.740	1.070
			41	0.530	0.675
			42	0.630	0.575

9.2 ESRI GridAscii Format

ncols	5
nrows	5
xllcorner	358700
yllcorner	5516400
cellsize	20
NODATA_value	-9999

100 100 99 57 99
100 97 96 97 96
99 99 98 95 94
97 94 93 94 97

9.3 Visual Basic Sample Code Extracted from RIDEM

The public sub-routine mStepCanal is a component of the CEA. mStepCanal creates an
array of enforced flow directions for canal pixels, an array with the location of dead end
pixels flagged, and a 3-dimensional array called CanalXYZ() that holds the row and
column coordinate of split flow locations, as well as the alternate flow direction (See
section 5.2.4 Calculation of the Flow Direction Matrix). This snippet of code calls sub-
routines that are not included in this appendix such as ReadIntegerAsciiFilie,
mTraceCaanal, and Write_AsciiFile.

```
Public Sub mStepCanal(strDrain As String, strCanalOrd As String, strCanalID As String, _
            strCanalEnt As String, strCanalDead As String)

    On Error GoTo ErrHandler
    'arrays to hold inputs
    Dim Canal() As Integer
    Dim CanalEnt() As Integer
    Dim EndLoop() As Integer
    Dim Drain() As Integer
    Dim CanalID() As Integer

    'Set variables for the header info from the ascii file
    Dim width As Integer, height As Integer, xll As Double, yll As Double
    Dim CellSize As Single, NoDataSym As Single

    'call a sub to read in the files
    frmMain.StatusBar1.Panels(2).Text = "Reading input files..."
    ReadIntegerAsciiFile Canal(), strCanalOrd, width, height, xll, yll, CellSize, NoDataSym
    ReadIntegerAsciiFile CanalEnt(), strCanalEnt, width, height, xll, yll, CellSize, NoDataSym
    ReadIntegerAsciiFile Drain(), strDrain, width, height, xll, yll, CellSize, NoDataSym
    ReadIntegerAsciiFile CanalID(), strCanalID, width, height, xll, yll, CellSize, NoDataSym
    ReadIntegerAsciiFile EndLoop(), strCanalDead, width, height, xll, yll, CellSize, NoDataSym


    Dim x As Integer, y As Integer
    Dim x2 As Integer, y2 As Integer

    frmMain.StatusBar1.Panels(2).Text = "Processing..."

    'Find the maximum value in the canal grid.
    'This represents the "stream order" of the canal network.
    Dim intCanalMax As Integer
    For x = 1 To height
      For y = 1 To width
```

154

```
    If Canal(x, y) > intCanalMax Then
      intCanalMax = Canal(x, y)
    End If
  Next y
Next x


'For each canal "stream order" greater than 1, declare an array
'to hold the row, column, and order values.
'This is a three dimensional array to hold
'X, Y, coordinates for each level (the 3rd dimension of the array)
Dim CanalXYZ() As Integer
ReDim CanalXYZ(50, 2, intCanalMax)
Dim Altfd() As Integer
ReDim Altfd(50, 3, intCanalMax)

For x = 1 To height
  For y = 1 To width
    If CanalEnt(x, y) > 0 Then
      ReDim CanalEnt(height, 1) As Integer
      GoTo EntryFound
    End If
  Next y
Next x

EntryFound:

  Dim outFlowD() As Integer
  ReDim outFlowD(height, width) As Integer
  Dim outDeadEnd() As Integer
  ReDim outDeadEnd(height, width) As Integer

  'Create a copy of the canal file.
  Dim canal_c() As Integer
  Dim canal_c2() As Integer
  ReDim canal_c(height, width) As Integer
  ReDim canal_c2(height, width) As Integer
  canal_c() = Canal()
  canal_c2() = Canal()

  Dim intCurrent As Integer
  intCurrent = 1

  frmMain.StatusBar1.Panels(2).Text = "Tracing main-canal..."

  'The pixelStart variable was required for canals that were only one
  'pixel long.  So that flow was not simply put back into the adjacent
  'lower order canal.
  Dim pixelStart As Byte
  pixelStart = 1

  'follow the main canal.
  mTraceCanal CanalXYZ(), 1, height, width, CanalEnt(), _
        canal_c(), x, y, outFlowD(), Drain(), NoDataSym, outDeadEnd(), _
        CanalID(), pixelStart, Altfd(), canal_c2(), EndLoop()

  'Start a loop to trace the next order of canals (2, 3, 4, kth...)
```

155

```
'Each call to mTraceCanal only ID's the next order.
'Determine how many X,Y pairs were identified.
Dim i As Integer, CurrO As Integer
i = 1
intCurrent = intCurrent + 1


For CurrO = 2 To intCanalMax
  frmMain.StatusBar1.Panels(2).Text = "Processing Canal Order " & CurrO & " of " & intCanalMax
  Dim boolDone As Boolean
  Do Until boolDone = True
    If CanalXYZ(i, 1, intCurrent) > 0 Then
      'copy the canal file
      canal_c() = Canal()
      pixelStart = 1

      'call private sub-routine mTraceflow
      'mTraceflow creates an enforced canal flow directin layer, populates
      'the 3-dimensional array CanalXYZ with the row and column coordinate of
      'split flow pixels, and records the alternate flow direction.
      mTraceCanal CanalXYZ(), intCurrent, height, width, CanalEnt(), _
          canal_c(), CanalXYZ(i, 1, intCurrent), CanalXYZ(i, 2, intCurrent), _
          outFlowD(), Drain(), NoDataSym, outDeadEnd(), CanalID(), pixelStart, _
          Altfd(), canal_c2(), EndLoop()
    Else
      boolDone = True
    End If
    i = i + 1
  Loop
  intCurrent = intCurrent + 1
  boolDone = False
  i = 1
Next CurrO

'check outputs for validity
For x = 1 To height
  For y = 1 To width
    If CanalID(x, y) > 0 And outFlowD(x, y) <= 0 Then
      MsgBox "Potential Error: The output grid does not include all canal segments." & vbCrLf & _
          "This can occur if the canal ID & canal order data layers are not continuous at " & _
          "canal intersections." & vbCrLf & "Check Input files and Output files...", vbInformation +
vbOKOnly, "Potential Error!"
      x = height
      y = width
    End If
  Next y
Next x

frmMain.StatusBar1.Panels(2).Text = "Writing Outputs..."

Dim strFileName As String

Dim boolIn As Boolean
Do
  strFileName = InputBox("Enter the name of the canal flow direction file.", "File Name:")
  If Len(strFileName) > 0 Then
```

156

```
    If Not IsNumeric(strFileName) Then
      boolIn = True
    End If
   End If
 Loop Until boolIn = True


 Write_AsciiFile outFlowD(), strFileName, width, height, xll, _
         yll, CellSize, NoDataSym


 boolIn = False
 Do
   strFileName = InputBox("Enter the name of the canal deadend file.", "File Name:")
   If Len(strFileName) > 0 Then
    If Not IsNumeric(strFileName) Then
      boolIn = True
    End If
   End If
 Loop Until boolIn = True

 Write_AsciiFile outDeadEnd(), strFileName, width, height, xll, _
         yll, CellSize, NoDataSym


 intCurrent = 1
 'this creates a log file with X, Y, Coords
 'and alternate flow directions for these pixels. The alternate flow
 'directions are the directions into lower order canals. These pixels
 'are, therefore, the pixels that disperse flow into more than one canal.


 'assigns an avialable integer value to the file to open
 Dim nFile As Integer
 nFile = FreeFile

 Dim Alt_row As Integer
 Dim Alt_column As Integer
 boolIn = False
 Do
   strFileName = InputBox("Enter file name for the alternate fd X/Y Coords and flow directions", "File
Name:")
   If Len(strFileName) > 0 Then
    If Not IsNumeric(strFileName) Then
      boolIn = True
    End If
   End If
 Loop Until boolIn = True


 If m_Directory = "" Then
    Open App.Path & "\" & strFileName For Output As #nFile
 Else
    Open m_Directory & "\" & strFileName For Output As #nFile
 End If
 Write #nFile, "ID", "XCoord", "YCoord", "Row", "Column", "FlowDirection", "CanalOrd"

 Dim pixelCount As Integer, Altfd2 As Integer
 Dim Alt_X As Long, Alt_Y As Long
```

157

```
    Dim canalOrdTo As Integer
    boolDone = False
    i = 1
    intCurrent = 2

    For CurrO = 2 To intCanalMax
       frmMain.StatusBar1.Panels(2).Text = "Part II: Processing Canal Order " & CurrO & " of " &
intCanalMax
       Do Until boolDone = True
         If Altfd(i, 1, intCurrent) > 0 Then
           pixelCount = pixelCount + 1

           'call a sub that searches the neighbours of each pixel for
           'a neighbour with a lower Canal Order.  This pixel will be the
           'pixel that will have alternate flow directions.
           Alt_X = (xll + ((Altfd(i, 2, CurrO) - 1) * CellSize)) + (CellSize / 2)
           Alt_Y = ((height - Altfd(i, 1, CurrO)) * CellSize) + yll + (CellSize / 2)
           Alt_row = Altfd(i, 1, intCurrent)
           Alt_column = Altfd(i, 2, intCurrent)
           Altfd2 = Altfd(i, 3, intCurrent)

           'call a sub to determine which canal order the canal is flowing to.
           mCanalOrdTo Alt_row, Alt_column, Altfd2, canal_c2(), canalOrdTo

           Write #nFile, pixelCount, Alt_X, Alt_Y, Alt_row, Alt_column, Altfd2, canalOrdTo
         Else
           boolDone = True
         End If
         i = i + 1
       Loop
       intCurrent = intCurrent + 1
       If intCurrent > intCanalMax Then
         boolDone = True
       Else
         boolDone = False
       End If

       i = 1
    Next CurrO

    Close #nFile
    Exit Sub

ErrHandler:
    ErrHandlerSub Err
End Sub
```

The public sub-routine aAssignFDs is a component of the REA. aAssignFDs assigns a

flow direction to each breach grid cell. First the DEM-derived (D8) flow direction is

assigned to the current breach grid cell. If the current breach grid cell does not loop back

into the current ditch segment it is used as the breach flow direction. If the DEM-derived

(D8) flow direction loops back to the current ditch segment it assigns a flow direction to

either the grid cell to the left or to the right of the DEM-derived downstream grid cell

based on the flow accumulation value. If all three DEM-derived (D8) flow directions

loop (breach grid cell flow direction, left grid cell flow direction, and right grid cell flow

direction) it moves the breach pixel to the grid cell with the highest flow accumulation

value in the current ditch segment. Following this step the sub-routine re-routes all of the

flow from the current ditch segment to the new breach pixel (See section 4.2.4

Calculation of the Runoff Collector Flow Directions). This snippet of code calls

subroutines that are not included in this appendix such as ReadIntegerAsciiFile,

ReadLongAsciiFile, ReadDoubleAsciiFile, mFindSegment, A_Edit888Fd,

A_Ditch_Segment_FDTracer, and Write_AsciiFile.

```
Public Sub aAssignFDs(strDitchFd As String, strDEMFD As String, strDEMacc As String, strDEM As
String, checkFor888 As Boolean, VariableCls As String)
    Dim DitchFD() As Integer
    Dim DEMfd() As Integer
    Dim DEMacc() As Long
    Dim DEM() As Double

    'Set variables for the header info from the ascii file
    Dim width As Integer, height As Integer, xll As Double, yll As Double
    Dim CellSize As Single, NoDataSym As Single

    frmMain.StatusBar1.Panels(2).Text = "Step 7...Reading Files"
    ReadIntegerAsciiFile DitchFD(), strDitchFd, width, height, xll, yll, CellSize, NoDataSym
    ReadIntegerAsciiFile DEMfd(), strDEMFD, width, height, xll, yll, CellSize, NoDataSym
    ReadLongAsciiFile DEMacc(), strDEMacc, width, height, xll, yll, CellSize, NoDataSym
    ReadDoubleAsciiFile DEM(), strDEM, width, height, xll, yll, CellSize, NoDataSym

    Dim OutPutFD() As Integer
    ReDim OutPutFD(height, width) As Integer
```

159

```
'Create an array to hold the breach points that were moved so
'loops were not created
'Dim move_count As Integer this declaration was moved to a global variable
Dim BreachMove() As Double
ReDim BreachMove(height, width) As Double


'This array will hold all the breach sites, including the ones that were moved
'but not including the where the old ones were moved from.
ReDim m_NewBreachSites(height, width) As Integer
m_NewBreachSites() = DitchFD()


Dim Left As Boolean, Right As Boolean
Dim LeftAcc As Long, RightAcc As Long
Dim looped As Boolean
Dim LeftLooped As Boolean


Dim BreachValue As Integer
BreachValue = 450
Dim x As Integer, y As Integer


Dim DitchFDCopy() As Integer
ReDim DitchFDCopy(height, width) As Integer
DitchFDCopy() = DitchFD()


For x = 1 To height
  For y = 1 To width
    If DitchFD(x, y) = BreachValue Then


        m_Looped = False
        LeftLooped = False
        Left = False
        Right = False
        Select Case DEMfd(x, y)
          Case 1
            If DitchFD(x, y + 1) < 1 Then 'The downstream pixel is not part of the ditch
             'OutPutFd(X, y) = 1 --- This was the only part of this if before July 2 2002


            'Identify the current ditch segment, the ditch pixels that flow to this one
            mFindSegment_s x, y, DitchFDCopy(), height, width


            'call the trace routing from the leftacc x, y position
            looped = A_Ditch_Segment_FDTracer(x, y, x, y, DEMfd(), DitchFD(), height, width)
            'if the DEMfd flow direction for this current breach pixel does not loop
            'back into this ditch segment then simply assign the flow direction
            If m_Looped = False Then
              OutPutFD(x, y) = 1
            Else
              'if the DEMfd does loop around call Edit888fd
              'this (Edit888fd) moves the breach to the location within the current ditchsegment with the
highest
              'flow accumulation value
              A_Edit888Fd OutPutFD(), DitchFD(), DEMacc(), DEMfd(), BreachMove(), x, y, height,
width, DEM()
            End If
```

160

Else
  LeftAcc = DEMacc(x - 1, y + 1)
  RightAcc = DEMacc(x + 1, y + 1)
  'Identify the current ditch segment, the ditch pixels that flow to this one
  mFindSegment_s x, y, DitchFDCopy(), height, width

  'Check to see if the pixel to the left and to the right are part of the ditch
  If DitchFD(x - 1, y + 1) > 0 Then
    'The pixel to the left is also part of the ditch grid
    Left = True
  End If
  If DitchFD(x + 1, y + 1) > 0 Then
    'The pixel to the right is also part of the ditch grid
    Right = True
  End If

  'Trace the flow path of the highest flow direction
  If Left = False Then
    'call the trace routing from the leftacc x, y position
    looped = A_Ditch_Segment_FDTracer(x, y, x - 1, y + 1, DEMfd(), DitchFD(), height,

width)

    If m_Looped = True Then LeftLooped = True
    If m_Looped = False Then
      OutPutFD(x, y) = 128
      GoTo Find_NextBreachPixel
    End If
  End If
  If Right = False Then
    'call the trace routing from the rightacc x, y position
    looped = A_Ditch_Segment_FDTracer(x, y, x + 1, y + 1, DEMfd(), DitchFD(), height,

width)

    If m_Looped = False Then
      'if the pixel to the left is a possibility but the right has a larger facc then assign the right

direction

      'if left was not a possibility then assign the right direction
      'if the left was a possibility but it looped assign the right direction
      If Left = False And RightAcc >= LeftAcc Or Left = True Or LeftLooped = True Then
        OutPutFD(x, y) = 2
        GoTo Find_NextBreachPixel
      End If
    End If
  End If
  'If we made it this far then either the left, right, or both option
  'pixels loop around.
  A_Edit888Fd OutPutFD(), DitchFD(), DEMacc(), DEMfd(), BreachMove(), x, y, height,
width, DEM()

  GoTo Find_NextBreachPixel
  End If
Case 2
  If DitchFD(x + 1, y + 1) < 1 Then
    'Identify the current ditch segment, the ditch pixels that flow to this one
    mFindSegment_s x, y, DitchFDCopy(), height, width

    'call the trace routing from the leftacc x, y position
    looped = A_Ditch_Segment_FDTracer(x, y, x, y, DEMfd(), DitchFD(), height, width)

161

'if the DEMfd flow direction for this current breach pixel does not loop
'back into this ditch segment then simply assign the flow direction
If m_Looped = False Then
    OutPutFD(x, y) = 2
Else
    'if the DEMfd does loop around call Edit888fd
    A_Edit888Fd OutPutFD(), DitchFD(), DEMacc(), DEMfd(), BreachMove(), x, y, height,
width, DEM()
End If

Else
    LeftAcc = DEMacc(x, y + 1)
    RightAcc = DEMacc(x + 1, y)
    'Identify the current ditch segment, the ditch pixels that flow to this one
    mFindSegment_s x, y, DitchFDCopy(), height, width

    'Check to see if the pixel to the left and to the right are part of the ditch
    If DitchFD(x, y + 1) > 0 Then
        'The pixel to the left is also part of the ditch grid
        Left = True
    End If
    If DitchFD(x + 1, y) > 0 Then
        'The pixel to the right is also part of the ditch grid
        Right = True
    End If

    'Trace the flow path of the highest flow direction
    If Left = False Then
        'call the trace routing from the leftacc x, y position
        looped = A_Ditch_Segment_FDTracer(x, y, x, y + 1, DEMfd(), DitchFD(), height, width)
        If m_Looped = True Then LeftLooped = True
        If m_Looped = False Then
            OutPutFD(x, y) = 1
            GoTo Find_NextBreachPixel
        End If
    End If
    If Right = False Then
        'call the trace routing from the rightacc x, y position
        looped = A_Ditch_Segment_FDTracer(x, y, x + 1, y, DEMfd(), DitchFD(), height, width)
        If m_Looped = False Then
            If Left = False And RightAcc >= LeftAcc Or Left = True Or LeftLooped = True Then
                OutPutFD(x, y) = 4
                GoTo Find_NextBreachPixel
            End If
        End If
    End If
    'If we made it this far then either the left, right, or both option
    'pixels loop around.
    A_Edit888Fd OutPutFD(), DitchFD(), DEMacc(), DEMfd(), BreachMove(), x, y, height,
width, DEM()
    GoTo Find_NextBreachPixel
End If

Case 4
    If DitchFD(x + 1, y) < 1 Then
        'Identify the current ditch segment, the ditch pixels that flow to this one

162

```
mFindSegment_s x, y, DitchFDCopy(), height, width

'call the trace routing from the leftacc x, y position
looped = A_Ditch_Segment_FDTracer(x, y, x, y, DEMfd(), DitchFD(), height, width)
'if the DEMfd flow direction for this current breach pixel does not loop
'back into this ditch segment then simply assign the flow direction
If m_Looped = False Then
   OutPutFD(x, y) = 4
Else
   'if the DEMfd does loop around call Edit888fd
   A_Edit888Fd OutPutFD(), DitchFD(), DEMacc(), DEMfd(), BreachMove(), x, y, height,
width, DEM()
End If
Else
   LeftAcc = DEMacc(x + 1, y + 1)
   RightAcc = DEMacc(x + 1, y - 1)
   'Identify the current ditch segment, the ditch pixels that flow to this one
   mFindSegment_s x, y, DitchFDCopy(), height, width

   'Check to see if the pixel to the left and to the right are part of the ditch
   If DitchFD(x + 1, y + 1) > 0 Then
      'The pixel to the left is also part of the ditch grid
      Left = True
   End If
   If DitchFD(x + 1, y - 1) > 0 Then
      'The pixel to the right is also part of the ditch grid
      Right = True
   End If

   'Trace the flow path of the highest flow direction
   If Left = False Then 'And LeftAcc >= RightAcc Then
      'call the trace routing from the leftacc x, y position
      looped = A_Ditch_Segment_FDTracer(x, y, x + 1, y + 1, DEMfd(), DitchFD(), height,
width)

      If m_Looped = True Then LeftLooped = True
      If m_Looped = False Then
         OutPutFD(x, y) = 2
         GoTo Find_NextBreachPixel
      End If
   End If
   If Right = False Then
      'call the trace routing from the rightacc x, y position
      looped = A_Ditch_Segment_FDTracer(x, y, x + 1, y - 1, DEMfd(), DitchFD(), height,
width)

      If m_Looped = False Then
         If Left = False And RightAcc >= LeftAcc Or Left = True Or LeftLooped = True Then
            OutPutFD(x, y) = 8
            GoTo Find_NextBreachPixel
         End If
      End If
   End If
   'If we made it this far then either the left, right, or both option
   'pixels loop around.
   A_Edit888Fd OutPutFD(), DitchFD(), DEMacc(), DEMfd(), BreachMove(), x, y, height,
width, DEM()
   GoTo Find_NextBreachPixel
```

163

End If

Case 8
  If DitchFD(x + 1, y - 1) < 1 Then
    'Identify the current ditch segment, the ditch pixels that flow to this one
    mFindSegment_s x, y, DitchFDCopy(), height, width

    'call the trace routing from the leftacc x, y position
    looped = A_Ditch_Segment_FDTracer(x, y, x, y, DEMfd(), DitchFD(), height, width)
    'if the DEMfd flow direction for this current breach pixel does not loop
    'back into this ditch segment then simply assign the flow direction
    If m_Looped = False Then
      OutPutFD(x, y) = 8
    Else
      'if the DEMfd does loop around call Edit888fd
      A_Edit888Fd OutPutFD(), DitchFD(), DEMacc(), DEMfd(), BreachMove(), x, y, height,
width, DEM()
    End If
  Else
    LeftAcc = DEMacc(x + 1, y)
    RightAcc = DEMacc(x, y - 1)
    'Identify the current ditch segment, the ditch pixels that flow to this one
    mFindSegment_s x, y, DitchFDCopy(), height, width

    'Check to see if the pixel to the left and to the right are part of the ditch
    If DitchFD(x + 1, y) > 0 Then
      'The pixel to the left is also part of the ditch grid
      Left = True
    End If
    If DitchFD(x, y - 1) > 0 Then
      'The pixel to the right is also part of the ditch grid
      Right = True
    End If

    'Trace the flow path of the highest flow direction
    If Left = False Then
      'call the trace routing from the leftacc x, y position
      looped = A_Ditch_Segment_FDTracer(x, y, x + 1, y, DEMfd(), DitchFD(), height, width)
      If m_Looped = True Then LeftLooped = True
      If m_Looped = False Then
        OutPutFD(x, y) = 4
        GoTo Find_NextBreachPixel
      End If
    End If
    If Right = False Then
      'call the trace routing from the rightacc x, y position
      looped = A_Ditch_Segment_FDTracer(x, y, x, y - 1, DEMfd(), DitchFD(), height, width)
      If m_Looped = False Then
        If Left = False And RightAcc >= LeftAcc Or Left = True Or LeftLooped = True Then
          OutPutFD(x, y) = 16
          GoTo Find_NextBreachPixel
        End If
      End If
    End If
  End If
  'If we made it this far then either the left, right, or both option
  'pixels loop around.

164

A_Edit888Fd OutPutFD(), DitchFD(), DEMacc(), DEMfd(), BreachMove(), x, y, height, width, DEM()
            GoTo Find_NextBreachPixel
        End If

    Case 16
        If DitchFD(x, y - 1) < 1 Then
            'Identify the current ditch segment, the ditch pixels that flow to this one
            mFindSegment_s x, y, DitchFDCopy(), height, width

            'call the trace routing from the leftacc x, y position
            looped = A_Ditch_Segment_FDTracer(x, y, x, y, DEMfd(), DitchFD(), height, width)
            'if the DEMfd flow direction for this current breach pixel does not loop
            'back into this ditch segment then simply assign the flow direction
            If m_Looped = False Then
                OutPutFD(x, y) = 16
            Else
                'if the DEMfd does loop around call Edit888fd
                A_Edit888Fd OutPutFD(), DitchFD(), DEMacc(), DEMfd(), BreachMove(), x, y, height, width, DEM()
            End If
        Else
            LeftAcc = DEMacc(x + 1, y - 1)
            RightAcc = DEMacc(x - 1, y - 1)
            'Identify the current ditch segment, the ditch pixels that flow to this one
            mFindSegment_s x, y, DitchFDCopy(), height, width

            'Check to see if the pixel to the left and to the right are part of the ditch
            If DitchFD(x + 1, y - 1) > 0 Then
                'The pixel to the left is also part of the ditch grid
                Left = True
            End If
            If DitchFD(x - 1, y - 1) > 0 Then
                'The pixel to the right is also part of the ditch grid
                Right = True
            End If

            'Trace the flow path of the highest flow direction
            If Left = False Then 'And LeftAcc >= RightAcc Then
                'call the trace routing from the leftacc x, y position
                looped = A_Ditch_Segment_FDTracer(x, y, x + 1, y - 1, DEMfd(), DitchFD(), height, width)
                If m_Looped = True Then LeftLooped = True
                If m_Looped = False Then
                    OutPutFD(x, y) = 8
                    GoTo Find_NextBreachPixel
                End If
            End If
            If Right = False Then 'And RightAcc >= LeftAcc Then
                'call the trace routing from the rightacc x, y position
                looped = A_Ditch_Segment_FDTracer(x, y, x - 1, y - 1, DEMfd(), DitchFD(), height, width)
                If m_Looped = False Then
                    If Left = False And RightAcc >= LeftAcc Or Left = True Or LeftLooped = True Then
                        OutPutFD(x, y) = 32
                        GoTo Find_NextBreachPixel
                    End If
            End If

165

```
            End If
        End If
        'If we made it this far then either the left, right, or both option
        'pixels loop around.
        A_Edit888Fd OutPutFD(), DitchFD(), DEMacc(), DEMfd(), BreachMove(), x, y, height,
width, DEM()
            GoTo Find_NextBreachPixel
        End If


    Case 32
        If DitchFD(x - 1, y - 1) < 1 Then
            'Identify the current ditch segment, the ditch pixels that flow to this one
            mFindSegment_s x, y, DitchFDCopy(), height, width


            'call the trace routing from the leftacc x, y position
            looped = A_Ditch_Segment_FDTracer(x, y, x, y, DEMfd(), DitchFD(), height, width)
            'if the DEMfd flow direction for this current breach pixel does not loop
            'back into this ditch segment then simply assign the flow direction
            If m_Looped = False Then
                OutPutFD(x, y) = 32
            Else
                'if the DEMfd does loop around call Edit888fd
                A_Edit888Fd OutPutFD(), DitchFD(), DEMacc(), DEMfd(), BreachMove(), x, y, height,
width, DEM()
            End If
        Else
            LeftAcc = DEMacc(x, y - 1)
            RightAcc = DEMacc(x - 1, y)
            'Identify the current ditch segment, the ditch pixels that flow to this one
            mFindSegment_s x, y, DitchFDCopy(), height, width


            'Check to see if the pixel to the left and to the right are part of the ditch
            If DitchFD(x, y - 1) > 0 Then
                'The pixel to the left is also part of the ditch grid
                Left = True
            End If
            If DitchFD(x - 1, y) > 0 Then
                'The pixel to the right is also part of the ditch grid
                Right = True
            End If


            'Trace the flow path of the highest flow direction
            If Left = False Then
                'call the trace routing from the leftacc x, y position
                looped = A_Ditch_Segment_FDTracer(x, y, x, y - 1, DEMfd(), DitchFD(), height, width)
                If m_Looped = True Then LeftLooped = True
                If m_Looped = False Then
                    OutPutFD(x, y) = 16
                    GoTo Find_NextBreachPixel
                End If
            End If
            If Right = False Then
                'call the trace routing from the rightacc x, y position
                looped = A_Ditch_Segment_FDTracer(x, y, x - 1, y, DEMfd(), DitchFD(), height, width)
                If m_Looped = False Then
                    If Left = False And RightAcc >= LeftAcc Or Left = True Or LeftLooped = True Then
```

166

```
              OutPutFD(x, y) = 64
              GoTo Find_NextBreachPixel
            End If
          End If
        End If
        'If we made it this far then either the left, right, or both option
        'pixels loop around.
        A_Edit888Fd OutPutFD(), DitchFD(), DEMacc(), DEMfd(), BreachMove(), x, y, height,
width, DEM()
            GoTo Find_NextBreachPixel
          End If


      Case 64
        If DitchFD(x - 1, y) < 1 Then
          'Identify the current ditch segment, the ditch pixels that flow to this one
          mFindSegment_s x, y, DitchFDCopy(), height, width


          'call the trace routing from the leftacc x, y position
          looped = A_Ditch_Segment_FDTracer(x, y, x, y, DEMfd(), DitchFD(), height, width)
          'if the DEMfd flow direction for this current breach pixel does not loop
          'back into this ditch segment then simply assign the flow direction
          If m_Looped = False Then
            OutPutFD(x, y) = 64
          Else
            'if the DEMfd does loop around call Edit888fd
            A_Edit888Fd OutPutFD(), DitchFD(), DEMacc(), DEMfd(), BreachMove(), x, y, height,
width, DEM()
          End If
        Else
          LeftAcc = DEMacc(x - 1, y - 1)
          RightAcc = DEMacc(x - 1, y + 1)
          'Identify the current ditch segment, the ditch pixels that flow to this one
          mFindSegment_s x, y, DitchFDCopy(), height, width


          'Check to see if the pixel to the left and to the right are part of the ditch
          If DitchFD(x - 1, y - 1) > 0 Then
            'The pixel to the left is also part of the ditch grid
            Left = True
          End If
          If DitchFD(x - 1, y + 1) > 0 Then
            'The pixel to the right is also part of the ditch grid
            Right = True
          End If


          'Trace the flow path of the highest flow direction
          If Left = False Then
            'call the trace routing from the leftacc x, y position
            looped = A_Ditch_Segment_FDTracer(x, y, x - 1, y - 1, DEMfd(), DitchFD(), height, width)
            If m_Looped = True Then LeftLooped = True
            If m_Looped = False Then
              OutPutFD(x, y) = 32
              GoTo Find_NextBreachPixel
            End If
          End If
          If Right = False Then
            'call the trace routing from the rightacc x, y position
```

167

```
            looped = A_Ditch_Segment_FDTracer(x, y, x - 1, y + 1, DEMfd(), DitchFD(), height,
width)
                If m_Looped = False Then
                  If Left = False And RightAcc >= LeftAcc Or Left = True Or LeftLooped = True Then
                  OutPutFD(x, y) = 128
                  GoTo Find_NextBreachPixel
                  End If
                End If
              End If
              'If we made it this far then either the left, right, or both option
              'pixels loop around.
              A_Edit888Fd OutPutFD(), DitchFD(), DEMacc(), DEMfd(), BreachMove(), x, y, height,
width, DEM()
            GoTo Find_NextBreachPixel
          End If


        Case 128
          If DitchFD(x - 1, y + 1) < 1 Then
            'Identify the current ditch segment, the ditch pixels that flow to this one
            mFindSegment_s x, y, DitchFDCopy(), height, width


            'call the trace routing from the leftacc x, y position
            looped = A_Ditch_Segment_FDTracer(x, y, x, y, DEMfd(), DitchFD(), height, width)
            'if the DEMfd flow direction for this current breach pixel does not loop
            'back into this ditch segment then simply assign the flow direction
            If m_Looped = False Then
              OutPutFD(x, y) = 128
            Else
              'if the DEMfd does loop around call Edit888fd
              A_Edit888Fd OutPutFD(), DitchFD(), DEMacc(), DEMfd(), BreachMove(), x, y, height,
width, DEM()
            End If
          Else
            LeftAcc = DEMacc(x - 1, y)
            RightAcc = DEMacc(x, y + 1)
            'Identify the current ditch segment, the ditch pixels that flow to this one
            mFindSegment_s x, y, DitchFDCopy(), height, width


            'Check to see if the pixel to the left and to the right are part of the ditch
            If DitchFD(x - 1, y) > 0 Then
              'The pixel to the left is also part of the ditch grid
              Left = True
            End If
            If DitchFD(x, y + 1) > 0 Then
              'The pixel to the right is also part of the ditch grid
              Right = True
            End If


            'Trace the flow path of the highest flow direction
            If Left = False Then
              'call the trace routing from the leftacc x, y position
              looped = A_Ditch_Segment_FDTracer(x, y, x - 1, y, DEMfd(), DitchFD(), height, width)
              If m_Looped = True Then LeftLooped = True
              If m_Looped = False Then
                OutPutFD(x, y) = 64
                GoTo Find_NextBreachPixel
```

168

```
                    End If
                End If
                If Right = False Then
                    'call the trace routing from the rightacc x, y position
                    looped = A_Ditch_Segment_FDTracer(x, y, x, y + 1, DEMfd(), DitchFD(), height, width)
                    If m_Looped = False Then
                        If Left = False And RightAcc >= LeftAcc Or Left = True Or LeftLooped = True Then
                            OutPutFD(x, y) = 1
                            GoTo Find_NextBreachPixel
                        End If
                    End If
                End If
                'If we made it this far then either the left, right, or both option
                'pixels loop around.
                A_Edit888Fd OutPutFD(), DitchFD(), DEMacc(), DEMfd(), BreachMove(), x, y, height,
width, DEM()
                GoTo Find_NextBreachPixel
            End If
        End Select
    End If
Find_NextBreachPixel:
    Next y
    frmMain.StatusBar1.Panels(2).Text = "Step 7: Processing row " & x & " of " & height
Next x


'MsgBox "888 meands left, right, or both alternate pixels loop around, therefore ID by hand" & _
' "999 means The alternate FD, the left and the right are all part of the ditch"


Dim vbFD() As Integer
ReDim vbFD(height, width) As Integer


'This was added on June 23, 2002
For x = 1 To height
    For y = 1 To width
        If OutPutFD(x, y) = 0 Then
            OutPutFD(x, y) = DitchFD(x, y)
        ElseIf OutPutFD(x, y) = 888 Or OutPutFD(x, y) = 999 Then
            checkFor888 = True
        End If
    Next y
Next x


'This was added during the automation.
For x = 1 To height
    For y = 1 To width
        If OutPutFD(x, y) > 0 Then
            vbFD(x, y) = OutPutFD(x, y)
        Else
            vbFD(x, y) = DEMfd(x, y)
        End If
    Next y
Next x


Dim asciiOutPut As String
asciiOutPut = "A_Enfor_fd.Asc"
Write_AsciiFile OutPutFD(), asciiOutPut, width, height, xll, yll, CellSize, NoDataSym
```

169

```
asciiOutPut = "A_vb_fds.asc"
Write_AsciiFile vbFD(), asciiOutPut, width, height, xll, yll, CellSize, NoDataSym

If move_count > 0 Then
    asciiOutPut = "A_moved_elev.Asc"
    Write_AsciiFile_Double BreachMove(), asciiOutPut, width, height, xll, yll, CellSize, NoDataSym
    asciiOutPut = "A_moved_fd.asc"
    Write_AsciiFile m_NewBreachSites(), asciiOutPut, width, height, xll, yll, CellSize, NoDataSym
Else

End If

frmMain.StatusBar1.Panels(2).Text = "Step 7 Complete"
End Sub
```